

University of New Hampshire

## University of New Hampshire Scholars' Repository

---

Master's Theses and Capstones

Student Scholarship

---

Spring 2009

### Electricity production from the management of municipal solid waste leachate with microbial fuel cells

Lisa Damiano

*University of New Hampshire, Durham*

Follow this and additional works at: <https://scholars.unh.edu/thesis>

---

#### Recommended Citation

Damiano, Lisa, "Electricity production from the management of municipal solid waste leachate with microbial fuel cells" (2009). *Master's Theses and Capstones*. 443.

<https://scholars.unh.edu/thesis/443>

This Thesis is brought to you for free and open access by the Student Scholarship at University of New Hampshire Scholars' Repository. It has been accepted for inclusion in Master's Theses and Capstones by an authorized administrator of University of New Hampshire Scholars' Repository. For more information, please contact [Scholarly.Communication@unh.edu](mailto:Scholarly.Communication@unh.edu).

**ELECTRICITY PRODUCTION  
FROM THE MANAGEMENT OF MUNICIPLE SOLID WASTE LEACHATE  
WITH MICROBIAL FUEL CELLS**

**BY**

**LISA DAMIANO**

**B.S., University of New Hampshire, 2007**

**THESIS**

**Submitted to the University of New Hampshire**

**in Partial Fulfillment of**

**the Requirements for the Degree of**

**Master of Science**

**In**

**Civil Engineering**

**May, 2009**

UMI Number: 1466926

### INFORMATION TO USERS

The quality of this reproduction is dependent upon the quality of the copy submitted. Broken or indistinct print, colored or poor quality illustrations and photographs, print bleed-through, substandard margins, and improper alignment can adversely affect reproduction.

In the unlikely event that the author did not send a complete manuscript and there are missing pages, these will be noted. Also, if unauthorized copyright material had to be removed, a note will indicate the deletion.

**UMI<sup>®</sup>**

---

UMI Microform 1466926  
Copyright 2009 by ProQuest LLC  
All rights reserved. This microform edition is protected against  
unauthorized copying under Title 17, United States Code.

---

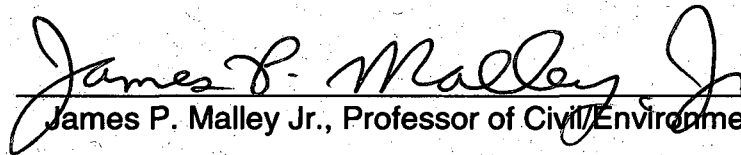
ProQuest LLC  
789 East Eisenhower Parkway  
P.O. Box 1346  
Ann Arbor, MI 48106-1346

This thesis has been examined and approved.



---

Thesis Director, Jenna R. Jambeck, Research Assistant Professor  
of Civil/Environmental Engineering



---

James P. Malley Jr., Professor of Civil/Environmental Engineering



---

*NE Kinner*  
Nancy E. Kinner, Professor of Civil/Environmental Engineering

5/6/09

---

Date

## TABLE OF CONTENTS

CHAPTER	PAGE
List of Tables .....	viii
List of Figures .....	x
Abstract .....	xii

CHAPTER	PAGE
CHAPTER 1 .....	1
1.1 Background.....	1
1.2 Objective and Scope.....	3
CHAPTER 2.....	5
2.1 Introduction .....	5
2.2 Composition and Formation of Municipal Solid Waste Leachate .....	5
2.3 Management of Municipal Solid Waste Leachate .....	10
2.4 The Beginning of Microbial Fuel Cells.....	11
2.5 Microbial Fuel Cell Technology.....	11
2.6 Microbiology.....	13
2.6.1 Bacterial Metabolism.....	13
2.6.2 Bacterial Metabolism in Microbial Fuel Cells.....	16
2.6.3 Electron Transfer.....	16
Artificial Mediators.....	17

Self-Produced Mediators.....	18
Direct Electron Transfer.....	19
2.6.4 Microbial Community.....	20
2.7 Mass transfer and Kinetics.....	22
2.8 Voltage and Power Generation.....	23
2.9 Factors that Affect the Cell Voltage.....	26
2.10 Designing an MFC.....	28
2.10.1 Materials.....	28
Anode.....	28
Cathode.....	32
Membranes.....	35
Catholyte.....	37
2.10.2 Architecture.....	37
Two Chamber MFC.....	38
Single Chamber MFC.....	39
Plate MFC.....	41
Tubular MFC.....	42
Microbial Fuel Cells in Series.....	43
2.11 Types of Substrates used in Microbial Fuel Cells.....	44
2.12 Other Types of Microbial Fuel Cells.....	46

2.12.1	Hydrogen Production .....	46
2.12.2	Sediment MFCs .....	47
2.12.3	MFCs for Bioremediation .....	47
CHAPTER 3.....		48
3.1	Overview.....	48
3.2	Materials .....	49
3.3.1	Landfill Leachate.....	49
3.2.1	Single Chamber Designs .....	50
	Square MFC.....	50
	Cylinder MFC.....	52
	Larger Scale MFC.....	54
3.3	Methods.....	56
3.3.2	MFC Operation.....	56
3.3.3	Electrical Measurements.....	58
	Data Acquisition.....	58
	Power Density Curve.....	58
3.3.4	Leachate Characterization .....	58
	Probe Readings.....	59
	COD.....	59
	TOC.....	61

Ammonia.....	61
Alkalinity.....	62
Nitrate, Nitrite, Sulfate, and Chloride.....	62
Total Phosphorus and Phosphate.....	62
Sulfide.....	63
Total Metals Analysis.....	63
3.2.2 Microbiology.....	65
CHAPTER 4.....	67
4.1 Introduction.....	67
4.2 Power Production.....	67
4.2.1 Square MFC.....	67
4.2.2 Circle MFC.....	74
4.2.3 Larger Scale MFC.....	80
4.2.4 Power Density and Coulombic Efficiency.....	82
4.3 Leachate Characterization.....	89
4.3.1 Square MFC.....	89
4.3.2 Circle MFC.....	93
4.3.3 Larger Scale MFC.....	97
4.3.4 Leachate Characterization Analysis.....	99
pH.....	102



Conductivity.....	103
Dissolved Oxygen. ....	104
Oxidation Reduction Potential (ORP).....	105
COD, BOD, and TOC.....	107
Alkalinity. ....	109
Ammonia. ....	109
Chloride.....	111
Nitrate/Nitrite. ....	113
Phosphate/Total Phosphorus . ....	113
Sulfate/Sulfide. ....	116
Cations. ....	117
4.4 Microbial Analysis .....	119
CHAPTER 5.....	124
REFERENCES.....	127
APPENDICES.....	135

## LIST OF TABLES

Table 2.1	Composition of landfill leachate (Kjeldsen et al. 2002).....	9
Table 4.1	Summary of voltage prod. for Square MFC, cycles 1a – 3a.....	71
Table 4.2	Summary of voltage prod. for Square MFC, cycles 4b – 7b.....	72
Table 4.3	Summary of voltage prod. for Circle MFC, cycles 1b-4b.....	75
Table 4.4	Summary of voltage prod. for Circle MFC, cycles 1c-3c .....	78
Table 4.5	Summary of voltage prod. for Larger Scale MFC, cycles 1c-2c .....	82
Table 4.6	Comparison of results with values from the literature.....	87
Table 4.7	Coulombic efficiencies for all MFC designs and cycles.....	89
Table 4.8	Leachate charact., Square MFC, cycle 1a (1/10/08 – 1/28/08) .....	90
Table 4.9	Leachate charact., Square MFC, cycle 2a (1/31/08 – 2/11/08) .....	90
Table 4.10	Leachate charact., Square MFC, cycle 3a (2/11/08 – 2/22/08) .....	91
Table 4.11	Leachate charact., Square MFC, cycle 4b (8/7/08 – 8/18/08) .....	91
Table 4.12	Leachate charact., Square MFC, cycle 5b (8/18/08 – 9/5/08) .....	92
Table 4.13	Leachate charact., Square MFC, cycle 6b (9/16/08–9/24/08) .....	92
Table 4.14	Leachate charact., Square MFC, cycle 7b (9/24/08–10/3/08) .....	93
Table 4.15	Leachate charact., Circle MFC, cycle 1b (8/7/08 – 8/23/08) .....	94
Table 4.16	Leachate charact., Circle MFC, cycle 2b (8/23/08 – 9/9/08) .....	95
Table 4.17	Leachate charact., Circle MFC, cycle 3b (9/15/08 –9/24/08) .....	95
Table 4.18	Leachate charact., Circle MFC, cycle 4b (9/24/08 –10/3/08) .....	96
Table 4.19	Leachate charact., Circle MFC, cycle 1c (1/16/09 – 2/2/09).....	96
Table 4.20	Leachate charact., Circle MFC, cycle 2c (2/2/09 – 2/16/09).....	97
Table 4.21	Leachate charact., Circle MFC, cycle 3c (2/16/09 –3/12/09).....	97

Table 4.22	Leachate charact., Larger Scale MFC, cycle 1c (2/2/09–2/16/09)....	98
Table 4.23	Leachate charact., Larger Scale MFC, cycle 2c (2/16/09 – 4/9/09)..	99
Table 4.24	Percent difference for Square MFC, cycles 1-3 a.....	100
Table 4.25	Percent difference for Square MFC, cycles 4-7 b.....	100
Table 4.26	Percent difference for Circle MFC, cycles 1-4 b.....	101
Table 4.27	Percent difference for Circle MFC, cycles 1-3 c.....	101
Table 4.28	Percent difference for Larger Scale MFC, cycles 1-2 c.....	102
Table 4.29	Cation conc. for influent and effluent leachate of Square MFC .....	118
Table 4.30	Cation conc. for influent and effluent leachate of Circle MFC .....	118

## LIST OF FIGURES

Figure 2.1 Reduction Reactions (Snoeyink and Jenkins 1980).....	8
Figure 2.2 Schematic of a basic microbial fuel cell (not to scale).....	13
Figure 3.1 Illustration of graphite anode used in Square MFC.....	50
Figure 3.2 Picture of Square MFC .....	51
Figure 3.3 Electrical breadboard with wiring used in MFC operations .....	52
Figure 3.4 Illustration of graphite anode used in Circle MFC (not to scale).....	53
Figure 3.5 Picture of Circle MFC.....	54
Figure 3.6 Illustration of graphite anode used in Larger Scale MFC .....	55
Figure 3.7 Picture of Larger Scale MFC.....	56
Figure 4.1 Square MFC, cycle 1a, voltage vs. time (1/10/08 – 1/28/08) .....	68
Figure 4.2 Square MFC, cycle 2a, voltage vs. time (1/31/08 – 2/11/08) .....	69
Figure 4.3 Square MFC, cycle 3a, voltage vs. time (2/11/08 – 2/22/08) .....	69
Figure 4.4 Square MFC, cycle 4b, voltage vs. time (8/07/08 – 8/18/08) .....	72
Figure 4.5 Square MFC, cycle 5b, voltage vs. time (8/18/08 – 9/05/08) .....	73
Figure 4.6 Square MFC, cycle 6b, voltage vs. time (9/16/08 – 9/24/08) .....	73
Figure 4.7 Square MFC, cycle 7b, voltage vs. time (9/24/08 – 10/03/08) .....	74
Figure 4.8 Circle MFC, cycle 1b, voltage vs. time (8/07/08 – 8/23/08).....	76
Figure 4.9 Circle MFC, cycle 2b, voltage vs. time (8/23/08 – 9/9/08).....	76
Figure 4.10 Circle MFC, cycle 3b, voltage vs. time (9/15/08 – 9/24/08).....	77
Figure 4.11 Circle MFC, cycle 4b, voltage vs. time (9/24/08 – 10/03/08).....	77
Figure 4.12 Circle MFC, cycle 1c, voltage vs. time (1/16/09 – 2/02/09) .....	79
Figure 4.13 Circle MFC, cycle 2c, voltage vs. time (2/02/09 – 2/16/09).....	79

Figure 4.14	Circle MFC, cycle 3c, voltage vs. time (2/16/09 – 3/12/09)	80
Figure 4.15	Larger Scale MFC, cycle 1c, voltage vs. time (2/02/09 – 2/16/09)	81
Figure 4.16	Larger Scale MFC, cycle 2c, voltage vs. time (2/16/09 – 4/09/09)	82
Figure 4.17	Power density and polarization curve (1) for Circle MFC	84
Figure 4.18	Power density and polarization curve (2) for Circle MFC	85
Figure 4.19	Power density and polarization curve for Square MFC	85
Figure 4.20	Percent increase of pH for all cycles of MFC designs	103
Figure 4.21	DO concentration of inf. and effluent leachate for all cycles	105
Figure 4.22	Cycle time and inf. leachate ORP (Square & Circle MFCs)	106
Figure 4.23	COD, BOD, and TOC removals for Circle & Large Scale MFCs	108
Figure 4.24	Ammonia removal for all MFC designs	111
Figure 4.25	Chloride increase for all MFC designs	113
Figure 4.26	% Difference of TP and ORP for Square and Circle MFC	115
Figure 4.27	Comparison of microbial communities (Major Phyla)	121
Figure 4.28	Microbial community analysis, Non-Producing,	121
Figure 4.29	Microbial community analysis, Pre-MFC,	122
Figure 4.30	Microbial community analysis, Post-MFC,	122
Figure 4.31	Microbial community analysis, Biofilm of MFC	123

## **ABSTRACT**

### **ELECTRICITY PRODUCTION FROM THE MANAGEMENT OF MUNICIPAL SOLID WASTE LEACHATE WITH MICROBIAL FUEL CELLS**

by,

Lisa L. Damiano

University of New Hampshire, May, 2009

Microbial fuel cells are a new technology that can be used for treating landfill leachate and simultaneously producing electricity. Three designs were tested in batch cycles using landfill leachate (908-3200 mg/L COD): a Square (995 mL), Circle (934 mL) and a Large Scale MFC (18.3 L). A total of seven cycles were completed for each the Square MFC and Circle MFC and two cycles for the Larger Scale MFC. Maximum power densities of 24-31 mW/m<sup>2</sup> (653 mW/m<sup>3</sup>-824 mW/m<sup>3</sup>) were achieved using the Circle MFC and a maximum voltage of 635 mV was produced using the Larger Scale MFC. BOD, TOC, and Ammonia were removed at 50-72%, 17-53 %, and 7-69%, respectively. The Larger Scale MFC achieved 47-86% BOD removal, 51% TOC removal and 60% ammonia reduction while operating over 52 days. These results demonstrate MFCs can be used to treat landfill leachate with the benefit of power generation.

## **CHAPTER 1**

### **INTRODUCTION**

#### **1.1 Background**

In 2007, 137.2 million tons of waste were produced and sent to landfills in the United States. While this number has been reduced by 5 million tons since 1990, landfills are expected to remain the dominant form of municipal solid waste management in the future (USEPA 2007). Microbial fuel cell (MFC) technology can benefit both the solid waste industry and contribute to reducing greenhouse gas emissions and dependence on fossil fuels. In a microbial fuel cell, organic matter is oxidized (degraded) by microorganisms and electrons are produced. These electrons flow through wiring and a resistor to produce electrical current and therefore direct electricity (Logan, 2008). This system has no energy input, yet can degrade organic matter and produce an energy output.

There is a growing need for alternative forms of energy as well as processes that reduce energy use in the global community. The climate of the world has increased in temperature and is continuing to do so with every passing day (IPCC 2007). Between 1970 and 2004, global green house gas emissions increased 70%, with carbon dioxide being the greatest anthropologic greenhouse gas (IPCC 2007). This steady increase in greenhouse gas levels, along with the depletion of the world's fossil fuel resources, requires the research and utilization

of technologies that can limit both the use of fossil fuels and the production of greenhouse gases.

MFCs can be used to treat landfill leachate while reducing energy needs and producing an alternative form of energy. Landfill leachate is liquid that infiltrates the landfill system or is produced by the waste within the system. Leachate must be collected and managed to protect the surrounding environment. Leachate can also be re-circulated in an operating landfill to manage the leachate as well as increase biodegradation of waste within the landfill and increase landfill gas production. While many organic constituents in the leachate can be treated through the biological processes within the landfill, ammonia can accumulate and resist treatment (Barlaz et al 2002). Ammonia can be toxic to bacteria and other organisms and inhibit accelerated biodegradation that can result from recirculation. MFCs could be used as a pre-treatment for the leachate prior to recirculation to lower concentrations of constituents, while producing electricity and limiting energy inputs into the system.

In the early 1990s, the United States Environmental Protection Agency (USEPA) began enforcing regulations for the disposal of nonhazardous waste in landfills under the Resource Conservation and Recovery Act (Subtitle D). As part of these regulations, a closed landfill must be monitored and maintained for the 'post-closure monitoring period' of 30 years, or a site-specific longer time period. Monitoring includes collection and treatment of leachate, monitoring of the groundwater, landfill gas monitoring, and inspection and maintenance of the final cover (USEPA 1991). Termination of monitoring after 30 years will be



agreed upon if the landfill is considered stable and no longer a harm to the environment without monitoring.

Landfill leachate will become a major factor in the determined stability of a landfill and whether management of the leachate prior to release will be needed (Barlaz et al. 2002). Dissolved organic matter, ammonia, and nutrients can pose environmental hazards if leachate is released into surface water or groundwater at increased levels with no management. From 1991 to 2007, the number of open landfills decreased from 5,812 to 1,754 (Municipal 2007). These numbers forecast that in the coming years, regulators will have many decisions to make on whether to terminate or continue monitoring landfills past the 30 year time period. While the owners of landfills cannot be expected to fund monitoring for infinite time, landfills must also remain safe to the environment after monitoring/treatment of leachate and landfill gas has been terminated. The MFC technology could be considered as a low operations and maintenance option for these situations that require management of leachate with minimal resources.

## **1.2 Objective and Scope**

Microbial fuel cells were researched utilizing landfill leachate as the substrate. Leachate characterization was completed to evaluate treatment for a number of constituents; electricity and power production were also monitored. At the inception of this research, there was no other published research utilizing an MFC of the design used for this research, with unaltered landfill leachate, and no outside inoculation of bacteria. This research provides the first in-depth analysis

of leachate constituents and the treatment that will occur within an MFC system.

The specific goals of this research were to;

- 1) Design and operate a single chamber MFC (previously developed by UNH for cow manure) to evaluate how the characteristics of the leachate change while producing electricity.
- 2) Determine the power density and efficiency of using landfill leachate as a substrate in a single chamber MFC.
- 3) Validate the hypothesis that no outside inoculation of anaerobic bacteria will be needed when using landfill leachate.
- 4) Create a larger scale MFC system that will help begin to evaluate the applicability of this technology.

## **CHAPTER 2**

### **LITERATURE REVIEW**

#### **2.1 Introduction**

This chapter includes historical research conducted that is relevant to microbial fuel cells (MFCs) and landfill leachate. It provides an overview of the generation and characteristics of landfill leachate, as well as the microbiology, architecture, voltage and power generation of MFCs.

#### **2.2 Composition and Formation of Municipal Solid Waste Leachate**

Modern sanitary landfills are engineered facilities used for the deposition of wastes and are designed to minimize the hazards to public health and safety. A basic landfill control system involves a liner, landfill leachate collection and extraction system, a landfill gas collection and extraction system, and both daily and final cover layers. Landfill liners and leachate collection systems are used to minimize the infiltration of leachate into soils below the landfill; limiting the potential for groundwater contamination. Leachate is liquid that is both released and produced from the waste during compaction and degradation in a landfill. Outside sources such as groundwater infiltration, precipitation, and/or surface drainage into the landfill also contribute to leachate volume within the system. Liquids percolate through the waste and both biological and chemical components are leached into the leachate (Tchobanoglous, Theisen, and Vigil 1993).

Every landfill is designed specifically for its location and the type of waste that is accepted. However, because of the organic content and compaction of waste within the structure, all landfills are anaerobic systems. This creates some similarities in leachate composition, although chemical composition of leachate will vary depending on the age of the landfill (Kjeldsen et al. 2002; Tchobanoglous, Theisen, and Vigil 1993).

There are four main categories of compounds in MSW landfill leachate; dissolved organic matter, inorganic macrocomponents, heavy metals, and xenobiotic compounds. Dissolved organic matter is measured by Chemical Oxygen Demand (COD), Total Organic Carbon (TOC), volatile fatty acids or other humic-like compounds. Calcium, magnesium, sodium, potassium, ammonium, iron, manganese, chloride, sulfate, and hydrogen carbonate are all considered inorganic macrocomponents. Common heavy metals that will be found in leachate are cadmium, chromium, copper, lead, nickel, and zinc. Xenobiotic organic compounds refer to household or industrial chemicals such as aromatic hydrocarbons, phenols, chlorinated aliphatics, pesticides, and plastizers. This category of pollutants is generally present in low concentrations; usually less than 1 mg/L. Other compounds found in leachate, such as borate, sulfide, barium, lithium, mercury, cobalt, arsenate, and selenate, are also found at low concentrations and are of less importance (Kjeldsen et al. 2002).

It is not uncommon for leachate to have low levels of nitrite and nitrate and have all nitrogen as ammonia in the system due to the biological process of the landfill. This can be explained by the basics of the nitrogen cycle in which  $\text{NH}_4^+$

is oxidized to  $\text{NO}_2^-$  followed by  $\text{NO}_3^-$  (nitrification),  $\text{NO}_3^-$  is reduced to  $\text{NO}_2^-$  to  $\text{NH}_4^+$  (nitrate reduction); and  $\text{NO}_3^-$  is can also be reduced to  $\text{N}_{2(g)}$  (denitrification). Nitrogen gas can then be reduced to  $\text{NH}_4^+$  and  $\text{NH}_4^+$  can be incorporate or released from organic matter (amination or ammonification).  $\text{NH}_4^+$ ,  $\text{NO}_2^-$ , and  $\text{NO}_3^-$  are all easily and quickly inter-convertible by nitrification and nitrate reduction (Snoeyink and Jenkins 1980).

For microorganisms to facilitate nitrification, nitrate reduction, and denitrification, it must be energetically favorable (as discussed in section 2.6.1). Typical electron acceptance reactions for aerobic and anaerobic systems are listed in Figure 2.1, from highest energy gain for the bacteria to least. In a landfill, oxygen will be used up first in aerobic respiration, however landfills are anaerobic systems, thus denitrification and nitrate reduction will then take place. Fermentation and sulfate reduction can also occur once this is energy favorable. Lastly, methane fermentation will take place. This is where many landfills exist, for they are actively producing landfill gas containing methane. This means that the more energy favorable reactions of denitrification and nitrate reduction would have occurred already and is the reason that little or no nitrate/nitrite is found in landfill leachate. Nitrogen gas is present in landfill gas at about 2-5%, reiterating the idea that denitrification is occurring within landfills (Tchobanoglous, Theisen, and Vigil, 1993).

1. $O_2 + 4H^+ + 4e^- \rightarrow 2H_2O$	(Aerobic Respiration)
2. $2NO_3^- + 12H^+ + 10e^- \rightarrow N_{2(g)} + 6H_2O$	(Denitrification)
3. $NO_3^- + 10H^+ + 8e^- \rightarrow NH_4^+ + 3H_2O$	(Nitrate Reduction)
4. $CH_2O + 2H^+ + 2e^- \rightarrow CH_3OH$	(Fermentation)
5. $SO_4^{2-} + 9H^+ + 8e^- \rightarrow HS^- + 4H_2O$	(Sulfate Reduction)
6. $CO_{2(g)} + 8H^+ + 8e^- \rightarrow CH_{4(g)} + 2H_2O$	(Methane Fermentation)

Figure 2.1 Reduction Reactions (Snoeyink and Jenkins 1980)

Table 2.1 summarizes general leachate parameter ranges, compiled by Kjeldsen et al. (2002). The table is applicable to newer landfills and is a compilation of 14 different studies from the years 1976-1997 (Kjeldsen et al. 2002). The ranges for many constituents are large, illustrating the vast differences that can be found between leachates from a single landfill as well as from multiple locations. The flow paths of leachate within the landfill are constantly changing, thus concentrations and types of constituents in the leachate can constantly change as well.

Table 2.1 Composition of landfill leachate (Kjeldsen et al. 2002)

Parameter	Range
(Values in mg/L unless otherwise noted)	
pH	4.5-9
Specific Conductivity ( $\mu\text{S}/\text{cm}$ )	2500-35000
Total Solids	2000-60000
<i>Organic Matter</i>	
Total Organic Carbon (TOC)	30-29000
Biological Oxygen Demand (BOD <sub>5</sub> )	20-57000
Chemical Oxygen Demand (COD)	140-152000
BOD <sub>5</sub> /COD ratio	0.02-0.80
Organic Nitrogen	14-2500
<i>Inorganic Macrocomponents</i>	
Total Phosphorous	0.1-23
Chloride	150-4500
Sulphate	8-7750
Hydrogen bicarbonate	610-7320
Sodium	70-7700
Potassium	50-3700
Ammonium-N	50-2200
Calcium	10-7200
Magnesium	30-15000
Iron	3-5500
Manganese	0.03-1400
Silica	4-70
<i>Heavy Metals</i>	
Arsenic	0.01-1
Cadmium	0.0001-0.40
Chromium	0.02-1.5
Cobalt	0.005-1.50
Copper	0.005-10
Lead	0.001-5
Mercury	0.00005-0.16
Nickel	0.015-13
Zinc	0.03-1000

### **2.3 Management of Municipal Solid Waste Leachate**

There are four categories of management practices for landfill leachate; recycling back into the landfill, evaporation, treatment followed by disposal, and discharge to a municipal wastewater collection system. Re-circulating the leachate back into the landfill can increase landfill gas production, which is a valuable energy source (Tchobanoglous, Theisen, and Vigil 1993). The landfill can also help to treat the leachate through chemical and biological processes.

Treatment of leachate can be one or a combination of biological, chemical, and physical processes. Biological treatment removes organics and nitrogen through processes such as activated sludge, trickling filters, and nitrification/denitrification. Chemical processes are used to control pH, precipitate metals, and remove some organics by oxidation and wet air oxidation. Suspended matter can be removed by the physical processes of sedimentation and filtration. Adsorption can be used to remove organics, while air and steam stripping can remove volatile organics. Ion exchange can also be used to remove dissolved inorganics (Tchobanoglous, Theisen, and Vigil 1993). These treatment technologies can be used to treat leachate for discharge (e.g. into surface waters), or as pre-treatment prior to transport to a municipal wastewater treatment facility for further treatment. Some wastewater treatment facilities may have the capabilities and be willing to accept the leachate with no treatment; however this can often be more expensive. All of these management options for leachate treatment, except for leachate recirculation, require energy input and will cost the landfill operation and maintenance fees with no additional benefit.



## **2.4 The Beginning of Microbial Fuel Cells**

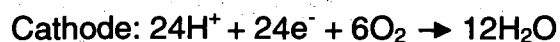
Microbial Fuel Cells harness the conversion of bacterial energy to electrical energy. By using electrodes, electrons from bacteria can be collected and used to produce electrical current through wiring and a resistor. It is accepted that in 1911, M.C. Potter was the first person to observe the electrical current that can be produced by bacteria (Potter 1911). There was very little interest or advances made in the technology from 1911-1967. The first patent to describe microbial fuel cell technology was issued to John Davis in 1967 (Biffinger and Ringeisen 2008). It was not until the 1990's that research truly began on microbial fuel cell technology and possible applications. Since 1967, there have been very few patents issued, most being given in the 2000's. The field has chosen to publish research, methods, and designs in scientific journals rather than apply for a large number of patents (Biffinger and Ringeisen 2008).

## **2.5 Microbial Fuel Cell Technology**

In a microbial fuel cell (MFC), organic matter is oxidized (degraded) by microorganisms and electrons are produced. The electrons are then transferred to a terminal electron acceptor (TEA) which is reduced by the electrons. TEA's such as oxygen, nitrate, and sulfate can diffuse into the cell and accept electrons to form new products that can then leave the cell. However, some bacteria can transfer their electrons outside the cell (exogenously) to the awaiting TEA. It is these bacteria that can produce power within an MFC system (Logan, 2008).

Figure 2.2 illustrates a basic microbial fuel cell system in which there is an anode and cathode chamber, separated by a membrane permeable to protons. The anode compartment is an anaerobic region (i.e. no oxygen) where the anaerobic bacteria are located. The cathode compartment is an aerobic region (i.e. oxygen is present). The membrane separation helps to maintain these conditions for each compartment, yet allows a charge transfer between the electrodes. Electrodes are placed in each chamber to facilitate the electron transfer process. Electrons and protons are produced through the oxidation of organic matter. The electrons are transferred to the anode electrode, in the anode compartment, and travel through a wire and resistor to the cathode electrode, where the wire is connected. Here, the electrons join with the protons which have diffused through the membrane from the anode compartment, and oxygen to form water. A catalyst at the cathode or a catholyte solution must be used to facilitate this reaction. The by-products of this reaction are carbon dioxide, from the decomposition of the organic matter, and small amounts of water at the cathode.

Using glucose as an example of an organic substrate; 24 electrons and 24 protons are released in the anode chamber. These protons and electrons both travel to the cathode chamber where 6 molecules of oxygen are needed to create 12 water molecules. Six carbon dioxide molecules are created at the anode.



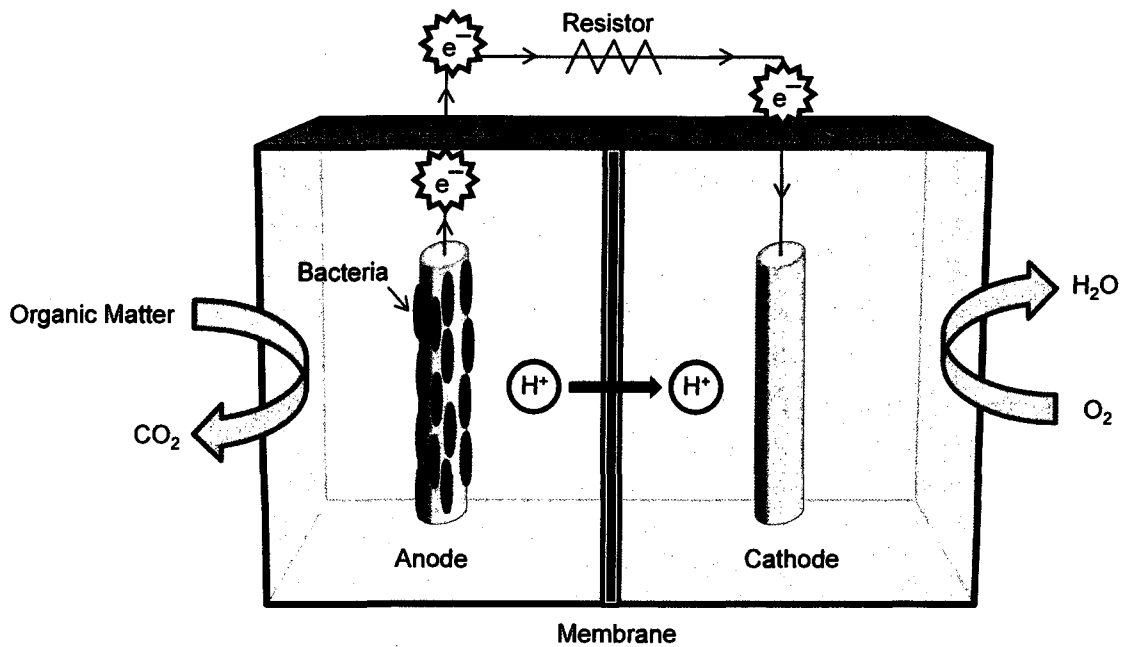


Figure 2.2 Schematic of a basic microbial fuel cell (not to scale)

## 2.6 Microbiology

### 2.6.1 Bacterial Metabolism

Bacteria are unicellular microorganisms characterized by the lack of a true nucleus. The foundation for life processes is the ability to utilize energy in an organized fashion, referred to as metabolism (Chapelle 2001). A cell must extract energy from organic compounds, then both store and use the energy to grow and maintain necessary functions. These energy transformations must follow the basic laws of thermodynamics.

The first law of thermodynamics states that energy can neither be created nor destroyed (Halliday, Resnick, and Walker 2003). For bacteria, this governs that there is a set amount of energy available in organic compounds and only this amount is available for use. The second law of thermodynamics states that in

closed, irreversible systems, entropy will always increase (Halliday, Resnick, and Walker 2003). The energy available in a system can be broken up into useable energy and unavailable energy. The unavailable energy goes to increasing the entropy of a system and is lost as heat. The amount of useful energy that is taken up or released during a reaction is called the Gibbs free energy change of the reaction ( $\Delta G$ ). If a reaction is energy-releasing, it has a negative  $\Delta G$ , while an energy-consuming reaction has a positive  $\Delta G$ . Bacteria combine both of these types of reactions into a system to operate cell functions. Intermediate reactants that temporarily store energy help join energy-releasing and consuming reactions so that it is possible to synthesize compounds that could otherwise not be created (Chapelle 2001).

Bacteria base the reactions that are chosen on what pathway will provide the highest energy gain. Depending on the terminal electron acceptor (TEA) present, two metabolic pathways can be used by the bacteria; respiration and fermentation (Schroder 2007). An electron acceptor is an inorganic compound that accepts electrons from bacteria and completes the oxidation of an organic substrate (Chapelle 2001). Respiration is a combination of the reduction of a TEA and the oxidation of an organic compound where the electrons are transferred through an electron transport chain to the final TEA. The higher the potential of the TEA, the higher the energy gain for the organism, thus the more favorable the reaction (Schroder 2007). The term potential refers to the tendency of the chemical species/solution/material to accept electrons. This can be related to Gibbs free energy by equation (2-1).

$$\Delta G^{\theta 1} = n F [E_{(\text{donor})}^{\theta 1} - E_{(\text{acceptor})}^{\theta 1}] \quad (2-1)$$

Where  $n$  is the number of electrons per reaction mole,  $F$  is Faraday's constant, and  $E^{\theta 1}$  is the standard biological potential of the electron donor and acceptor, respectively (Schroder 2007).

Aerobic respiration is the most energetically favorable pathway, however anaerobic respiration will be used when oxygen is not present (Schroder 2007). For this transfer of electrons to occur, an electron must first be moved through an electron transport chain within the cell; a mechanism that can also conserve energy by synthesizing ATP. Adenosine triphosphate (ATP) is the most important compound that living cells use for temporary storage of energy. The formation of this compound stores energy within a phosphate bond which can be liberated once the bond is broken. Nicotine adenine (NAD) is another intermediate compound for storing energy that can be reduced to NADH or oxidized to  $\text{NAD}^+$  (Chapelle 2001).

The electron transport system uses both hydrogen carriers and electron carriers (NADH). As the electron is transported through the transport chain, protons are transferred in and out of the cell. This transfer of protons causes a proton gradient between the inside and outside of the cell membrane which has potential energy associated with it. The cell is able to capture this energy through membrane-bound enzymes called ATP synthase complex. As protons diffuse through these enzymes, the potential energy is captured and stored

chemically as ATP. This process is called chemiosmosis. The final step in this process is for the electron to be transported to the TEA (Chapelle 2001).

### **2.6.2 Bacterial Metabolism in Microbial Fuel Cells**

Microbial fuel cells harness the extracellular electron transfer of anaerobic bacteria. Therefore, the anode compartment of an MFC must not contain oxygen (based upon Gibbs free energy, if oxygen is present at the anode, it is the more energy favorable TEA). Fermentation is an important anaerobic mechanism for degrading organic matter; however it is not a process that creates electricity in MFCs. Many electrons remain within fermentation products, not readily reacting with electrodes. Effective anaerobic oxidation must combine fermentation products with other constituents (e.g. long-chain fatty acids and aromatic compounds) to complete electron transfer to the electrode (Lovley 2006).

Because of the need for anaerobic bacteria, every MFC is inoculated initially. Generally, this inoculation comes from bacteria from a wastewater, sludge, or sediment. Bacteria from an MFC that has already been in operation can also be used for a new MFC (Logan 2008).

### **2.6.3 Electron Transfer**

Once electrons have left the cell, they must be transferred to an electrode to produce current. A natural world comparison of the transfer of electrons to an electrode is the transfer of electrons to  $\text{Fe}^{3+}$  oxides, for they are an insoluble, extracellular electron acceptor. Organic matter is oxidized while  $\text{Fe}^{3+}$  oxides are

reduced, similar to the process in an MFC. This process requires both fermentative and  $\text{Fe}^{3+}$  reducing microorganisms. (Lovley 2006).

In a microbial fuel cell there are three main mechanisms for microorganisms to transfer electrons to an exocellular electrode. The transfer can occur with the addition of artificial mediators, self-produced mediators, and/or direct contact with the electrode (Lovley 2006). Not all bacteria can accomplish this extracellular transfer; some can only use soluble compounds such as sulfate that diffuse through the cell membrane to receive electrons. The field of microbial fuel cell technology has termed bacteria that can directly transport electrons outside of the cell “exoelectrogens” (Logan 2008). These bacteria are essential to microbial fuel cell technology because without the exocellular electron transfer, no power could be produced.

#### Artificial Mediators.

Early in MFC research, the addition of artificial mediators was used to facilitate electron transfer. *Escherichia coli* is an example of a bacteria used in MFCs that required an artificial mediator (Park and Zeikus 2000). Artificial mediators can cross cell membranes and accept electrons, exiting the cell in a reduced form to transfer the electrons to the electrode (Lovley 2006). Examples of such artificial mediators are neutral red, iron chelates, various phenazines, 4-naphthoquinone, and thionine (Lovley 2006). These mediators posed a set of problems for MFC technology. Many mediators are toxic to humans and not easily disposed of. Mediators input more energy into the life cycle analysis of MFCs since they must be manufactured and replaced regularly. Lastly, it has not

been demonstrated that using artificial mediators will be able to sustain the bacteria within the MFC for extended periods of time due to a lack of available electrons for cell maintenance and growth. The artificial mediators remove more electrons than the natural transfer to a terminal electron acceptor would remove (Lovley 2006).

For these reasons as well as new discoveries, artificial mediators are no longer used by most researchers. Rabaey and other researchers proved that artificial exogenous mediators were not necessary in microbial fuel cells for electron transfer (Rabaey et al. 2004; Rabaey et al. 2005a). Self-produced mediators such as pyocyanin can shuttle electrons and produce electricity. This mechanism was first proposed as a mechanism for the electron transfer to  $\text{Fe}^{3+}$  (Rabaey et al. 2004).

#### Self-Produced Mediators.

It is unclear whether self-produced mediators, also called shuttles, are generated specifically for exocellular electron transfer or if they serve multiple purposes. These mediators are molecules that can be oxidized faster at the electrode, causing fewer overpotential losses, and assist in the transfer of electrons to the electron acceptor. It has been shown that mediators produced by one type of bacteria can be used by other species of bacteria and improve the electron transfer of the overall system (Rabaey et al. 2005a).

The major advantage of self-produced electron mediators is long-range interaction between the bacteria and anode. The microorganisms do not need to be in direct contact with the electrode for the transfer of electrons to occur. G.



*fermentans* displayed this ability while producing a thick extracellular matrix to reduce the possibility of losing the mediator to the bulk solution (Bond and Lovley 2005). *Shewanella oneidensis* was also shown to produce an electron shuttle while converting lactate to electricity in an MFC (Lanthier, Gregory, and Lovley 2007). A great deal of energy is used by a microorganism to biosynthesize an electron mediator, thus it must be used repeatedly to be considered energetically worthwhile for the cell. This spent energy can cause the mechanism to be at a competitive disadvantage; especially in a flowing system where the mediator could easily be lost to the bulk liquid (Lovely 2006).

#### Direct Electron Transfer.

Electron transfer can occur through direct contact between the microorganisms and the electrode or with the use of nanowires. Direct contact requires that the organisms have membrane bound electron transport protein relays, such as c-type cytochromes, to facilitate the transfer of electrons out of the cell (Schroder 2007). However, this transfer allows for only one layer of bacteria in direct contact with the electrode, to transfer electrons. Nanowires are conductive appendages that are hypothesized to carry electrons from the bacterial cell to the surface of the anode (Gorby et al. 2006). These appendages allow for multiple layers of bacteria on the anode to transfer electrons as well as interspecies transfer and transfer from the bulk liquid to the anode (Logan 2008).

The bacteria *Shewanella oneidensis* MR-1 was found to have nanowires with heights of 5-10 nm. The photosynthetic cyanobacterium, *Synechocystis* strain PCC 6803 and a thermophilic fermentative bacterium *Pelotomaculum*

*thermopropionicum* were also found to utilize nanowires (Gorby et al. 2006). Similar conductive appendages have been observed often in research employing *Geobacter sulfurreducens*. While nanowires are not required for electron transfer to the anode, a lack of nanowires resulted in more than a 70% reduction in current production (Reguera et al. 2006). It was also found that when nanowire production was inhibited, 60% of the cells attached to the anode of an MFC were dead. The only living population was in direct contact with the anode (Reguera et al. 2006). Bacteria can attach to the anode of the MFC and form a biofilm, which is a multi-layer community of bacteria that can theoretically grow to any thickness. Nanowires can connect cells of the outer layers of a biofilm to the inside of the system and facilitate electron transfer to the anode (Logan 2008). This can allow thicker biofilms to develop while providing increased current production from the MFC system.

#### **2.6.4 Microbial Community**

The microbial fuel cell environment will select a microbial community that will self-mediate electron transfer. Bacteria that were isolated from a plate MFC were mostly facultative anaerobic bacteria that accumulated fewer organic acids and were more electrochemically active. *Alcaligenes faecalis*, *Enterococcus gallinarum*, and *Pseudomonas aeruginosa* have all been found to participate in MFC current production (Rabaey et al. 2004). *Shewanella* and *Geobacter* are also commonly found within MFC biofilms (Logan and Regan 2006). There are no specific trends to the major species found within MFC microbial communities

however common bacteria that are reported are proteobacteria (alpha-, beta-, delta-, and gamma-), firmicutes, and bacteroidetes (Logan and Regan 2006; Logan 2008). While in some cases, alpha-proteobacteria dominate the community; other times gamma- or beta- dominate, or there was no dominate type (Logan 2008). These categories are broad classifications of bacteria that encompass many different types of bacteria.

Firmicutes are a phylum of bacteria that can be iron reducing while bacteroidetes are a phylum of mostly anaerobic bacteria. Some bacteroidetes are hydrogen and formate requiring microorganisms. Proteobacteria are a phylum of bacteria that are divided into classes termed alpha-, beta-, gamma- and delta-. These broad categories include aerobic and anaerobic bacteria as well as fermentative bacteria and pathogens (Garrity et al. 2005).

There is an ongoing debate in MFC literature as to the benefits of using a mixed community of bacteria versus a single strain of bacteria that is known to have efficient extracellular electron transfer (Logan 2008). Data exists for each side of the argument and a consensus has yet to be reached as to which will produce greater power. Microbiologists in the field have started using genetic engineering to create an ideal exoelectrogen strain of bacteria (Logan 2008). Both *Rhodopseudomonas palustris* DX-1 and *G. sulfureducens* were recently shown to produce larger voltages than mixed cultures of bacteria in MFCs (Xing et al. 2008; Nevin et al. 2008).

## **2.7 Mass transfer and Kinetics**

The bacteria that are transferring electrons exocellularly can attach and grow on the electrode forming a biofilm. These biofilms are made up of numerous microorganisms and can theoretically grow to any thickness; however other factors usually limit growth. Ramasamy et al. (2008) found that initial biofilm growth had a beneficial effect on the kinetics of the bio-electrochemical system and decreased activation losses (discussed in section 2.9 ) (Ramasamy et al. 2008). Biofilms in microbial fuel cells display unique characteristics. For example, in a wastewater environment, the active bacteria are located where the biofilm interacts with the surrounding fluid. In an MFC, the active bacteria are not at this interface but within the biofilm itself; interacting with the electrode (Logan 2008). While this placement is beneficial to the transfer of electrons, it also causes other challenges.

As these biofilms become thicker, mass transfer of nutrients and substrate to the microorganisms attached to the electrode can become the limiting factor in power production rather than the rate of substrate oxidation by the bacteria. Mass transfer of waste products out of the biofilm can also be an important factor in bacterial health and thus power production. If the bulk liquid is not mixed and is a stationary system, mass transfer of the substrate to the biofilm itself could be the limiting factor also (Logan 2008).

## 2.8 Voltage and Power Generation

Voltage generation in a microbial fuel cell can be complicated to predict for it is dependent on the activities of living organisms. However voltage or current can be calculated by equation (2-2) if the cell potential (voltage) E or the current (I) are measured and the external resistance of the system, R, is known.

$$E = I * R \quad (2-2)$$

Electricity can only be generated in a microbial fuel cell if the overall reaction is thermodynamically favorable (Logan et al. 2006). Gibbs free energy, explained in section 2.6.1, can be used to determine the maximum amount of work that can be obtained from this reaction by the equation,

$$\Delta G_r = \Delta G_r^0 + RT \ln ( II ) \quad (2-3)$$

Where  $\Delta G_r$  is the Gibbs free energy for the specific conditions,  $\Delta G_r^0$  is the Gibbs free energy under standard conditions (298.15 K, 1 bar pressure, and 1 M concentration for all species), R is the universal gas constant, T is the temperature in Kelvin, and II is a reaction quotient of the activities of the products divided by the activities of the reactants (Logan et al. 2006; Oldham and Myland 1994). This equation can be written in terms of the cell voltage, also called the electromotive force,  $E_{emf}$  for standard conditions where II = 1;

$$E_{emf}^0 = - \frac{\Delta G_r^0}{nF} \quad (2-4)$$

$$E_{emf} = E_{emf}^0 - \frac{RT}{nF} \ln II \quad (2-5)$$

Where  $E_{emf}^0$  is the standard cell electromotive force and  $n$  is the number of electrons per reaction mole. Values of standard cell electromotive forces can be found in various textbooks and resources (Logan et al. 2006; Logan 2008; Oldham and Myland 1994).

The total cell potential can be calculated using the half cell reactions that are occurring at the anode and cathode of the microbial fuel cell.  $E_{emf}$  can be calculated for the anode ( $E_{an}$ ) and cathode ( $E_{cat}$ ) using equation (2-5), resulting in equation (2-6) for the total cell potential. This equation can only be used if the anode and cathode are running at the same pH (Logan et al. 2006; Logan 2008).

$$E_{emf} = E_{cat} - E_{an} \quad (2-6)$$

Cell voltage is recorded during all microbial fuel cell testing because current can be difficult to measure. Current can be calculated from equation (2-2) with a known external resistance. Power is a common way for researchers to report voltage data and is calculated by equation (2-7) (Logan 2008).

$$P = \frac{E_{MFC}^2}{R_{ext}} \quad (2-7)$$

Where  $E_{MFC}$  is the voltage recorded from the microbial fuel cell. Because of the variation in MFC system architectures and materials, researches normalize power when reporting data. It is common to normalize based upon the anode (an) or cathode (cat) surface area (Equation (2-8)) or upon the volume (v) of the microbial fuel cell anode compartment (Equation (2-9)).

$$P_{an/cat} = \frac{E_{MFC}^2}{A_{an/cat} R_{ext}} \quad (2-8)$$

$$P_v = \frac{E_{MFC}^2}{v R_{ext}} \quad (2-9)$$

When reporting results, the coulombic efficiency of the system is an important calculated value to describe overall efficiency of the MFC. The goal of MFC technology is to utilize as many electrons as possible for current production. Coulombic efficiency is the fraction of electrons that are recovered as current versus the electrons that were in the starting substrate (organic matter). For a fed batch system, this fraction creates the equation,

$$C_E = \frac{M_s \int_0^{t_b} I dt}{F b_{es} v_{an} \Delta c} \quad (2-10)$$

Where  $M_s$  is the molecular weight of the substrate,  $I$  is the current,  $F$  is Faraday's constant (96,500 C/mole<sup>-</sup>),  $b_{es}$  is the moles of electrons removed through oxidation,  $v_{An}$  is the volume of the anode compartment liquid, and  $\Delta c$  is the substrate concentration change over the batch cycle (Logan 2008). This equation

can be altered for more complex substrates where COD is used as the measure of substrate concentration and an average current value over the cycle is used.

$$C_E = \frac{8 \cdot I \cdot t}{F V_{An} \Delta \text{COD}} \quad (2-11)$$

Where 8 is a constant used for COD ( $M_s$  is equal to 32 (molecular weight of oxygen) and  $b_{es}$  equals 4 (the number of electrons exchanged per mole of oxygen)) and  $\Delta \text{COD}$  is the change in COD concentration over time  $t$  (Logan 2008).

## **2.9 Factors that Affect the Cell Voltage**

Based upon the voltages which can be calculated from the equations of section 2.8, the maximum cell voltage for an optimum MFC using an air cathode and a set substrate of acetate is 1.1 V. However, this theoretical value has never been reached in the laboratory setting. This is because of the overall internal resistance of the system; which is made up of overpotentials and ohmic losses. The overpotentials of the system can be the result of three main types of losses; activation losses, bacterial metabolism losses and mass transfer losses. Activation losses are caused by energy lost as heat in the initiation of reactions as well as in the transfer of electrons. These losses can be reduced through the use of improved catalysts at the cathode (section 2.10.2), using different types of bacteria, or improving the overall electron transfer mechanisms of the system. The losses associated with bacterial metabolism are due to the loss of energy in



utilizing substrate oxidation for energy (Logan 2008). There is little that can be changed within the MFC system to reduce these losses.

Mass transfer losses are the result of insufficient movement of reactants or products within the bulk liquid or biofilm of the system. These losses were examined in section 2.7. Research has been published that shows the flux within the biofilm at the anode can negatively affect voltage generation. Protons can accumulate within the biofilm and cause a localized increase in pH at the anode which will affect the kinetics of the system (Kim et al. 2007; Torres, Marcus, Rittmann 2008). Even when the bulk liquid pH is buffered and remains neutral during operation, the pH at the anode can still be lowered substantially (Torres, Marcus, and Rittmann 2008). In a system where high substrate concentrations are present, this lack of proton transport away from the anode can cause low current generation.

Ohmic losses are a result of the MFC architecture and the resistance that arises from inefficiencies in the system. Resistance of proton movement through the solution, electrode, connecting wire or other internal connections all contribute to ohmic losses. These losses can be improved by optimizing electrode spacing, membrane materials, connections, and the conductivity of the solution (Logan 2008). A delicate balance between optimizing conditions to reduce these losses and no addition of new problems must be reached. For example, while electrodes need to be in close proximity to each other, each requires different operation conditions (aerobic/anaerobic) thus space between them is necessary. It has been shown recently that the cathode and catholyte of an MFC contribute

around 50% of the internal resistance of the system while the anode only accounts for about 5% (Fan Sharbrough, and Liu 2008). This suggests that it is the ohmic losses of the cathode that contributes to the reduction in power production more than any other factor.

## **2.10 Designing an MFC**

There are many inherent challenges in designing an efficient microbial fuel cell. Construction, materials, and the architecture must maximize power generation, yet minimize cost and be applicable to real world and future use of the technology. There are three major elements of an MFC; the anode, cathode, and for certain designs, a membrane. Numerous variations in design that utilize new inventive materials as well as traditional materials in new applications have been constructed.

### **2.10.1 Materials**

#### **Anode.**

There are eight properties that an anode material must fulfill to be applicable for use in a microbial fuel cell. It must be conductive, non-corrosive, non-fouling, porous, inexpensive, easy to make, applicable to larger size systems and contain a large surface area. Conductivity is one of the most important attributes of these materials because electrons must flow through the material from the point of transfer by the microorganism to the collection point. While many metals fit this important characteristic, they fall short in applicability due to

their corrosive nature and lack of a suitable surface for bacteria attachment. The use of carbon-based electrodes is very common in MFC research for they meet much of the criteria stated above (Logan 2008).

Carbon cloth and carbon paper are used frequently throughout the literature because they provide increased conductivity and facilitate bacterial growth (Logan 2008). Reticulated vitreous carbon (RVC), which is a very porous foam made from glass-like carbon with high electrical conductivity, has also been used as both a cathode and anode by researchers (He, Minteer, and Angenent 2005). Although this material provides high surface areas, it can be very brittle and create new problems for the system.

Graphite is a carbon based material that is used in microbial fuel cells because it is durable and has easily definable surface areas due to low internal porosity (Chaudhuri and Lovley 2003; Liu, Ramarayanan, and Logan 2004). Graphite can be utilized in many different forms including plates, sheets, and rods. A comparison was completed on the power production of graphite rods, felt, and foam in identical MFC systems. Graphite felt produced large power densities because it contained almost 3 times more surface area than that of the graphite rod (Chaudhuri and Lovley, 2003). However, when current production was normalized to surface area, the felt and rod had comparable values of 28 mA/m<sup>2</sup> and 31 mA/m<sup>2</sup> respectively. The graphite foam produced the greatest power density of 74 mA/m<sup>2</sup>; attributed to more cells attaching to the foam because of its structure (Chaudhuri and Lovley, 2003). This conclusion

accentuates the importance of material choice on the overall performance of the MFC.

Graphite granules were first used by Rabaey et al (2005b) in a tubular MFC design. Granules are small pieces of graphite, usually 1.5-5 mm in diameter that can be used for both the anode and cathode. Although the granules are electrically conductive, there must be consistent contact between all the pieces for current to be efficiently transported through them to the collection point. A graphite rod can be placed within the granules to help maintain this contact as well as provide a connection for the wiring of the MFC (Rabaey et al. 2005b). Graphite granules have been used in multiple packed bed reactor MFC architectures in the literature (Aelterman et al. 2006a; Rabaey et al. 2006, Clauwawert et al. 2007b).

New anode materials, designs, and methods have been researched in recent years to maximize the surface area available for bacteria to colonize. A graphite fiber brush (2.5 cm outer diameter and 2.5 cm length) was first used by Logan et al. (2007) to achieve a surface area of 0.22 m<sup>2</sup>. The fibers were 7.2 μm in diameter and wrapped with titanium, a non-corrosive metal, using normal industrial brush machines. . A larger brush (5 cm in diameter and 7 cm long) provided 1.06 m<sup>2</sup> of surface area. Because these brushes have a porosity of 95% and 98% respectively, minimal volume is used to house them within the MFC. In a cylinder MFC (described in section 2.10.2), these brushes produced a 2400 mW/m<sup>2</sup> power density, normalized to cathode surface area (Logan et al.

2007). This is one of the highest power densities that have been published in the literature to date.

This high power density of the brush is also attributed to an ammonia treatment prior to use in the MFC (Logan et al. 2007). This energy intensive treatment process involves heating the material to 700° C for an hour in a 5% NH<sub>3</sub> helium gas. The positive surface charge of the material is increased due to the formation of nitrogen-containing surface functional groups. Acclimation time was reduced by 50% and power density increased from 1640 mW/m<sup>2</sup> to 1970 mW/m<sup>2</sup> after treatment. This ammonia treatment provides new material characteristics that result in better and faster bacterial adhesion and improved electron transfer at the anode (Cheng and Logan 2007).

Metals and metal coatings have been researched as possible anode materials to improve MFC performance. Iron oxide-coated electrodes were compared to porous carbon paper and although the iron oxide electrode (30 mW/m<sup>2</sup>) did perform better than the regular carbon paper (8 mW/m<sup>2</sup>); an electrode with a biofilm transplanted from a working MFC produced 40 mW/m<sup>2</sup>. The iron coating did not increase maximum power; however it did decrease the acclimation time for the bacteria (Kim, Min and Logan 2005). An anode utilizing Mn<sup>4+</sup> and a substrate of sewage sludge with the bacteria *E. coli*, outperformed plain graphite 1000 fold (788 mW/m<sup>2</sup>) (Park and Zeikus 2003). Stainless steel, titanium, tungsten, and aluminum oxide have also been tested for anode applications. Tungsten was the only material to decrease acclimation time, similar to the iron oxide-coated electrodes, and also had little effect on power

production. Use of the other metals resulted in negative effects on the power production of the MFCs (Logan 2008).

In recent years, the anode potential has been researched as an aspect of design that can be altered to increase power production. As discussed in the thermodynamics section and equation (2-1) of this paper; if the energy gain for the bacteria can be increased, they are more likely to use the electrode as the TEA. A potentiostat is used to input potential to the anode to increase power production. The lower the anode potential is, the less energy available per electron transferred for cell growth and maintenance (Aelterman et al. 2008b). However if this method is used, the MFC system will need an energy input.

It can be difficult to directly compare anode materials when trying to determine what materials are ideal for use in an MFC. For example, if the overall internal resistance of the system is too high, increasing the anode surface area or changing the material may not affect the power output of the cell at all because the internal resistance is controlling the system (Logan 2008). Caution must be used in drawing conclusions on the applicability of materials and designs in MFC systems.

### Cathode.

Research on MFC cathodes has been increasing in recent years. With the use of graphite brushes and other such high surface area materials, the anode is no longer a limiting factor for power production. The cathode poses the biggest challenges in design and materials because electrons, protons, and oxygen must all be transported to the area and react with a catalyst. An effective

cathode must be constructed from conductive material containing a catalyst and be in contact with the anode substrate and air. All of the carbon based materials discussed in the previous section for applications as an anode can also be used as cathode material, with the addition of a catalyst.

Two of the most commonly used cathode materials are carbon paper or carbon cloth. When used in a single chamber MFC, these materials will be wet-proofed due to the architecture of the system. The carbon paper and cloth can be purchased with a Platinum (Pt) catalyst already applied to the surface or this can be done in the laboratory by the researcher. A paste is created by combining a chemical binder, such as 5% Nafion liquid solution and a Pt/carbon powder product and is then applied to the material being utilized as the cathode (Cheng, Liu, and Logan 2006c). Research has indicated that this 'homemade' cathode, using the Pt/carbon/Nafion paste, increased power by 68% over a system using a purchased cathode with catalyst (Liu, Cheng, and Logan 2005).

The use of platinum at the cathode of MFCs increases the cost of this technology. Cobalttetramethoxyphenylporphyrin (CoTMPP) has been found to be a cheaper alternative to platinum as a catalyst on the cathode. The maximum power produced using CoTMPP was only 12% less than the power produced using a high Pt loading of 0.5 mg/cm<sup>2</sup>. This same study found that Pt loadings can be reduced to 0.1 mg/cm<sup>2</sup> with only a 19% reduction in power production. Using CoTMPP or reducing the amount of platinum catalyst at the cathode can be cost saving options for MFCs with minimum reductions in power production. (Cheng, Liu, and Logan 2006c). A further study in 2007 found that using Iron

phthalocyanine on Ketjen black carbon as a catalyst at the cathode actually performed better than platinum in a cylinder single chamber MFC design (Yu et al. 2007). Research will need to continue into the future to find more sustainable and cost effective catalysts that can be used at the cathode.

In a single chamber MFC system, the anode is located in an anaerobic chamber with the substrate while the cathode is in contact with both the substrate and open air (described further in section 2.10.2). To reduce oxygen diffusion through the cathode to the anode compartment, diffusion layers can be applied to the air-facing side of the material. Oxygen diffusion results in lower coulombic efficiencies ( $C_E$ ) due to loss of the substrate through aerobic degradation. Diffusion layers allow for oxygen to reach the cathode to complete the reaction with protons and electrons while limiting water loss and excessive oxygen diffusion into the anode compartment. Polytetrafluoroethylene (60%) can be applied as a diffusion layer and increase  $C_E$  values by as much as 171% (Cheng, Liu, and Logan 2006a).

New innovations in cathode construction have yielded tubular and biological cathodes. Tubular cathodes are made from ultrafiltration membranes, which have been used in water and wastewater treatment. These high surface area materials are coated with graphite paint on the air-facing side of the material to provide electrical conductivity. A catalyst, such as CoTMPP, is then added to the cathode. Using a graphite fiber brush as the anode and 2 tubular cathodes, a power density of  $17.7 \text{ mW/m}^3$  (normalized to reactor volume) was produced. While internal resistance of this system was greater,  $C_E$  values were



in the range of 70-74% (Zuo et al. 2007). Anion exchange membranes have also been studied in this same MFC set up and performed better with a power density of 728 mW/m<sup>2</sup> (Zuo, Cheng, and Logan 2008). Both of these membrane cathodes are promising developments in cathode research which can improve power densities of MFCs as well as create scalable systems.

Clauwaert et al. (2007) were the first research group to demonstrate the possibility of biocathodes while researching denitrification in MFCs. Through the use of a tubular MFC, with an internal cathode using a Cation exchange membrane, microorganisms at the cathode used electrons supplied by the microorganisms at the anode to produce a power density of 4mW/m<sup>3</sup> (normalized to the cathode chamber volume) while removing organics in both compartments (Clauwaert et al. 2007b). This research continued by testing a biocathode in a non-denitrification MFC. This system combined a tubular anode with a continuously wetted cathode, open to the air and produced 83 W/m<sup>3</sup> from a batch system (Clauwaert et al. 2007a). Application of such cathodes could eliminate the need for chemical catalysts at the cathode of an MFC.

### Membranes.

Membranes are used extensively in hydrogen fuel cells to separate the hydrogen and oxygen while allowing proton transfer within the system. They have a similar application in microbial fuel cells for separating two components while allowing proton exchange. However, membranes are only used in two chamber MFC systems. It was found by Liu and Logan in 2004 that a single

chamber MFC lacking a membrane performs better than a single chamber using a membrane fused to the cathode (Liu and Logan 2004).

In two chambered systems, cation exchange membranes, anion exchange membranes, and ultrafiltration membranes have all been researched. Cation exchange membranes (CEM), also called proton exchange membranes (PEM), are the most commonly used type of membrane; specifically a Nafion 117 Dupont brand. These membranes were developed for use in hydrogen fuel cells thus they are designed to create a conductive environment. However they were not designed for the saturation conditions of an MFC, and therefore do not have the same efficiencies as those in a hydrogen fuel cell (Logan 2008). Membranes such as Nafion, help increase the coulombic efficiency of the system (Kim et al. 2007). However, Nafion has a high oxygen diffusion transfer coefficient and has the tendency to transfer not only protons through the membrane (Kim et al. 2007; Rozendal, Hamelers, and Buisman 2006; Chae et al. 2008). PEMs still transfer other positive cations such as  $\text{Na}^+$ ,  $\text{K}^+$ ,  $\text{NH}_4^+$ ,  $\text{Ca}^{2+}$ , and  $\text{Mg}^{2+}$ . These species can be responsible for the positive charge transfer to the cathode rather than protons and were found in  $10^5$  times higher concentrations than protons at the cathode. This can cause the pH in the anode compartment to decrease as the pH at the cathode increases (Rozendal, Hamelers, and Buisman 2006). This change in pH can affect the bacterial respiration of the anode compartment.

The major disadvantages of using membranes in MFC systems are cost and fouling. Membranes are expensive and would be impractical for larger MFC systems. Fouling can cause oxygen and substrate diffusion between the

chambers as well as a decrease in proton transport. Membranes also increase the internal resistance of the system which can decrease power production (Logan 2008).

### Catholyte.

When air is not used at the cathode, a catholyte must be used instead of a catalyst to facilitate the reaction. Common catholytes used in literature are ferricyanide, hexacyanoferrate, permanganate, and iron. Although these catholytes have provided some of the highest power densities in the literature; they must be chemically regenerated or replaced after use in the MFC (Logan 2008). All of these catholytes are made from unsustainable materials and could never be used for a full scale application of the technology due to cost, large volumes, and toxicities.

### 2.10.2 Architecture

There are a large variety of microbial fuel cell designs that have been utilized in research. MFC design is controlled by the application that it will be used in. Basic MFC designs can be used to study small aspects of the microbial fuel cell system or to test one specific parameter. However, these systems will generally not result in power densities comparable to the most efficient systems that have been constructed. These highly efficient systems have been designed solely for the purpose of maximizing power production of the microbial fuel cell system. Each group of researchers has a preferential design and materials that are used in testing.

### Two Chamber MFC.

The most basic MFC design is a two-chambered system, illustrated and described in section 2.5 (Figure 2.2). These systems consist of two chambers separated by a PEM. The anode chamber is filled with an organic substrate and anode, while the cathode chamber is filled with a catholyte and cathode. Three different studies using the same two chamber, 310 mL anode volume (PEM, carbon paper electrodes, with Pt catalyst) produced maximum power densities of up to 45 mW/m<sup>2</sup> (Min et al. 2005; Oh, Min and Logan 2004, Oh and Logan 2006). A cheaper alternative that can be used in place of a PEM is a salt bridge, made from agar and salt (Logan 2008). While this two chamber system is a good option for simple demonstrations of the MFC technology, this design cannot compete in power production with a system using a PEM or a single chamber system.

Water sparged with air can be used in the cathode chamber, however other more efficient catholytes, such as phosphate buffer solution are often used. This solution has increased ionic strength and helps to maintain pH of the system (Min et al. 2005). Injecting air into the cathode compartment can help the cathode reaction and increase power production by 15.8% (Oh and Logan 2006). The nutrient medium often used in laboratory settings as organic matter in the anode compartment, can also serve as the catholyte in two chambered systems (Oh, Min, and Logan 2004; Oh and Logan 2006). When these substances are used, a catalyst must be applied to the cathode. As stated above, these systems

have limited power production due to the electrode spacing and the proton transfer efficiency of the PEM.

Non-sustainable chemical catholytes such as ferricyanide and permanganate can be used to increase power production. Ferricyanide increases mass transfer efficiencies and creates a larger cathode potential (Oh and Logan 2006; Oh, Min and Logan 2004). One of the largest power densities reported, 4310 mW/m<sup>2</sup>, was achieved using ferricyanide (Rabaey et al. 2004). Permanganate also creates a higher cathode potential and has been shown to outperform ferricyanide in power density results (Logan 2008).

Power production in two chamber MFCs can also be increased by changing the size of the PEM, anode, and cathode. A larger PEM can help increase proton transfer, however oxygen diffusion will result in a loss of substrate to aerobic processes and decrease the coulombic efficiency of the system (Oh and Logan 2006). The surface area of the PEM limits power production when the surface area is smaller than that of the electrodes; however when the PEM surface area is of sufficient size for the system, power output is proportional to the cathode surface area (Oh and Logan 2006). Results of any research must be analyzed closely due to the numerous influencing factors upon power production.

#### Single Chamber MFC.

Single chamber MFC systems are more efficient and applicable to uses outside laboratory research. In these systems, there is only an anode compartment; the cathode compartment becomes the open air around the MFC.

Generally, a cathode with platinum catalyst is open to the air on one side while maintaining contact with the substrate in the anode compartment on the other side to allow proton transport.

One of the most common single chamber MFC designs that is used in the literature was designed by Liu and Logan (2004) to test the necessity of a PEM. The single chamber system is a cylinder with a 28 mL empty bed volume (4 cm long with a 3 cm diameter). It uses a carbon paper anode on one side of the chamber with a carbon cloth cathode on the opposite side which is exposed to air. This carbon cloth is wet proofed and has a 0.5 mg/cm<sup>2</sup> Pt loading that faces the liquid-side of the reactor. Using wastewater as the substrate, 146 ± 8 mW/m<sup>2</sup> was produced with no membrane present. While the coulombic efficiencies of the system were reduced from 40-55% to 9-12% without a CEM due to oxygen diffusion into the system, this demonstrated that the absence of a membrane improves power densities (Liu and Logan 2004).

Optimum space between the anode and cathode of this design was determined to be 2 cm. This spacing reduced the internal resistance of the system from 161Ω for 4 cm spacing to 77 Ω and produced a power density of 1210 mW/m<sup>2</sup>. Both the cathode and anode potentials were increased as well; improving the coulombic efficiency of the MFC (Liu, Cheng, and Logan 2005). Electrode spacing of 1 cm caused a drop in power density due to oxygen diffusion to the anode, however when advective flow was used within the system power density was increased to 1540 mW/m<sup>2</sup>. This flow from the anode to

cathode helped reduce the oxygen diffusion that resulted from minimal electrode spacing (Cheng, Liu, and Logan 2006b).

Other improvements can be applied to this cylinder MFC design, which have been discussed already in section 2.6.5. Graphite brushes with or without an ammonia treatment can replace the anode carbon cloth to increase power production (Logan et al. 2007; Cheng and Logan 2007). Diffusion layers can also be added to the air cathode as well as using CoTMPP instead of platinum for the cathode catalyst (Cheng, Liu, and Logan 2006c). Tubular cathodes can be utilized in this system as well in place of the carbon cloth cathode (Zuo et al. 2007).

#### Plate MFC.

A variation on this basic single chamber MFC design has been the construction of a plate microbial fuel cell; similar to designs used in hydrogen fuel cells. This MFC is made of two non-conductive plates with a serpentine channel cut out of each to allow the flow of substrate on one side and the flow of air on the other side. The cathode is a hot-pressed PEM and carbon cloth with Pt combination that is placed in between the two plates and the anode is a carbon paper. This system produced 56 mW/m<sup>2</sup> from a domestic wastewater substrate and reached 309 mW/m<sup>2</sup> using acetate. This system did not operate as efficiently as the cylinder MFC, possibly because the proximity of the anode and cathode was too close, causing oxygen diffusion into the anode region (Min and Logan 2004).

A 2008 design by Liu et al. combined the cylinder design and characteristics of the plate MFC to construct a large MFC of 520 mL. The anode compartment contains baffles which allow for a plug-flow type treatment system. The carbon cloth anode was attached to all surfaces of this baffled compartment, totaling 757 cm<sup>2</sup> in surface area. The cathode (Pt catalyst, wet-proofing, and 4 diffusion layers) was placed on top of the anode compartment and sealed with a plastic cover with holes drilled to allow oxygen diffusion. This system produced 520 mW/m<sup>2</sup> in batch mode, and 695 mW/m<sup>2</sup> in continuous flow mode. Increasing the anode surface by using graphite granules and graphite brushes, in this design, had little effect on power due to the cathode limiting power production (Liu et al. 2008).

#### Tubular MFC.

Tubular MFCs can be single or two chamber designs and use oxygen or chemical catholytes in the system. A single chamber tubular MFC was made by Liu, Ramarayanan, and Logan (2004) and used wastewater as a substrate. This MFC was made by hot pressing a PEM to a carbon cloth with Pt catalyst and placing it around a tube with holes drilled into it to allow oxygen transfer. Eight graphite rods were placed around this tubular cathode and the system was enclosed by a plastic chamber. The tubular cathode was open on each end to allow oxygen diffusion to the cathode while the wastewater was fed continuously to the system. A maximum power density of 26 mW/m<sup>2</sup> was produced in this continuous flow system. When air was forced through the cathode, power production was reduced; reiterating the problems caused by increased levels of



oxygen diffusion into the anode compartment of an MFC (Liu, Ramarayanan, and Logan 2004).

Glass beads and wool were also used as separation in a two chamber column MFC lacking a membrane. Artificial wastewater was fed through an anode chamber with graphite felt, through the glass beads and wool, to the cathode chamber containing graphite felt and sparged with air. This system only produced 1.3 mW/m<sup>2</sup>; with the limiting factor most likely being the mass transfer of protons between the two electrodes (Jang et al. 2004). A similar system was constructed using graphite rods in place of graphite felt for both the anode and cathode. A maximum power density of 10.9 mW/m<sup>2</sup> was reported (Ghangrekar and Shinde, 2007). The glass beads and wool have also been replaced with a perforated polyacrylic plate in other MFC designs (Moon et al. 2005; Moon, Chang, and Kim 2006). Tubular systems using graphite granules have been used by multiple researchers in the literature as well. These systems generally use the graphite granules for the anode with a PEM/carbon cloth system encapsulating the granules (Clauwaert et al 2007a; You et al. 2007). A catholyte can be applied to the outside of these cathodes to improve power production (Rabaey et al. 2005c).

#### Microbial Fuel Cells in Series.

Many of the different MFC designs can be operated in series in a variety of different configurations. A cassette electrode MFC consists of 12 separate MFC systems, termed 'cassettes'. Each cassette consists, from left to right, of an anode, PEM, cathode, plastic frame to allow air to reach the cathode,

cathode, PEM, and anode. In total this system produced a maximum of 899 mW/m<sup>2</sup> (Shimoyama et al. 2008). For treating larger volumes of organic substrate, the best option for MFCs could be this compartmentalization of the volume. Greater power densities can be produced with multiple smaller units placed in a series-parallel configuration (Ieropoulos, Greenman, and Melhuish 2008). Interestingly, a parallel connection between multiple MFCs resulted in higher current, yet a series connection resulted in higher voltage (Aelterman et al. 2006a).

In all of the above designs, wiring can be copper, titanium, or any other conductive material of choice. While copper is an easy option, it can be toxic to bacteria thus must be sealed to reduce this risk.

### **2.11 Types of Substrates used in Microbial Fuel Cells**

There is a wide range of substrates that are acceptable candidates for use in microbial fuel cells for treatment and power production. In laboratory testing, it is common to see acetate and glucose used with additions of nutrients and buffer solutions. These substrates are used for optimum results, however many complex organic substrates can also be used.

Domestic wastewater has been used in multiple MFC systems with success. With a basic cylinder MFC design, 146 mW/m<sup>2</sup> was produced using wastewater with at a strength of 200-300 mg/L chemical oxygen demand (COD) (Liu and Logan 2004). In this same cylinder design, swine wastewater (8320 ± 190 mg/L soluble COD) was treated and produced a power density of 261 mW/m<sup>2</sup>. This system saw removals of both ammonia and soluble COD (Min et

al. 2005). Wastewater from a potato processing factory and a hospital (600-2300 mg/L COD) were used in a study using a two chambered system with a chemical catholyte (Aelterman et al. 2006b). A brewery wastewater was used in the cylinder MFC design with the addition of a high buffer concentration solution of 200 mM and produced 528 mW/m<sup>2</sup> at a COD of 2250 ± 418 mg/L (Feng et al. 2008). MFCs have been found to also efficiently utilize proteins as a substrate. Bovine serum albumin (354 ± 10 mW/m<sup>2</sup>), peptone (269 ± 14 mW/m<sup>2</sup>), and meat packaging wastewater (80 ± 1 mW/m<sup>2</sup>) were all treated in a single chamber system (Heilmann and Logan 2006).

Steam-exploded corn stover biomass has been used in MFCs and produced power densities from 367-371 mW/m<sup>2</sup> in conjunction with high biological oxygen demand (BOD) and COD removals (Zuo, Maness, and Logan 2006). A synthetic acid-mine drainage water was tested in the cylinder MFC design as well and produced about 48% of the power that can be produced with acetate (Cheng, Dempsey, and Logan 2007). Another interesting application of MFC technology was in a sediment MFC, utilizing soil for the bacteria and organic source. This design was operated using rice plants and the rhizodeposits from the plant to produce power and increased power production to seven times what it had been without the presence of plants (Schampelaire et al. 2008). Reed Mannagrass was also used in a similar design with promising results as a method of nondestructive harvesting of bioenergy that is carbon neutral. Research has begun to study algae as an organic substrate for MFCs with a maximum power density of 110 mW/m<sup>2</sup> reported (Strik et al. 2008).

## **2.12 Other Types of Microbial Fuel Cells**

Microbial fuel cells can be utilized for more than just the production of direct electricity. Chang et al. (2004 and 2005) researched the use of MFCs as biological oxygen demand (BOD) sensors. MFCs could be a quicker and easier method to determine BOD through a linear relation of current and BOD concentrations (Chang et al. 2004). MFCs can also be designed for specific removal needs, such as a denitrification system (Clauwaert et al. 2007b). Odors from swine wastewater can also be controlled by using the wastewater in an MFC for power production as well as treatment. Volatile organic acids which cause the odors were reduced by 99.76% in an MFC with power densities of 228 mW/m<sup>2</sup> and 84% sCOD removals (Kim et al. 2008)

### **2.12.1 Hydrogen Production**

MFCs can be employed for hydrogen production rather than direct electricity production. Hydrogen gas can be produced in greater amounts in an MFC than those from the current methods of fermentation and water electrolysis. In an MFC designed for hydrogen production, the cathode is sealed to eliminate air entering the system and a voltage is applied to the system. This energy input is necessary because hydrogen formation from acetate or other substrates is not a spontaneous process. Using a membrane-less basic cylinder design, with an applied voltage of 0.8 V, an overall energy efficiency of 78 % was reported (in

relation to the energy applied and the energy of the substrate) (Call and Logan 2008).

### **2.12.2 Sediment MFCs**

Marine sediments provide an ideal environment to operate a microbial fuel cell because the microorganisms, organic matter, and catholyte are all naturally present. Sediment MFCs employ the anaerobic bacteria that are naturally present to produce power by placing an anode in the anaerobic sediment. The organic matter in the sediment is used as the substrate for the MFC. The aerobic saltwater is used as the catholyte by placing a cathode in the ocean above the anode (Logan 2008). This microbial fuel cell is already in use in marine sediments at multiple locations and holds the most promise for easy and practical application of the MFC technology.

### **2.12.3 MFCs for Bioremediation**

Electrodes can be used as electron donors as well as electron acceptors in an MFC, as discussed with the concept of biocathodes. This concept can be used for bioremediation of sediments using an MFC. *Geobacteraceae* was found to reduce nitrate and fumarate using a graphite electrode poised at a -500 mV potential (Gregory, Bond, and Lovley 2004). Uranium groundwater contamination as well as perchlorate contamination have both been researched using MFCs (Logan 2008).

## **CHAPTER 3**

### **METHODS AND MATERIALS**

#### **3.1 Overview**

Laboratory testing was completed on all microbial fuel cell designs and involved both electrical generation evaluation and leachate characterization. An initial MFC was constructed in a square shape and will be called Square MFC. The MFC architecture evolved during research and an improved MFC was constructed with a cylindrical shape, which is termed Circle MFC for its cross-sectional shape. Finally, a larger scale MFC was designed, built, and labeled Larger Scale MFC. Power density and polarization curves were created using electrical test methods. Temperature, dissolved oxygen (DO), pH, oxidation reduction potential (ORP), and conductivity were all measured along with chemical oxygen demand (COD), biological oxygen demand (BOD), total organic carbon (TOC), ammonia, alkalinity, nitrite, nitrate, sulfate, total phosphorus, phosphate, chloride, sulfide, and a suite of metals. Influent and effluent levels were measured for each cycle of the MFCs to determine percent difference. A microbial analysis was also completed on the landfill leachate and biofilm that formed on the anode of the MFC.

## **3.2 Materials**

### **3.3.1 Landfill Leachate**

Landfill leachate was collected from the Turnkey Recycling and Environmental Enterprises (TREE) facility in Rochester, NH. Influent from the landfill leachate treatment facility was used, as well as leachate directly from Cell III, Phases 1 and 2. The leachate treatment facility accepts leachate from three different cells of operation, labeled TLR I, II, and III. TLR I accepted waste from 1979 until it was closed in 1992, while TLR II accepted waste from 1990-1997. TLR III is currently accepting waste and the facility plans to close the cell in 2012. Phase 1 and 2 of TLR III were opened in 1995 and 1996 respectively, with a third phase opened in 1997. TREE personnel stated that a small portion of leachate collected from TLR III may have been saturating landfill gas wells prior to being transported to the pumping station.

Leachate flow in a landfill is a dynamic system which can change at any time, resulting in changes in leachate characteristics. The leachate sampling location was changed multiple times due to the characteristics of the leachate and the necessity for consistent values during sampling. At TLR III (Phase 1 and 2), leachate was collected directly from the pumping station. At all locations, the leachate was transported in either 2 L or 19 L HDPE plastic containers and placed in the MFCs within an hour of arrival at UNH, with the exception of cycle 7b of the Square MFC, and cycles 2b and 4b of the Circle MFC. In these cases, the leachate was stored at 8-9° C for 1 week prior to use.

### **3.2.1 Single Chamber Designs**

#### **Square MFC.**

The anode chamber was constructed from Plexiglas (11 cm x 11 cm x 9 cm) and sealed with aquarium grade 100% silicone. It had a total volume of 1089 mL with a working volume of 1005 mL, considering the space the anode consumed. The anode was constructed using a 10 cm x 10 cm x 0.9525 cm dense fine grain graphite plate and nine 0.48 cm diameter by 5.5 cm long graphite rods. The plate was cut into an x shape and the rods were attached with silver epoxy (EE129-4, Epo-tek) as illustrated in Figure 3.1. The anode had a total surface area of 276 cm<sup>2</sup> (0.308 m<sup>2</sup>).

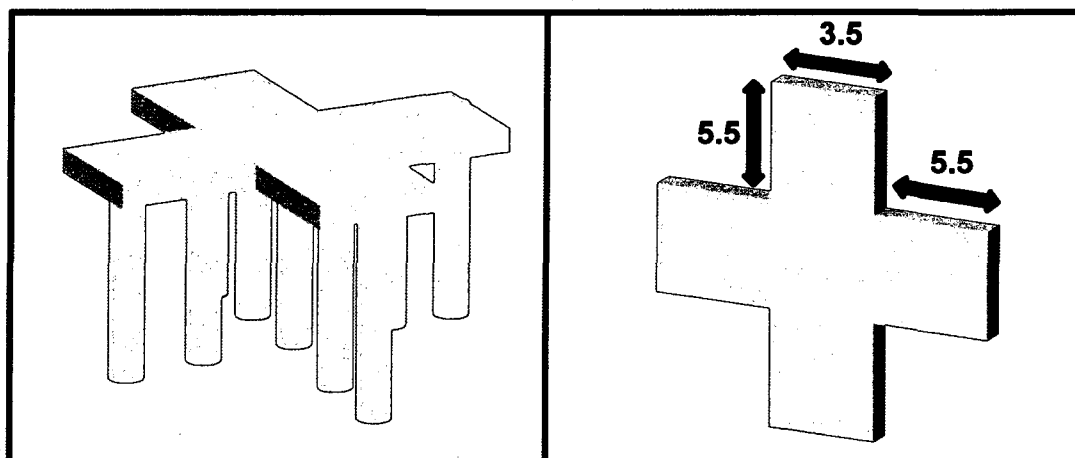


Figure 3.1 Illustration of graphite anode used in Square MFC (not to scale)

The cathode was composed of wet proofed woven carbon cloth coated with 1 mg/cm<sup>2</sup> platinum with dimensions 10 cm X 10 cm (100 cm<sup>2</sup>). The carbon cloth (designation A, E-Tek) was purchased with 30% wet proofing to limit the release of substrate through the cloth. The platinum was purchased as 10% HP



Platinum on Vulcan XC-72, a carbon black powder. This mixture was combined with a chemical binder of Dupont dispersion, 5% (by weight) Nafion liquid solution to form a paste of  $7\mu\text{L}$ -binder per mg-Pt/C catalyst (Cheng et al 2006c; Logan 2008). The paste was then applied to one side of the carbon cloth and allowed to dry for 24 hours at room temperature. The cathode sits 1 cm above the anode when installed. Silver epoxy (EE129-4, Epo-tek) was used to connect insulated copper wire to both the anode and carbon cloth. This system is pictured in Figure 3.2.

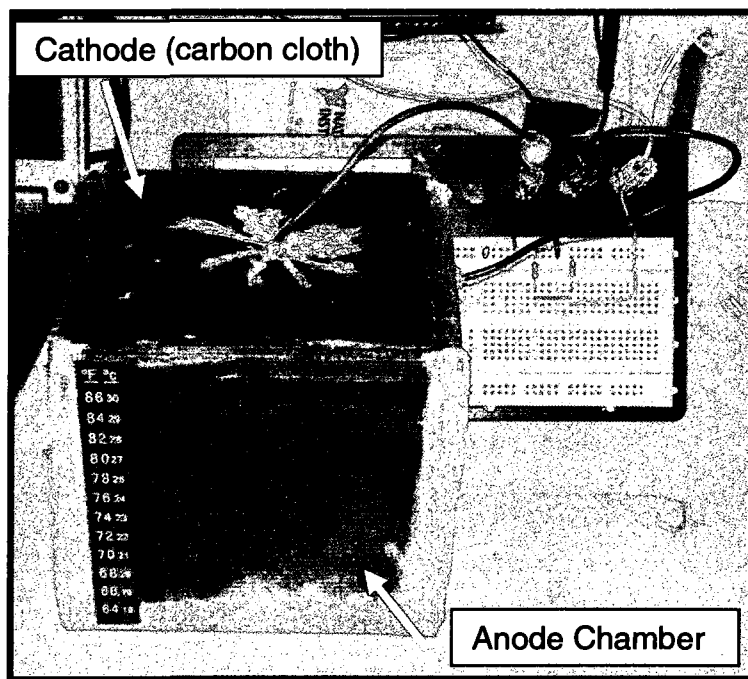


Figure 3.2 Picture of Square MFC

An electrical breadboard was used for the wiring of this system. Alligator clips were attached to the ends of the anode and cathode wiring. These clips were then attached to the breadboard which contained a capacitor to

compensate for electrical noise within the system, a 1  $\Omega$  resistor to compensate for the resistance of the data acquisition unit, and a 470  $\Omega$  resistor to provide a load for the system. This resistance was based upon values found in literature, as well as the results of prior UNH research (Microcellutions 2007). The internal resistance of this system is 400-500  $\Omega$  (discussed in the results). For optimum operation of an MFC, the external resistance should be equal to that of the internal resistance (Aelterman et al. 2008a). Thus the resistance was maintained at 470  $\Omega$  and provided optimum power production. The breadboard and wiring are pictured in Figure 3.3.

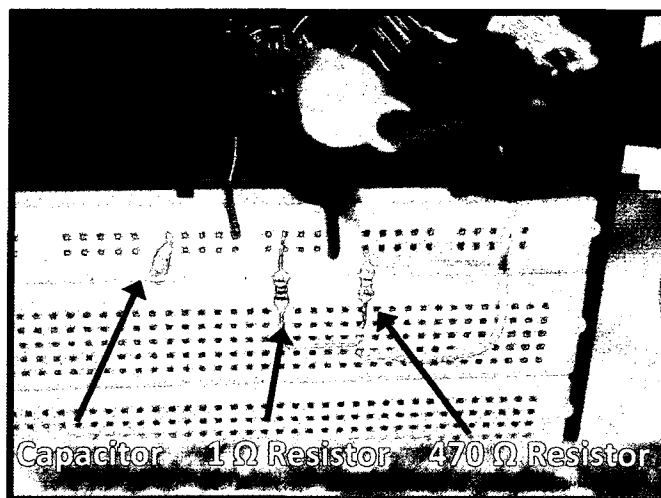


Figure 3.3 Electrical breadboard with wiring used in MFC operations

### Cylinder MFC.

This MFC design was created after using the Square MFC system and therefore improved upon some of the aspects of that design. The anode chamber was made from a 1000 mL Nalgene plastic cylindrical container, with a

working volume of 934 mL. The anode was constructed using a 11 cm x 11 cm x 0.9525 cm dense fine grain graphite plate and nine 0.48 cm diameter by 7.5 cm long graphite rods. The plate was cut into an x shape and the rods were attached with silver epoxy (EE129-4, Epo-tek) as illustrated in Figure 3.4. The anode had a total surface area of 258 cm<sup>2</sup> (0.258 m<sup>2</sup>).

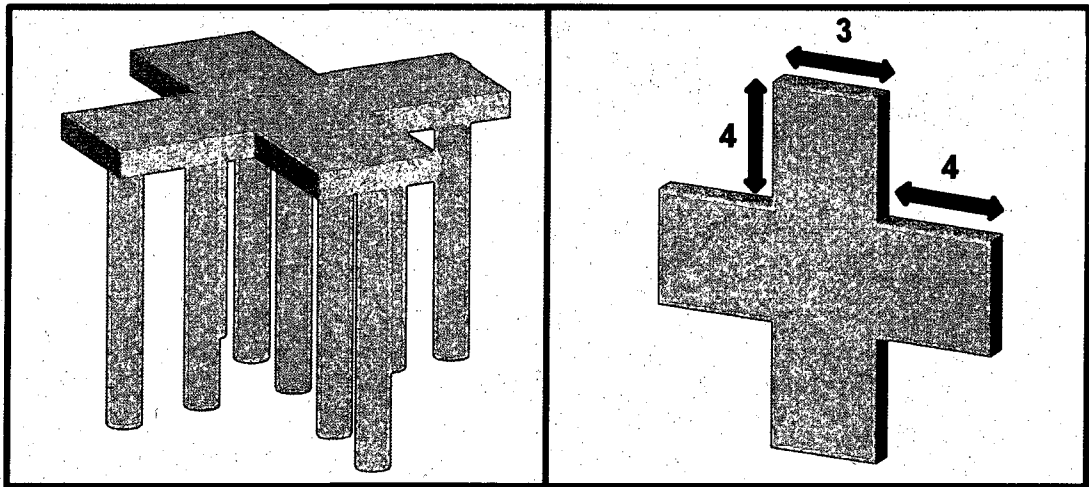


Figure 3.4 Illustration of graphite anode used in Circle MFC (not to scale)

The cathode was composed of wet proofed woven carbon cloth coated with 1 mg/cm<sup>2</sup> platinum with an inside diameter of 10 cm and an area with diameter of 8 cm exposed to air (50 cm<sup>2</sup>). The carbon cloth (designation A, E-Tek) was purchased with 30% wet proofing to provide containment of the leachate. The cathode was constructed in the same manner as the Square cathode. The center of the pre-fabricated lid of the plastic container was removed and the cathode was sealed in place using aquarium grade 100% silicon. The cathode sits 1 cm above the anode when installed. Silver epoxy

(EE129-4, Epo-tek) was used to connect insulated copper wire to both the anode and carbon cloth. Once the lid was tightened into place, this system was placed on its side to create constant contact between the cathode and leachate, as pictured in Figure 3.5. The wiring was identical to that used for the Square MFC. A small hole was drilled into the top of the MFC for leachate additions during the cycle time and was sealed when not in use

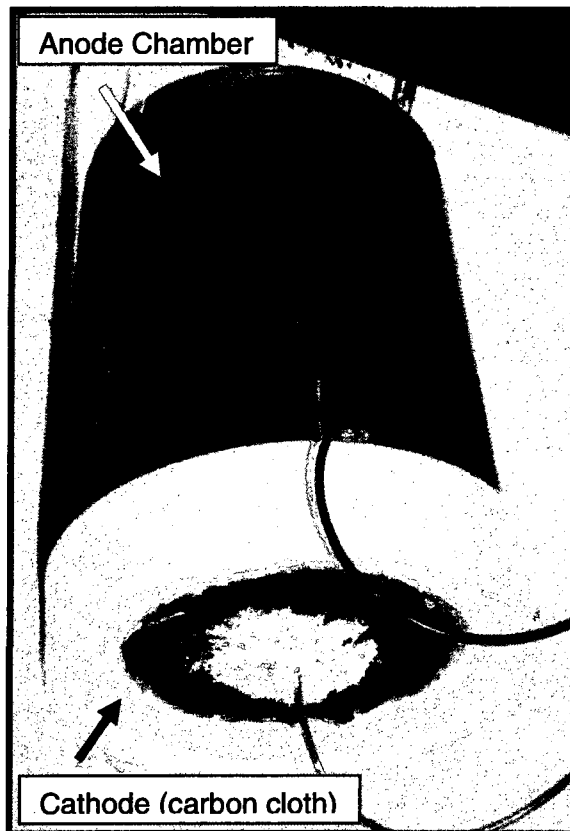


Figure 3.5 Picture of Circle MFC

#### Larger Scale MFC.

A larger MFC was created to determine electrical output and treatment capabilities of a scaled up MFC. The anode chamber was made from a 5 gallon

high-density polyethylene bucket with a diameter of 28 cm and 34 cm height. There was a total volume of 1.89 L, with a working volume of 1.83 L. The anode was constructed using a medium extruded graphite plate 30.5 cm x 30.5 cm x 0.635 cm and nine 1.27 cm diameter by 30.5 cm long fine extruded graphite rods. The plate was cut into an x shape and the rods were attached with silver epoxy (EE129-4, Epo-tek) as illustrated in Figure 3.6. The anode had a total surface area of 1,942 cm<sup>2</sup> (1.942 m<sup>2</sup>).

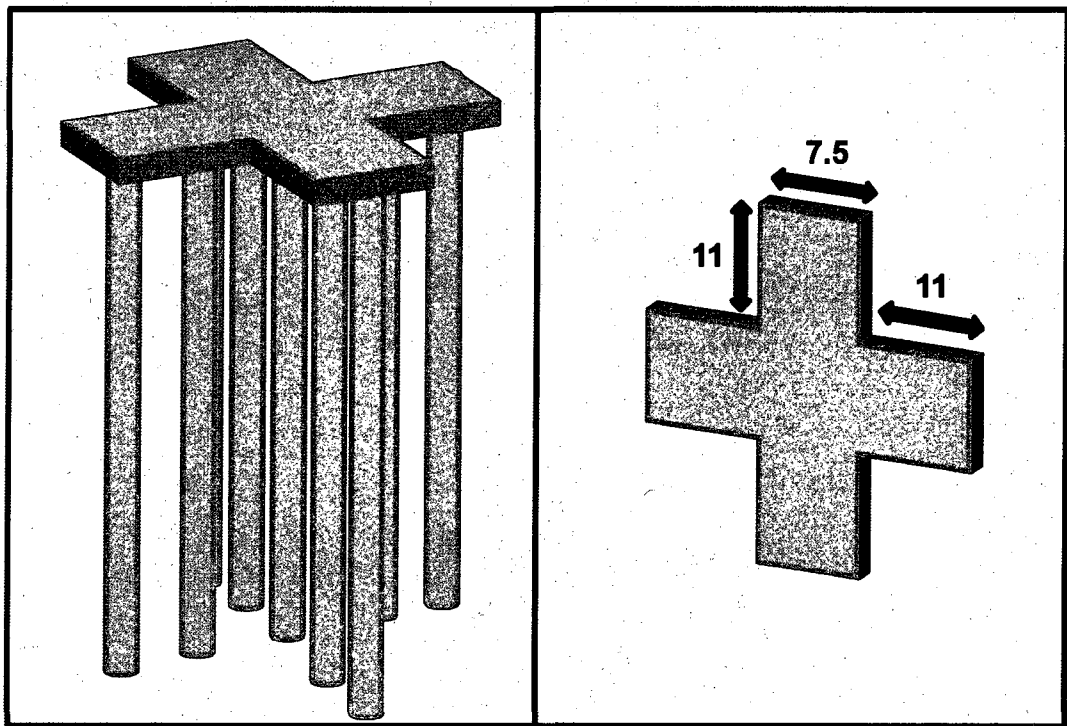


Figure 3.6 Illustration of graphite anode used in Larger Scale MFC (not to scale)

The cathode was composed of wet proofed woven carbon cloth coated with 1 mg/cm<sup>2</sup> platinum with a diameter of 30 cm (707 cm<sup>2</sup>). The carbon cloth (designation A, E-Tek) was purchased with 30% wet proofing to provide containment of the leachate and was constructed in the same manner as the

Square cathode. The cathode was allowed to float on the surface of the leachate to allow constant contact in this upright system. However, overlapping on the sides of the container was allowed to minimize air infiltration. The cathode sits 1 cm above the anode when installed. Silver epoxy (EE129-4, Epo-tek) was used to connect insulated copper wire to both the anode and carbon cloth. This system is pictured in Figure 3.7. The wiring was identical to that used for the Square MFC.

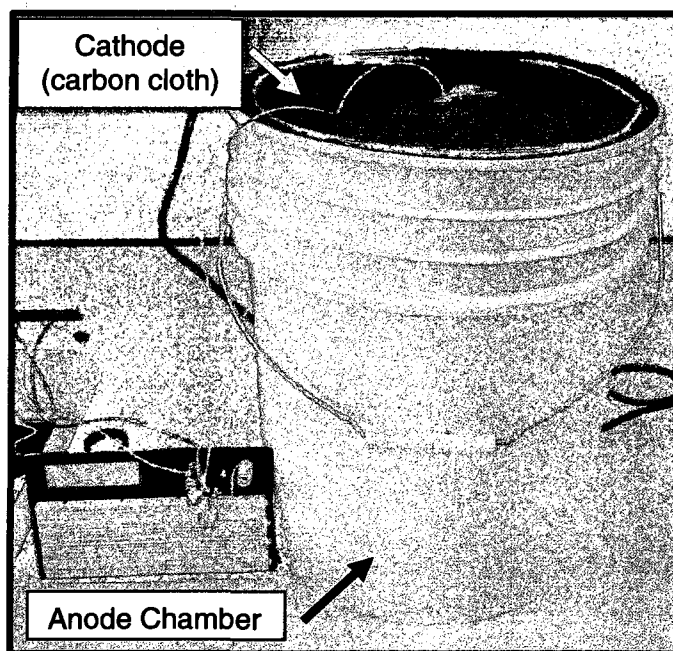


Figure 3.7 Picture of Larger Scale MFC

### 3.3 Methods

#### 3.3.2 MFC Operation

Leachate was used as both the substrate and inoculum in this research. No additional anaerobic bacteria or nutrient were added to the system. Leachate was added and removed between cycles with caution to limit disturbance of any biofilm formation on the anode. No cleaning was done between consecutive cycles of MFC operation so that continual growth of an exoelectrogen community could be achieved.

Because of evaporation and utilization, the level of leachate in the Square MFC slowly decreased resulting in inconsistent contact between the cathode and leachate. When there is no contact between the cathode and leachate, protons released in the anode compartment cannot reach the cathode and the MFC reaction is not completed. The MFC was checked each week day and leachate was added to the MFC when necessary to reestablish contact. Data on these additions can be found on page 136 of Appendix A. Although the Circle MFC was more resistant to oxygen infiltration; there still appeared to be evaporation of the leachate through the carbon cloth cathode of this design, as well as utilization. An empty space would form at the top of the MFC, void of leachate and leachate was added as needed (frequency and volumes presented on page 137 of Appendix A). The Larger Scale MFC had the same problems as the Square MFC. Additions of leachate were at greater volumes and frequency due to the large surface area of the cathode (Data on page 138 of Appendix A).

A cycle of operation for these MFCs began with the addition of recently sampled leachate into system. The cycle ideally ended when voltage produced dropped below 50 mV. This voltage was chosen so that the microbial community

within the MFC could be sustained, yet batch conditions for effluent testing of the leachate could be created. Variations in ending voltage did occur due to testing and laboratory constraints. All efforts were made to take the MFC offline as close to 50 mV as possible to maintain consistency.

### **3.3.3 Electrical Measurements**

#### **Data Acquisition.**

A data acquisition unit was used with a desktop computer and software to measure and record data from the microbial fuel cells. A National Instruments (USB 6210) unit with 16 inputs, 16-bit, 250 kS/s, multifunction I/O was used to measure the voltage from the MFCs every 2 minutes during a cycle. This unit was connected to a computer with Labview 8.5 software that allowed the data to be stored in an Excel file for subsequent analysis.

#### **Power Density Curve.**

A RS-500 Elenco Electronics resistor box was used to vary external resistance of the system operating in open circuit voltage (infinite resistance) from 40,000 $\Omega$  to 10 $\Omega$ . Voltage was recorded for each resistance when readings had stabilized. A description of how the curves were calculated can be found in Section 4.2.4.

### **3.3.4 Leachate Characterization**

For all measurements, data was recorded for the leachate prior to input into the MFC system and after treatment. Further description of residence times



can be found in the results section of this paper. All analyses were completed at UNH except for BOD, TOC, alkalinity, ammonia, chloride, nitrate/nitrite, phosphate, sulfate and total phosphorus.

#### Probe Readings.

Temperature (Celsius), pH, oxidation reduction potential (ORP) (mV), dissolved oxygen (mg/L and %), conductivity (mS/cm) and specific conductivity ( $\mu\text{S}/\text{cm}$ ) were all measured using a YSI 556 MPS probe. A YSI 5580 confidence solution (prepared by NCL of Wisconsin Inc.) was used before each analysis to determine if calibration was needed for ORP, pH, and specific conductivity. If calibration was needed for pH, a 3 point calibration was used with buffered solutions of pH 4 (YSI 2821), 7 (YSI 2822), and 10 (YSI 2823). A 10,000  $\mu\text{S}/\text{cm}$  or 1,000 $\mu\text{S}/\text{cm}$  conductivity solution (YSI 2167, prepared by NCL of Wisconsin Inc.) was used to calibrate specific conductivity. ORP and DO did not require additional calibration during testing because the values remained in the appropriate range for the calibration solution. Instrument accuracy and precision data can be found on page 139 of Appendix B.

#### COD.

Chemical oxygen demand (COD) is an indirect measure of the amount of organic compounds in a substance. Organic compounds are fully oxidized under acidic conditions. Units for COD are mg/L of oxygen consumed. Hach Method 8000, reactor digestion method (0-1500 ppm range) was used. This method is USEPA approved. Due to COD levels being high in this leachate, all samples were diluted 1 mL into 25 mL of reverse osmosis (RO) water prior to testing. 2

mL of sample were combined with the provided COD digestion reagent containing silver sulfate, sulfuric acid, demineralized water, chromic acid, and mercuric acid. The COD vials were then inverted gently several times to mix the contents and digested at 150°C for 2 hours using a Hach COD Reactor. The vials were allowed to cool to 120°C or less before removing them from the reactor and were then inverted several times while still warm and placed in a rack to cool to room temperature. A Hach DR/2400 Portable Spectrophotometer was used to measure the COD concentration using the High Range COD program. This test was run with triplicate samples and a blank. Instrument accuracy and precision data can be found on page 139 of Appendix B.

#### BOD.

Biochemical oxygen demand (BOD) measures the amount of molecular oxygen that is utilized during a period of time for the degradation of organic matter. This is a common test to predict the oxygen demand associated with a substrate released into a water body. BOD concentrations can cause oxygen depletion in the receiving water and thus negatively affect the ecosystem. It can be used to determine the treatment efficiencies of processes meant to improve the quality of a wastewater prior to release.

This testing was completed according to Standard Method 5210 B. An airtight bottle is completely filled with sample and incubated for 5 days at a specified temperature. Dissolved oxygen is measured initially and after incubation and BOD can then be calculated from this data. Reagents, seeding, and dilutions are utilized to complete the pre-treatment and test (Clesceri,

Greenberg, and Eaton 1998). Instrument accuracy and precision data can be found on page 140 of Appendix B.

### TOC

Total organic carbon (TOC) is the amount of organic carbon in a substrate, independent from the oxidation state of any matter and inorganics that can contribute to BOD and COD measurements. EPA method 415.1 was used for this testing. Organic carbon is converted to carbon dioxide by catalytic combustion or a wet chemical oxidation. This carbon dioxide can then be measured by an infrared detector or by a flame ionization detector once it has been converted to methane. These amounts are directly proportional to the concentration of organic carbon in the sample (Clesceri, Greenberg, and Eaton 1998). Instrument accuracy and precision data can be found on page 140 of Appendix B.

### Ammonia

Ammonia is a constituent of concern for recirculation of leachate as well as for effluent quality. Receiving waters can be overburdened with high nitrogen concentrations from ammonia levels in landfill leachate. Standard Method 4500-NH<sub>3</sub> D was utilized to complete this testing. An ammonia-selective electrode is used with a hydrophobic gas-permeable membrane to separate the electrode internal solution of ammonium chloride from the sample solution (Clesceri, Greenberg, and Eaton 1998). Instrument accuracy and precision data can be found on page 140 of Appendix B.

### Alkalinity.

Alkalinity is the acid-neutralizing capacity of a substrate, which is the sum of all of the titratable bases. Standard Method 2320 B was used to determine alkalinity levels. A titration curve is recorded through successive small additions of titrant and the corresponding pH (Clesceri, Greenberg, and Eaton 1998). Instrument accuracy and precision data can be found on page 140 of Appendix B.

### Nitrate, Nitrite, Sulfate, and Chloride.

These tests were administered according to EPA Method 300.0 A. A small volume of sample is placed in an ion chromatograph and the anions of interest are separated and measured. This is completed by a system containing a guard column, suppressor device, and conductivity detector (Pfaff 1993). Instrument accuracy and precision data can be found on page 140 of Appendix B.

### Total Phosphorus and Phosphate.

These tests were completed according to EPA Method 365.3. Antimony potassium tartrate and ammonium molybdate react with dilute solutions of in an acid medium to form an antimony-phospho-molybdate complex. A blue-colored complex is created by reducing this complex using ascorbic acid. Polyphosphates and some organic phosphorous compounds can be converted to orthophosphates by sulfuric acid hydrolysis or persulfate digestion. The blue color of the final complex is proportional to the concentration of the substrate

(USEPA 2009). Instrument accuracy and precision data can be found on page 140 of Appendix B.

### Sulfide.

Sulfide is an important constituent to examine for it can cause odor issues when it forms hydrogen sulfide. Gaseous hydrogen sulfide can be toxic and if it is oxidized biologically to  $H_2SO_4$ ; it can corrode metals and become toxic to organisms. Testing was completed using the Hach method 813, Methylene Blue Method, equivalent to USEPA Method 376.2 and Standard Method 4500-S<sup>2</sup> D. A clean sample cell was filled with 25 mL of sample and 1.0 mL of Sulfide 1 Reagent (Demineralized water and sulfuric acid) was added. The cell was swirled to mix and 1.0 mL of Sulfide 2 Reagent (Demineralized water and Potassium Dichromate) was then added to the cell and immediately mixed by swirling again. The cell was allowed to react for 5 minutes and then sulfide levels were read using a Hach DR/2000 Direct Reading Spectrophotometer. Method 690 was used at a wavelength of 665 nm. This test was run in triplicate and a blank was also run. Instrument accuracy and precision data can be found on page 139 of Appendix B.

### Total Metals Analysis.

Inductively Coupled Plasma-Atomic Emission Spectroscopy (ICP-AES) was used to detect inorganic (trace) metals in the Total Metals Analysis test. A Varian Vista AX machine was used following the EPA method 6010C. Samples were digested following EPA method 3052 for microwave assisted acid digestion. Teflon coated HDPE reaction vessels were filled with 50 mL of  $HNO_3$  Microwave

Cleaning Solution and placed in the microwave acceleration reaction system 5 (MARS5). An entire digestion cycle was completed and the containers were cleaned with demineralized water and allowed to dry. 45 mL of sample were then placed in the reaction container and 5 mL of high purity 70% nitric acid were added to the sample. This mixture was allowed to react for about 5 minutes before being sealed and digested in the microwave acceleration reaction system 5 (MARS5). The temperature was increase from ambient to 180° C in 10 minutes, then held at this temperature for 10 minutes. The sample was then allowed to cool before removal. Samples were run in triplicate and a blank was also run.

Samples were analyzed for the presence and concentration of aluminum, arsenic, antimony, barium, beryllium, cadmium, calcium, cobalt, chromium, copper, iron, potassium, magnesium, manganese, nickel, selenium, silver, sodium, strontium, thallium, vanadium, and zinc. NIST standards, calibration blanks, and calibration verifications were used for each analysis to ensure quality of the data. The calibration verifications and NIST standards were included at least every 20 samples to ensure the calibration remained consistent over the entire analysis, and that various labs, conducting the same trace metal analysis were detecting similar concentrations of the same solution. Solution matrix spikes were performed to make sure elemental interferences were not affecting the detection capabilities of the analysis. Aluminum, antimony, beryllium, calcium, cadmium, magnesium, potassium, sodium, and thallium results could

not be used for analysis because the concentrations were not in the range of 80%-120% of the calibration verification solution values.

### **3.2.2 Microbiology**

Microbial analysis was completed by David B. Ringelberg of the US Army Corps of Engineers as the Cold Regions Research and Engineering Laboratory, Engineer Research and Development Center. Leachate samples were cultured by spread plating 100  $\mu$ l onto R2A, TSA, NA and PTYG agar as well as incubating 100  $\mu$ l in the respective broths to enrich cells for total lipid fatty acids analysis (TLFA), terminal restriction fragment length polymorphism (T-RFLP) and MIDI analysis (MIDI is a rapid microbial identification system developed by MIDI Inc.).

A TLFA was completed by filtering 50 mL of leachate sample onto a 0.02  $\mu$ m anodisc inorganic membrane filter. This provided a good biomass for analysis. The filter was extracted in 3.8 ml total volume of CHCl<sub>3</sub>:MeOH:H<sub>2</sub>O (1:2:0.8, v:v:v), followed by a separation of the phases with an additional 2 mL of CHCl<sub>3</sub>:H<sub>2</sub>O (1:1, v:v). The fatty acids were then transesterified into methyl esters with 2 mL of CHCl<sub>3</sub>:MeOH:HCl (1:10:1, v:v:v) at 100°C for 1 hour. The fatty acid methyl esters were recovered in 2 mL hexane:CHCl<sub>3</sub> (4:1, v:v) and analyzed by GC/MS.

T-RFLP was then completed with a filtered 50 mL sample. DNA was extracted using a MOBIO microbial DNA kit, followed by amplification of 16S rDNA using primers 27F-926R. The amplicon was purified with the Qiagen PCR

kit, then digested with restriction enzymes HhaI, MspI and RsaI. The digests were desalted with the Qiagen endonuclease kit and analyzed via capillary electrophoresis.



## **CHAPTER 4**

### **RESULTS AND DISCUSSION**

#### **4.1 Introduction**

Microbial fuel cells were successfully operated using landfill leachate throughout the data collection of this research. Testing and analysis were completed using all three microbial fuel cell designs. Three sets of data were obtained; electrical production, leachate treatment, and microbial characterization. The MFCs were operated in batch mode and data was collected for each cycle of operation; referred to as 'cycle' in the following sections and will be consecutively numbered, starting with 1. Three different locations of leachate sampling were used for MFC operations. Leachate taken directly from the influent to the landfill leachate treatment facility is designated 'a'. Leachate taken from closed cell, TLR III, Phase 1 is designated 'b' and leachate from closed cell TLR III, Phase 2 is designated 'c'.

#### **4.2 Power Production**

##### **4.2.1 Square MFC**

Initial testing of the Square MFC was completed in January and February 2008 using leachate from the influent of the leachate treatment facility (a). Three continuous cycles of operation were completed and voltage was plotted versus

time in Figure 4.1, 4.2 and 4.3. The variable voltage readings are a result of the design of this particular MFC and the additions of leachate that were required due to evaporation.

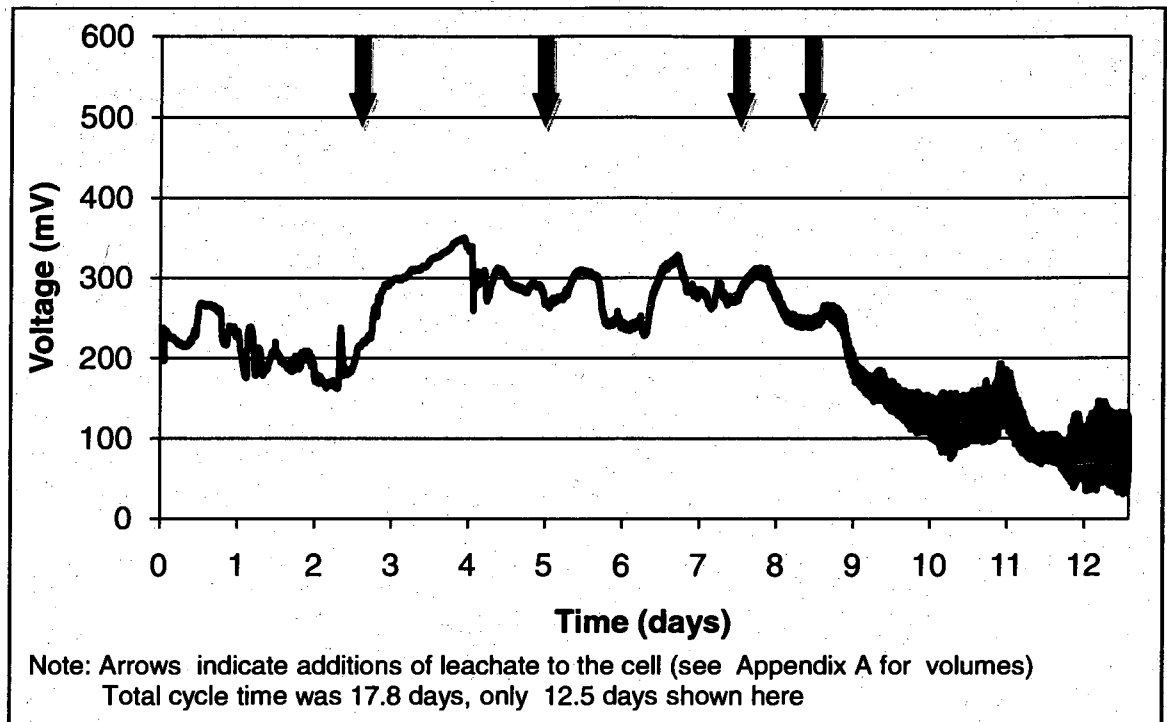


Figure 4.1 Square MFC, cycle 1a, voltage vs. time (1/10/08 – 1/28/08)

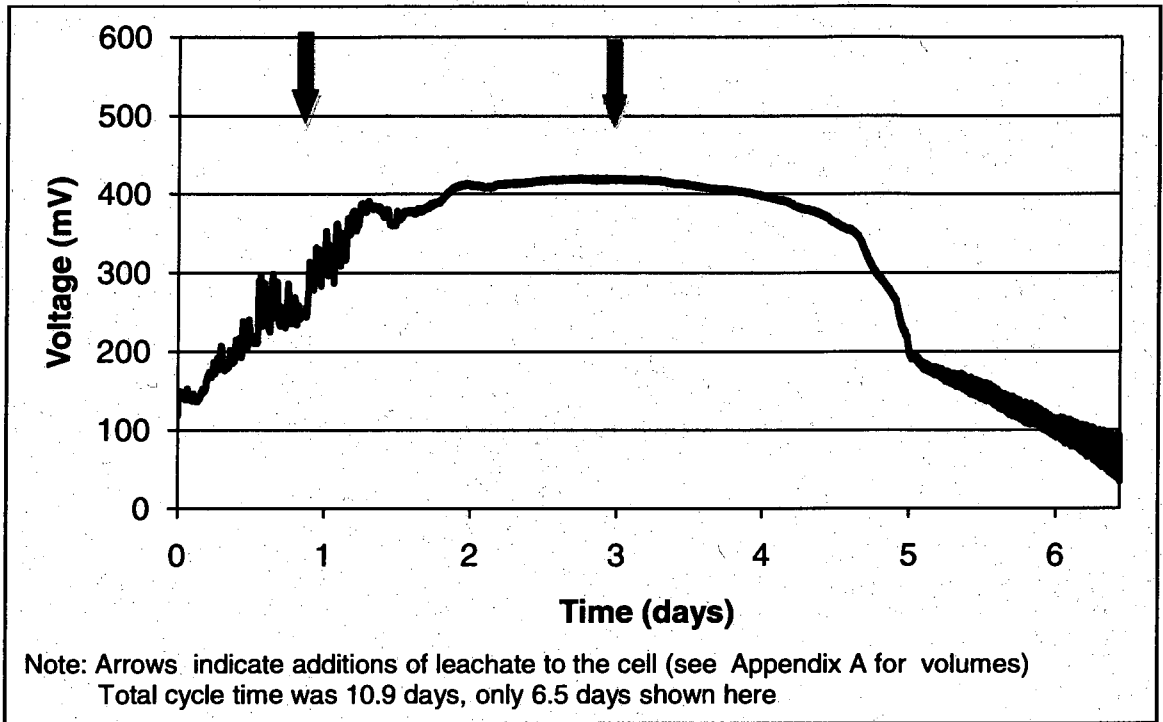


Figure 4.2 Square MFC, cycle 2a, voltage vs. time (1/31/08 – 2/11/08)

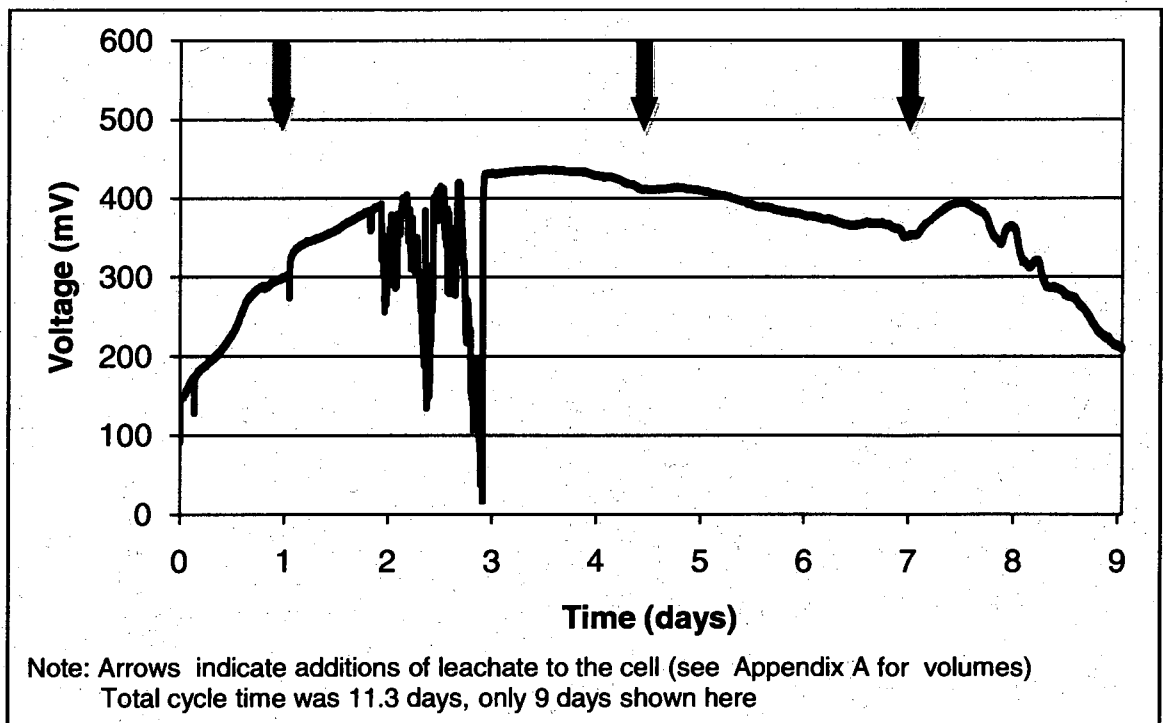


Figure 4.3 Square MFC, cycle 3a, voltage vs. time (2/11/08 – 2/22/08)

Table 4.1 summarizes the dates and voltages for the start, peak, and end of each cycle of the MFC. Cycle time was varied from 11 days to 18 days. With each consecutive cycle of the Square MFC, the peak voltage increased from 349 mV to 421 mV and then to 438 mV. These results suggest that a microbial community conducive to extracellular electron transfer was becoming established within the MFC over time. Exoelectrogens have a competitive advantage in microbial fuel cells due to their ability to use the anode material as a terminal electron acceptor. This population can increase over time and therefore increase the amount of electron transfer in the system.

Each of the voltage versus time plots mimic the phases that are typical in bacterial growth. The growth process begins with a lag phase as bacteria become accustomed to the environmental conditions and little growth is observed. This phase is followed by exponential growth of the microbial population and then a stationary phase where little growth is seen, but living cells are maintained. Lastly, a negative growth phase occurs if no new nutrients and carbon source are supplied to the bacteria. This batch process is how the MFCs were operated. Electricity generation in Figures 4.1, 4.2 and 4.3 followed the growth and establishment of the bacteria that are transferring the electrons. The absence of a lag phase could be a result of an existing microbial community within the system (no cleaning of the MFCs were conducted between consecutive cycles of operation). Once these bacteria begin to die due to the exhaust of the carbon source and/or nutrients in the leachate, electricity generation begins to decrease as well.

Table 4.1 Summary of voltage production for Square MFC, cycles 1a – 3a

	Cycle 1a	Cycle 2a	Cycle 3a
Start Date	01/10/08	1/31/08	2/11/08
Start Voltage (mV)	4	128	138
Peak Voltage Date	01/15/08	2/3/2008	2/14/08
Peak Voltage (mV)	349	421	438
Time to Peak Voltage (days)	4.8	2.8	3.5
Date of End Voltage	01/28/08	2/11/08	2/22/08
End Voltage (mV)	42	51	2
Total Cycle Time (days)	17.8	10.9	11.3

Further testing was completed on the Square MFC from August to October 2008. Landfill leachate from TLR III, Phase 1 (b) was used for these cycles. Plots of the electricity produced in voltage versus time are shown in Figures 4.4, 4.5, 4.6, and 4.7. Each of these graphs mimics bacterial growth similar to cycles 1a-3a. Additions of leachate were also made during these cycles to compensate for evaporation and the data can be found on page 136 of Appendix B. Figure 4.5 shows more variation in the voltage values than previous cycles. After evaluation, it was found that this voltage variability was because of corrosion of the silver epoxy and wiring as well as inconsistent contact between the cathode and leachate. This problem was resolved by constructing a new cathode that was used in cycles 6b and 7b.

Table 4.2 summarizes the results for cycles 4b – 7b. Peak voltages for these cycles were higher than those of 1a-3a. Each cycle's voltage peaked over 500 mV, which could have resulted from different leachate characteristics or a different initial microbial community in the leachate. Total time for cycles 6b and 7b were significantly shorter than those of the first two cycles. This could be due

to a steep decrease in COD levels of the influent leachate (shown in Table 4.12 and 4.13 and discussed in a subsequent section).

Table 4.2 Summary of voltage production for Square MFC, cycles 4b – 7b

	Cycle 4b	Cycle 5b	Cycle 6b	Cycle 7b
Start Date	8/7/08	8/18/08	9/16/08	9/24/08
Start Voltage (mV)	86.3	123.2	230.6	4.4
Peak Voltage Date	8/11/08	8/21/08	9/18/08	9/25/08
Peak Voltage (mV)	513.3	507.7	541.9	517.9
Time to Peak Voltage (days)	4.3	3.0	1.8	0.8
Date of End Voltage	8/18/08	9/5/08	9/24/08	10/3/08
End Voltage (mV)	76.3	16.9	10.4	9.2
Total Cycle Time (days)	10.8	18.0	7.8	9.0

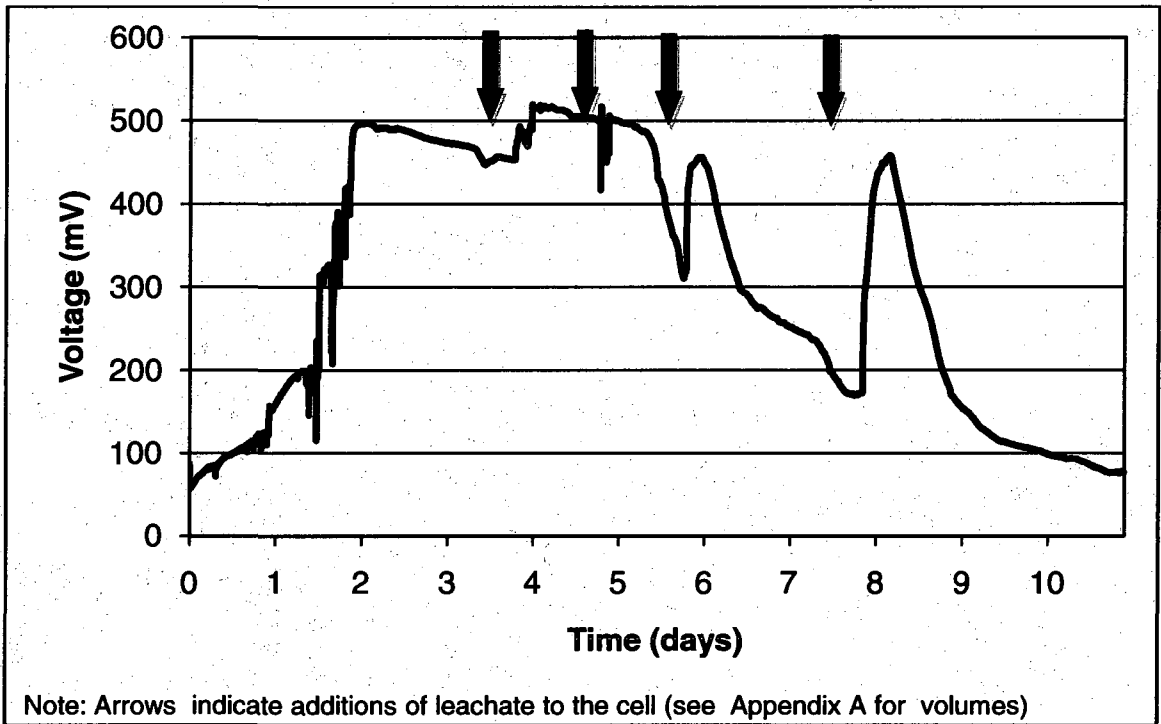


Figure 4.4 Square MFC, cycle 4b, voltage vs. time (8/07/08 – 8/18/08)

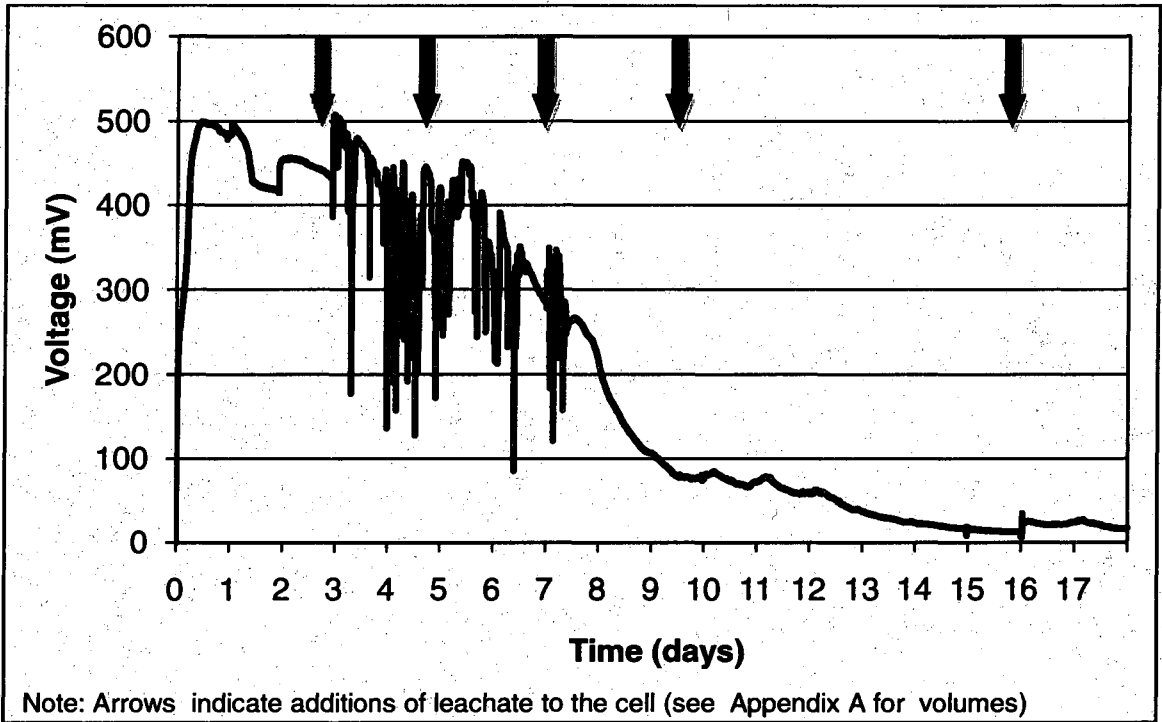


Figure 4.5 Square MFC, cycle 5b, voltage vs. time (8/18/08 – 9/05/08)

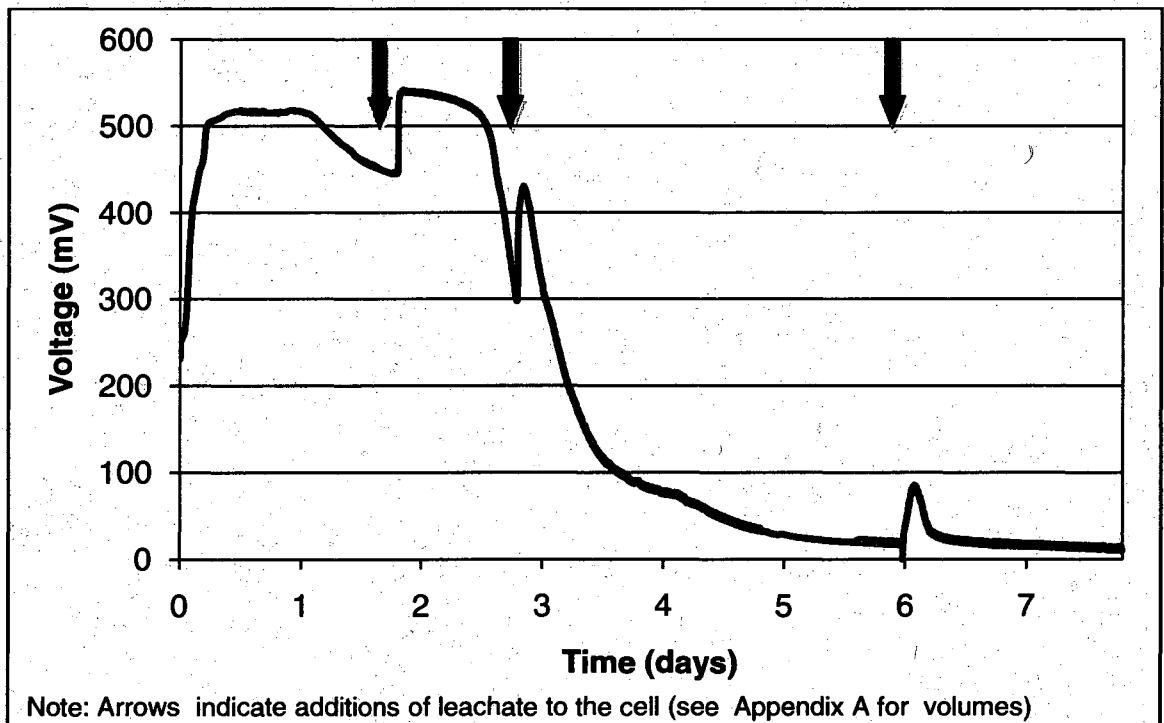


Figure 4.6 Square MFC, cycle 6b, voltage vs. time (9/16/08 – 9/24/08)

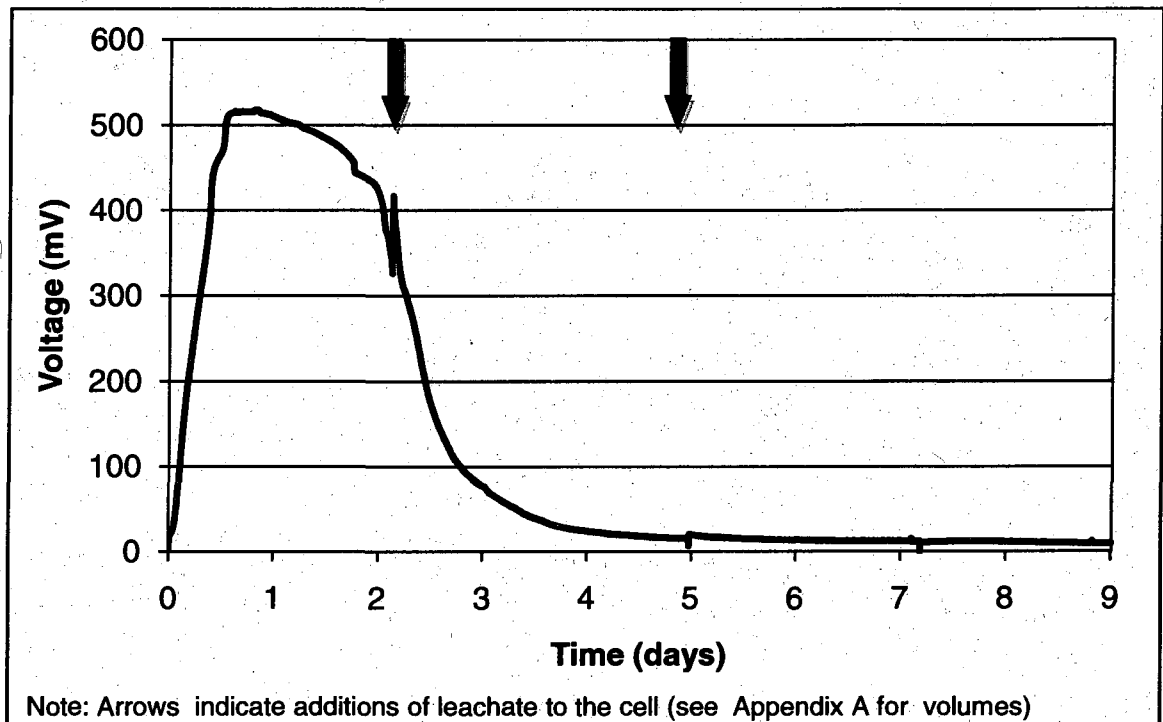


Figure 4.7 Square MFC, cycle 7b, voltage vs. time (9/24/08 – 10/03/08)

#### **4.2.2 Circle MFC**

Initial testing of the Circle MFC was completed in conjunction with the Square MFC from August to October 2008. Landfill leachate from TLR III, Phase 1 (b) was used for these cycles. The Circle MFC was designed to address the problem of inconsistent contact between the cathode and leachate of the Square MFC due to evaporation. Voltage was successively produced and four continuous cycles of operation were completed. Table 4.3 summarizes the results for cycles 1b – 4b, while plots of the data can be seen in Figures 4.8, 4.9, 4.10 and 4.11. Peak voltages for this design were greater than those of the Square while using the same influent leachate, which is likely because of the reduction of air entering the system, providing a more anaerobic environment



and consistent contact between the substrate and cathode. In this design, the cathode was attached to the lid of the container and actually screwed into place. This created a more air tight seal and constant contact between the cathode and leachate. There would be less competition from aerobic bacteria within the system, providing greater voltage production.

Figures 4.8, 4.9, 4.10, and 4.11 also mimic bacterial activity (as discussed in section 4.2.1), however with a faster growth phase and longer stable peak voltage production than those of the Square MFC. It is likely that the higher efficiencies in design caused these improvements in results. Similar to the Square MFC cycles 6b and 7b using the same leachate, the Circle MFC cycles 3b and 4b had significantly shorter run times. This can potentially be attributed to the decreased COD levels of the influent leachate of 908 and 1075 mg/L. Some of the variation in voltage readings in Figures 4.8,, 4.9, 4.10, and 4.11 are due to a decrease in voltage because of evaporation out of the system and the subsequent additions of leachate that caused a return to optimum operating conditions.

Table 4.3 Summary of voltage production for Circle MFC, cycles 1b-4b

	Cycle1b	Cycle 2b	Cycle 3b	Cycle 4b
Start Date	8/7/08	8/23/08	9/15/08	9/24/08
Start Voltage (mV)	30.4	39.3	77.5	25.2
Peak Voltage Date	8/12/08	8/26/08	9/18/08	9/26/08
Peak Voltage (mV)	490.3	479.2	530.6	533.7
Time to Peak Voltage (days)	5.1	2.5	3.4	2.1
Date of End Voltage	8/23/08	9/9/08	9/24/08	10/3/08
End Voltage (mV)	41.6	53.6	26.1	15.9
Total Cycle Time (days)	16.1	16.7	9.0	9.0

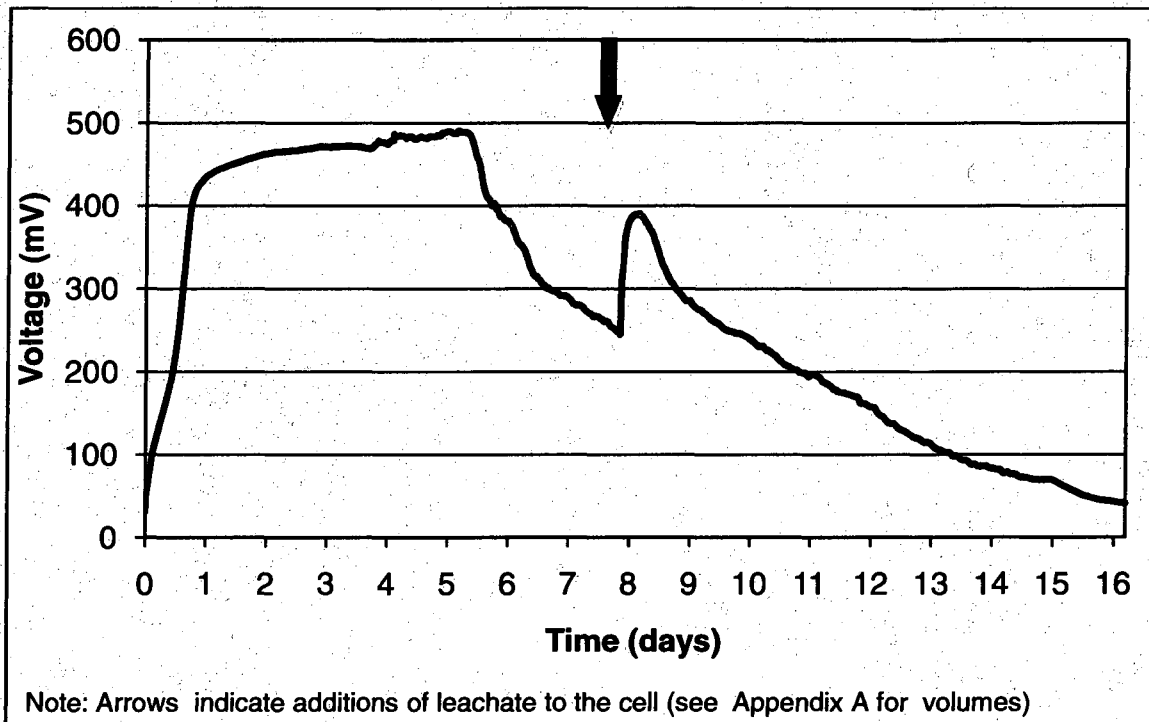


Figure 4.8 Circle MFC, cycle 1b, voltage vs. time (8/07/08 – 8/23/08)

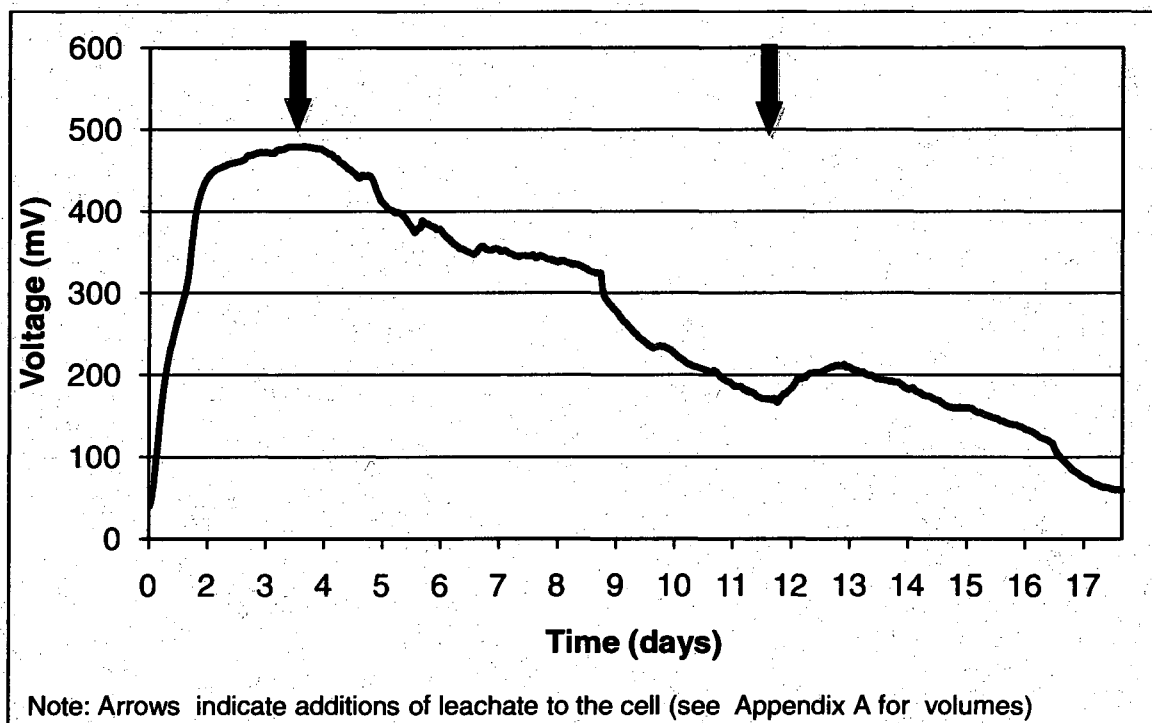


Figure 4.9 Circle MFC, cycle 2b, voltage vs. time (8/23/08 – 9/9/08)

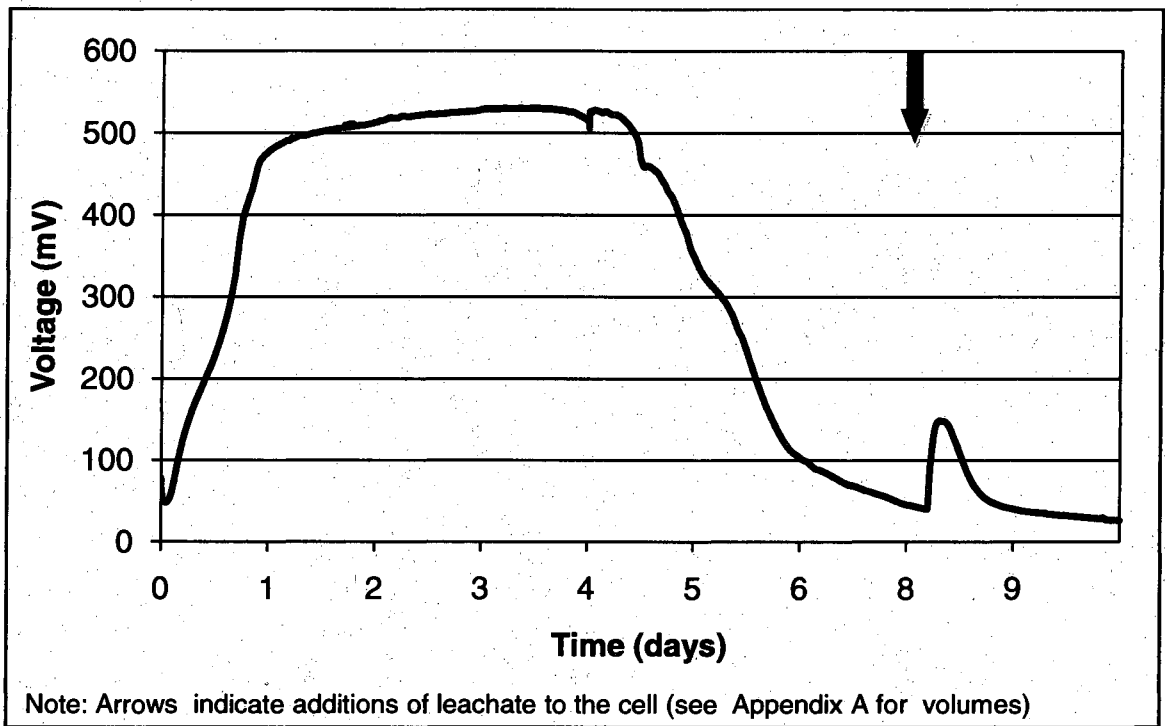


Figure 4.10 Circle MFC, cycle 3b, voltage vs. time (9/15/08 – 9/24/08)

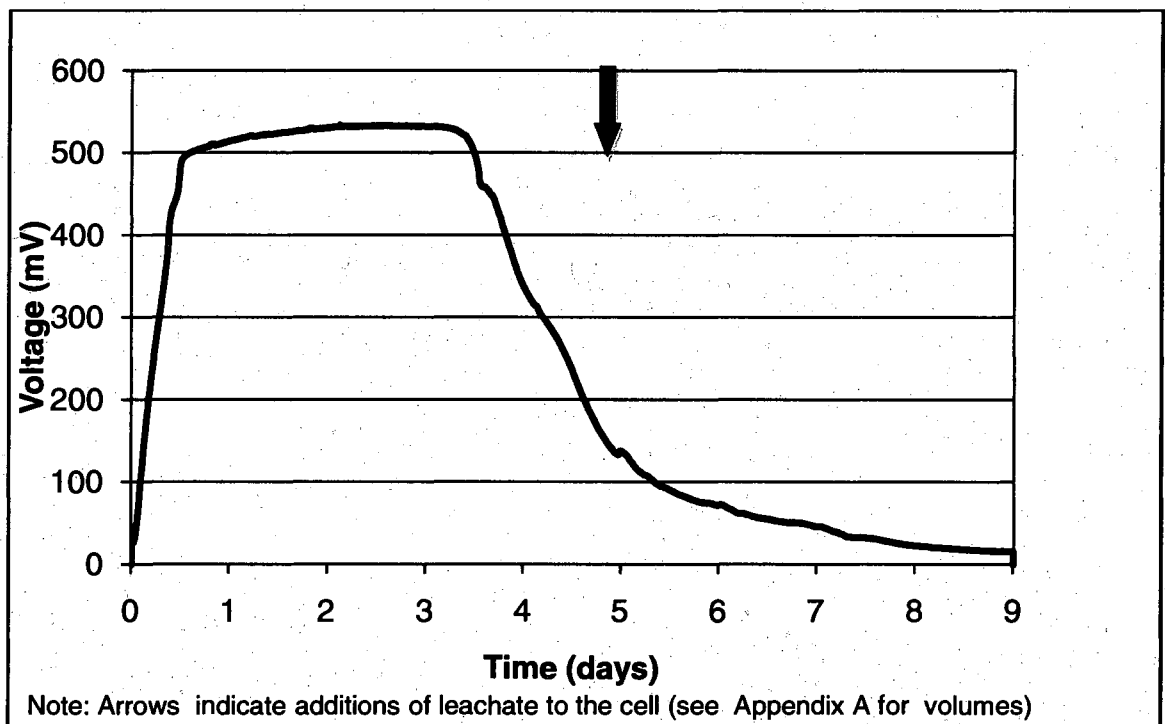


Figure 4.11 Circle MFC, cycle 4b, voltage vs. time (9/24/08 – 10/03/08)

Further testing was completed on the Circle MFC from January to February 2009. These cycles evaluated COD, BOD, TOC, and sulfide characteristics of influent and effluent leachate from the system. Because of timing constraints and contract laboratory error, BOD, TOC, and sulfide data were not collected in the previous cycles. Landfill leachate from TLR III, Phase 2 (c) was used in cycles 1-3c. The plots of voltage vs. time for these cycles can be found in Figures 4.12, 4.13 and 4.14. Each of these cycles were similar to those of cycles 1b-4b and followed the same trends in mimicking bacterial growth. Peak voltages were 526 mV, 504 mV, and 513mV which were in the range of cycles 1b-4b, however cycle 3c was significantly longer than any previous cycle in the Circle or Square MFCs. This was potentially because the BOD content of the influent was double what it had been, increasing from 180-200 mg/L to 430 mg/L. Voltage generation was sustained for nearly a month before the MFC was taken offline (still producing 110 mV) because of timing constraints of providing a microbial sample for analysis.

Table 4.4 Summary of voltage production for Circle MFC, cycles 1c-3c

	Cycle 1c	Cycle 2c	Cycle 3c
Start Date	1/16/09	2/2/09	2/16/09
Start Voltage (mV)	208.5	53.1	66.1
Peak Voltage Date	1/19/09	2/4/09	2/20/09
Peak Voltage (mV)	525.5	504.4	513.3
Time to Peak Voltage (days)	3.2	1.9	4.1
Date of End Voltage	2/2/09	2/16/09	3/12/09
End Voltage (mV)	52.9	55.1	109.5
Total Cycle Time (days)	17.1	13.9	24.1

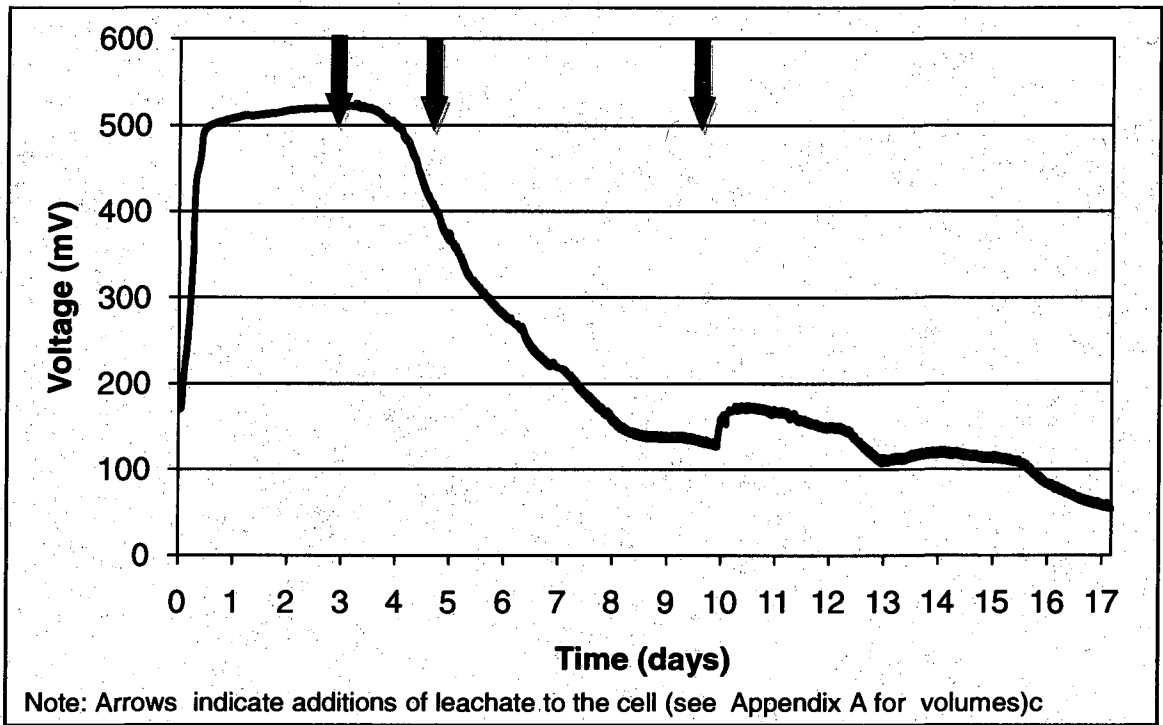


Figure 4.12 Circle MFC, cycle 1c, voltage vs. time (1/16/09 – 2/02/09)

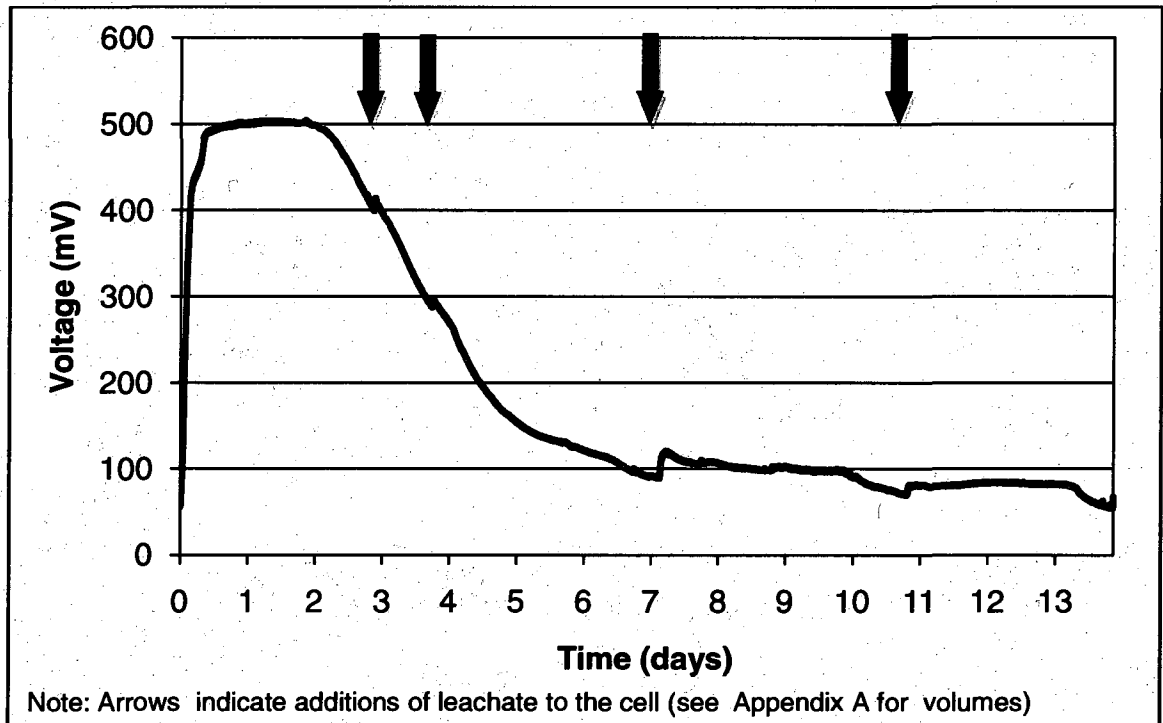


Figure 4.13 Circle MFC, cycle 2c, voltage vs. time (2/02/09 – 2/16/09)

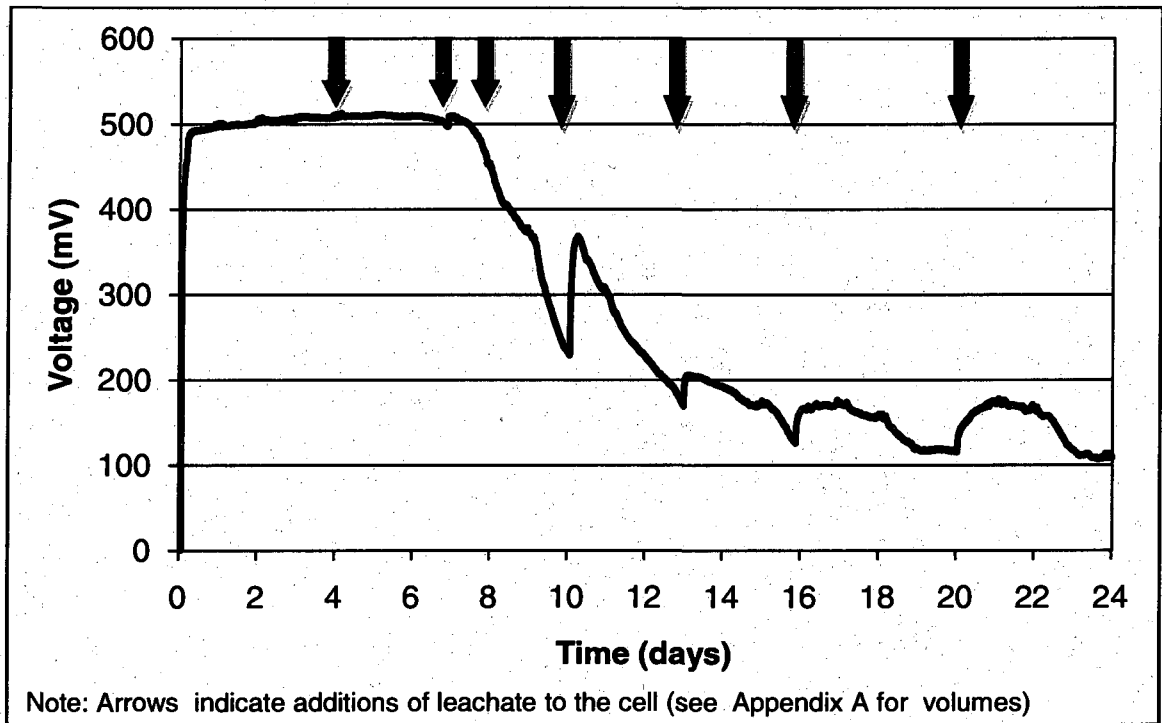


Figure 4.14 Circle MFC, cycle 3c, voltage vs. time (2/16/09 – 3/12/09)

### **4.2.3 Larger Scale MFC**

Testing was completed on the Larger Scale MFC from February to April 2009, using landfill leachate from TLR III, Phase 2. This MFC was designed to begin investigation into larger and 'scaled up' MFCs. This MFC design increased the volume of leachate used to 19 L, however it was uncertain how much voltage would be produced by the system for there is not a linear correlation between an increase in volume or surface area and voltage production. Upon scale-up, significant internal resistance is added to the system, with both protons and electrons having longer paths to travel to complete the circuit and reaction. Voltage was produced by the scaled-up MFC, but quickly decreased, most likely due to the use of new materials for MFC construction and necessary acclimation

of the bacteria (Figure 4.15). A second cycle was completed where voltage was maintained 52+ days and had a peak of 635 mV. These results are an increase from the Circle and Square designs; however this was only a ~100 mV increase even though leachate volume in the MFC increased more than 20 times from previous designs.

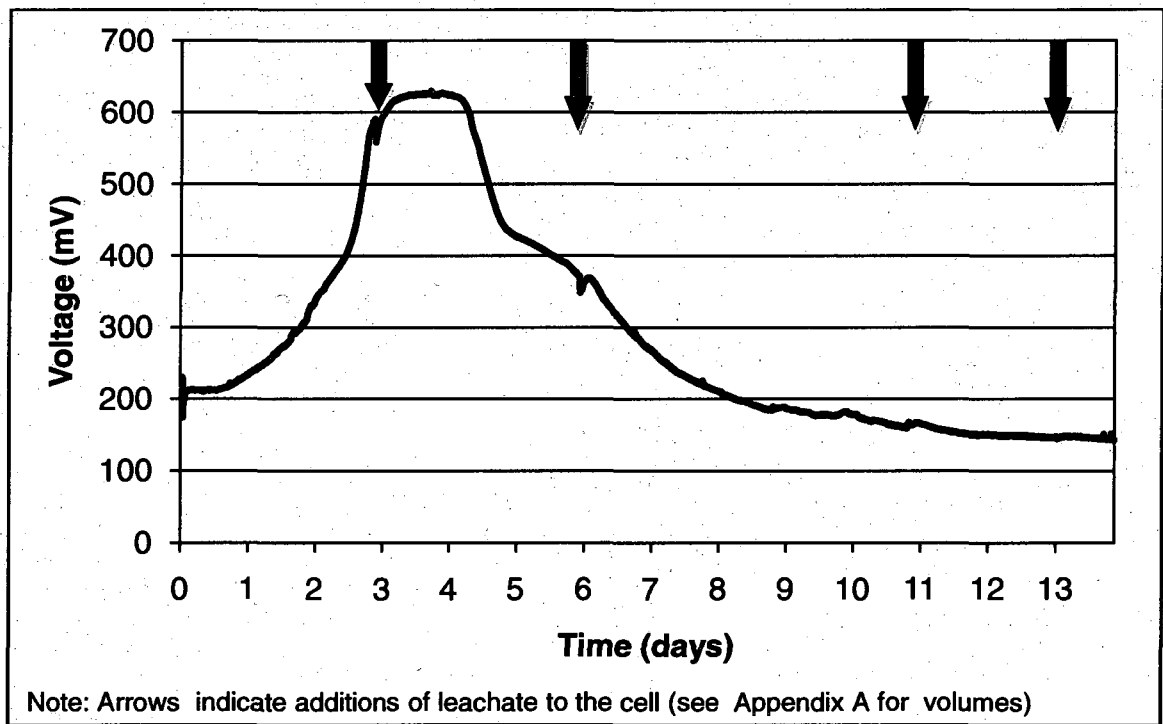


Figure 4.15 Larger Scale MFC, cycle 1c, voltage vs. time (2/02/09 – 2/16/09)

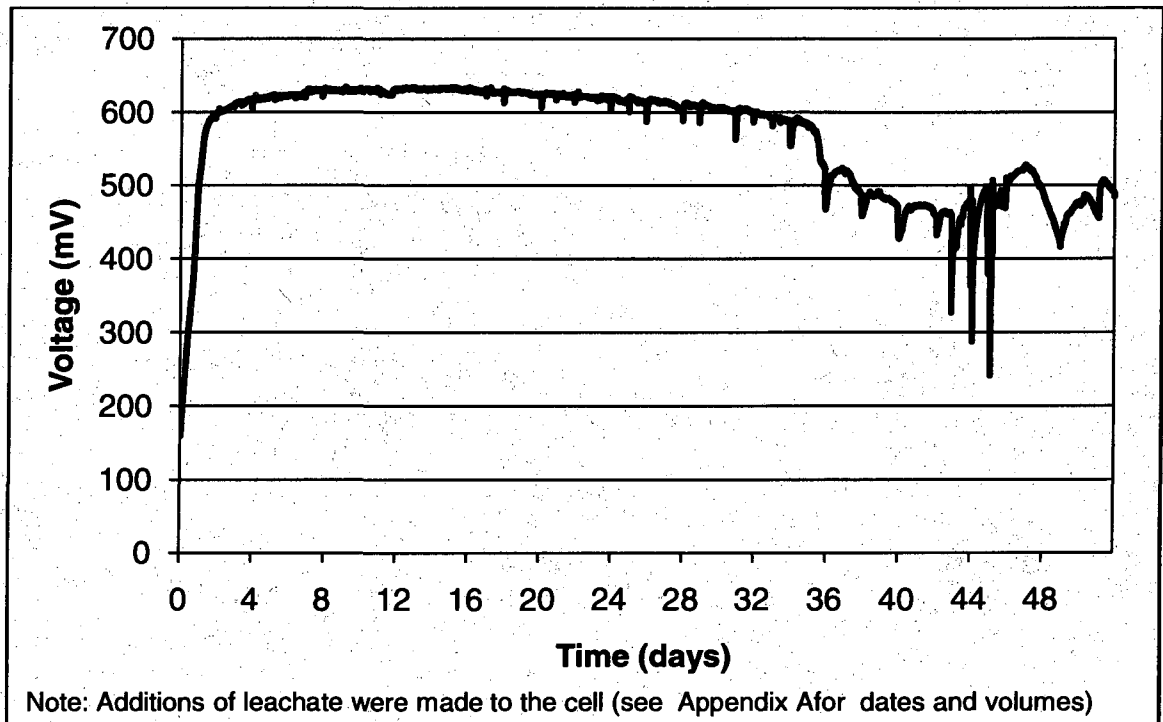


Figure 4.16 Larger Scale MFC, cycle 2c, voltage vs. time (2/16/09 – 4/09/09)

Table 4.5 Summary of voltage production for Larger Scale MFC, cycles 1c-2c

	Run 1c	Run 2c
Start Date	2/2/09	2/16/09
Start Voltage (mV)	229.6	162.7
Peak Voltage Date	2/6/09	2/24/09
Peak Voltage (mV)	629.7	635.0
Time to Peak Voltage (days)	3.7	8.0
Date of End Voltage	2/16/09	4/09/09
End Voltage (mV)	143.1	484
Total Run Time (days)	13.9	52

#### **4.2.4 Power Density and Coulombic Efficiency**

Power densities for both the Square and Circle MFCs were calculated using equations (2-8) and (2-9) (Sample calculations can be found on page 141-



142 of Appendix C). To obtain voltages to use for these calculations, power density curves were completed for each design. The open circuit voltage (OCV) of an MFC is the maximum voltage that can be obtained at infinite external resistance. Once the MFC has been operated at this condition and the maximum OCV has been reached, the external resistance is subsequently reduced and voltage is recorded (once it has stabilized) at each resistance. For this research, resistance ranged from 40,000 $\Omega$  (10,000 $\Omega$  for Square) to 10 $\Omega$ . Power density is then calculated in units of mW/m<sup>2</sup> or mW/m<sup>3</sup> depending on if it is normalized to surface area of the anode or volume. Power density curves are shown in Figures 4.17 and 4.18 for the Circle MFC and Figure 4.19 for the Square MFC.

A polarization curve has also been graphed with power density in Figures 4.17, 4.18 and 4.19. This curve is the current density, calculated from voltage, external resistance and anode surface area, versus the recorded cell voltage (Sample calculations can be found on page 142 of Appendix C). Polarization curves illustrate how well the MFC can maintain voltage as a function of current production. This curve is characterized by three general regions of decrease; an initial region with a fast voltage drop, a linear decrease in voltage, and a second rapid voltage drop when current density is at the greatest (Logan 2008). These three regions of decrease are a result of activation losses, bacterial metabolic losses, mass transfer losses, and ohmic losses. Activation losses are generally shown in the first region of voltage decrease; however none of the polarization curves (Figures 4.17, 4.18 and 4.19) experienced an initial rapid decrease of

voltage. This did not appear to be an anomaly as both power density curves from each trial of the Circle and Square MFC resulted in similar plots.

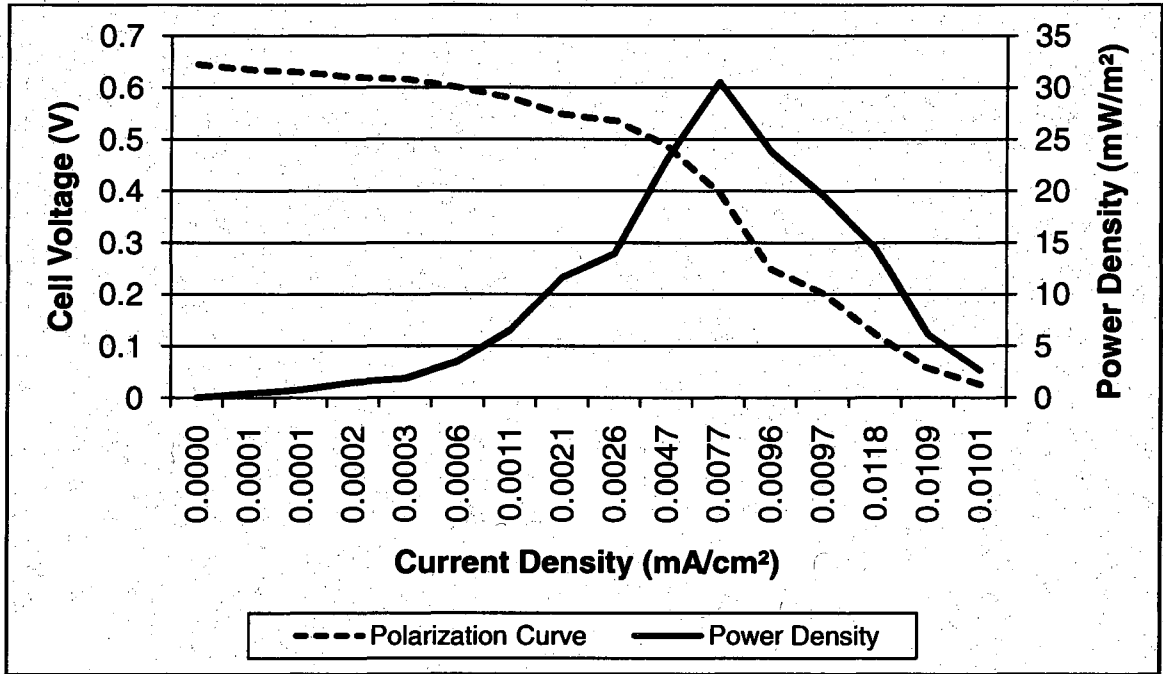


Figure 4.17 Power density and polarization curve (1) for Circle MFC

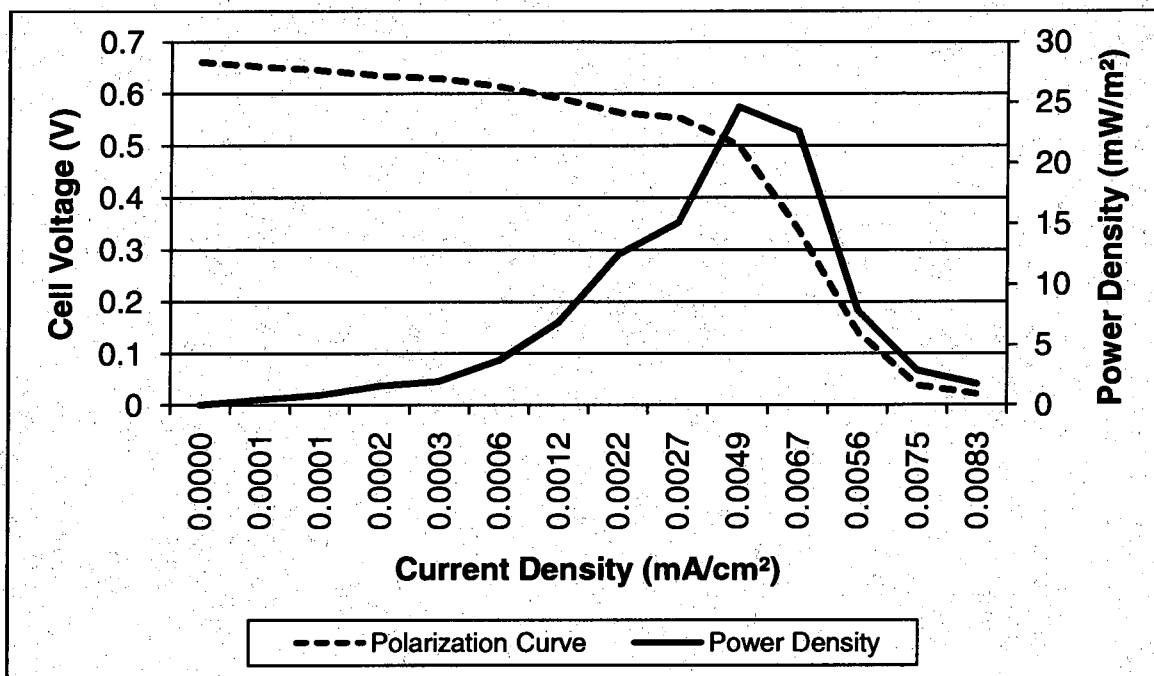


Figure 4.18 Power density and polarization curve (2) for Circle MFC

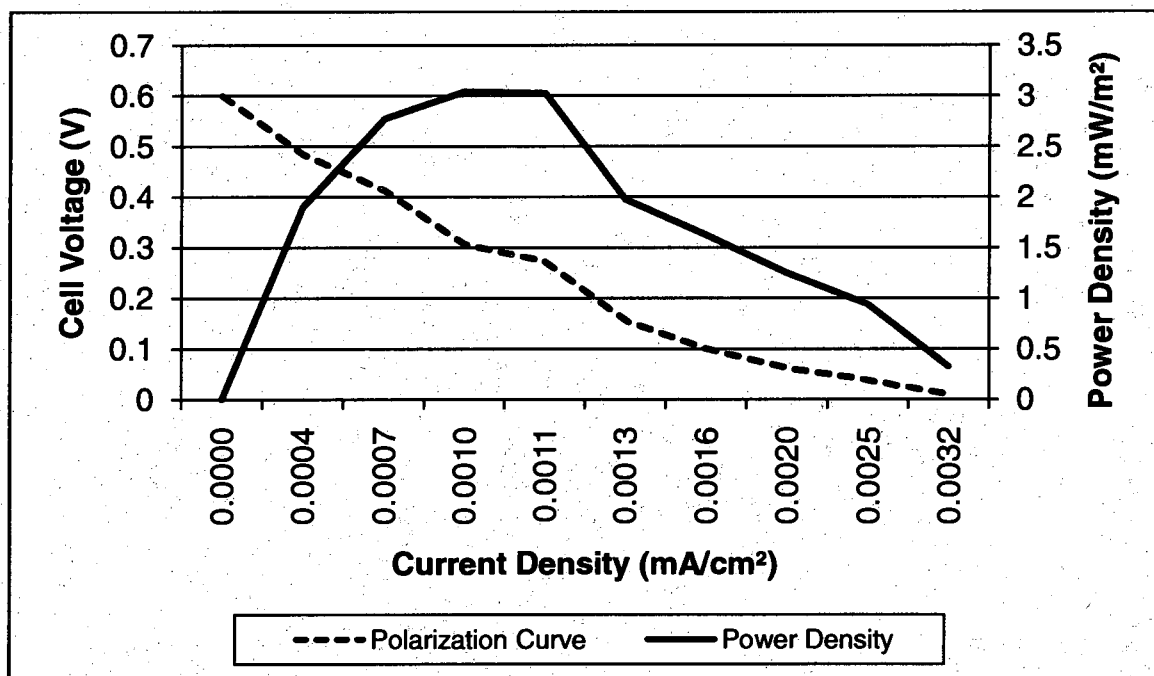


Figure 4.19 Power density and polarization curve for Square MFC

Power densities for the Square MFC were 3 mW/m<sup>2</sup> and 94 mW/m<sup>3</sup>. Maximum power densities for the Circle MFC were 24-31 mW/m<sup>2</sup> or 669-844 mW/m<sup>3</sup>. There have only been two other sets of research published utilizing landfill leachate in MFCs. However, because of varying architectures and operation differences, a direct comparison of results is difficult. One study obtained a power density of 6817.4 mW/m<sup>3</sup>, using landfill leachate in a small 40 mL volume single chamber MFC, using dilute leachate and anaerobic sludge inoculum (You et al. 2006). The greater power density of the You et al. (2006) research can be attributed to the smaller scale MFC and the amended leachate substrate. Another study found in the literature utilized a tubular MFC with a membrane and a continuous feed of leachate and recorded a maximum power density of 1.38 mW/m<sup>2</sup> (Greenman et al. 2009). Similar to the Square and Circle MFCs, the MFCs in this literature study were not inoculated with any outside source of bacteria and had a volume of approximately 0.9 L. Both the Square and Circle MFC outperformed the max power densities of the tubular design.

Looking beyond the use of landfill leachate in MFCs, the variability in results is large for many types of MFC systems. The results of this research are compared with the findings of research utilizing different types of wastewaters as well as the two studies using landfill leachate in Table 4.6. These systems are not directly comparable to this research due to high variations in operation and design.

Table 4.6 Comparison of results with values from the literature

Type	Substrate	Vol. (mL)	Power Density (mW/m <sup>2</sup> )	COD removal (%)	C <sub>E</sub> (%)	Source
Single Chamber, cylinder	Brewery Wastewater	28	205	87	10	Feng et al. 2008
Single Chamber, cylinder	Paper Recycling Wastewater w/ 50 mM PBS	300	144 ± 7 501 ± 20	51 ± 2 76 ± 4	NR* 16 ± 2	Huang and Logan 2008
Single Chamber, cylinder	Swine Wastewater	28	228	84	NR*	Kim et al. 2008
Single Chamber, cylinder	Swine Wastewater	28	261	86 ± 6	8	Min et al. 2005
Single Chamber, Plate	Domestic Wastewater	22	72 ± 1	42	NR*	Min and Logan 2004
Single Chamber, tubular	Domestic Wastewater	388	9	50-70	NR*	Liu, Ramarayanan and Logan 2004
Single Chamber, cylinder	Landfill Leachate (dilute)	40	6817.4 mW/m <sup>3</sup>	70-98	3.4	You et al. 2006
Single Chamber, column	Landfill Leachate	900	1.38	57-66 (BOD)	NR*	Greenman et al. 2009
Single Chamber, Square	Landfill Leachate	995	4	43	17	This Research
Single Chamber, Circular	Landfill Leachate	934	31	48	41	This Research

\*NR = No Result

Coulombic efficiency,  $C_E$ , (the fraction of electrons that are recovered as current versus the electrons that were in the starting substrate) is a calculation that is often used to describe the efficiency of MFC systems.  $C_E$  was calculated for all cycles of each MFC using equation (2-11) and all results are shown in Table 4.7 (Sample calculations can be found on page 143 of Appendix C). It should be noted that there are large ranges of  $C_E$  values for all of the designs and this is most likely due to inefficient use of the leachate for purely voltage production. When complex substrates are used in MFCs,  $C_E$  is calculated based upon COD removals as a representation of the amount of organic degradation being achieved in the system. Because COD removals were inconsistent in this research, possibly due to interference from inorganics in the measurement,  $C_E$  values may not be accurate representations of efficiencies. A negative  $C_E$  value represents an increase in COD values during the cycle of the MFC. This system is focused on both treatment of the leachate as well as electricity production, thus  $C_E$  values were not extremely important characteristics. The work of You et al. recorded a  $C_E$  of 3.4%, while Greenman et al. did not specify a value when using landfill leachate. This low value, along with the low values found in this research, are attributable to the complex nature of leachate and the organic substrate that is contained within it. Coulombic efficiencies of other MFCs utilizing wastewaters can be found in Table 4.6.

Table 4.7 Coulombic efficiencies for all MFC designs and cycles

Square MFC		Circle MFC		Larger Scale MFC	
Cycle	C <sub>E</sub> (%)	Cycle	C <sub>E</sub> (%)	Cycle	C <sub>E</sub> (%)
1a	150.3	1b	7.9	1c	5.2
2a	10.1	2b	11.2	2c	-13.6
3a	17.1	3b	41.0		
4b	6.4	4b	9.3		
5b	11.1	5c	-21.1		
6b	14.5	6c	29.4		
b	3.9	7c	-247.2		

### **4.3 Leachate Characterization**

Terminology that is used is as follows; influent refers to the values prior to placement in the MFC, effluent values were recorded at the end of the cycle and the percent difference in these values was then calculated. A negative value in percent difference means that there was an increase of that particular constituent during MFC operation.

#### **4.3.1 Square MFC**

Data from initial testing of the Square MFC, cycles 1-3a is displayed in Table 4.8, 4.9 and 4.10. This testing was completed using leachate from the influent of the leachate treatment facility. Data from further testing in conjunction with the Circle MFC using leachate from TLR III, Phase 1 (cycles 4-7b) is given in Table 4.11, 4.12, 4.13 and 4.14. All of these results will be discussed in detail in section 4.3.4, however all of the influent values were within the range that leachate from municipal solid waste landfills is typically observed (Table 2.1, Kjeldsen et al. 2002).

Table 4.8 Leachate characterization, Square MFC, cycle 1a (1/10/08 – 1/28/08)

	Influent	Effluent	% Difference
Temperature (°C)	23.4	20.3	13.4%
pH	7.8	8.9	-13.5%
Conductivity (mS/cm)	13.7	11.5	16.3%
DO (mg/L)	1.2	1.7	-40.7%
ORP (mV)	-73.6	95.7	230.0%
	mg/L	mg/L	%
COD	1975	1942	1.7%
BOD	240	122	49.2%
Alkalinity	4500	2800	37.8%
Ammonia	954	521	45.4%
Chloride	2178	2729	-25.3%
Nitrate <sup>a</sup>	0.05	0.05	0.0%
Nitrite <sup>b</sup>	2.0	2.0	0.0%
Phosphate	4.4	3.4	23.0%
Sulfate	12	17	-39.0%
Total Phosphorus	7.2	6.9	4.4%

<sup>a</sup> 0.05 Detection Limit    <sup>b</sup> 2.0 Detection Limit

Table 4.9 Leachate characterization, Square MFC, cycle 2a (1/31/08 – 2/11/08)

	Influent	Effluent	% Difference
Temperature (°C)	21.8	20.5	5.9%
pH	7.8	8.9	-14.5%
Conductivity (mS/cm)	14.3	14.1	1.8%
DO (mg/L)	1.2	0.67	42.2%
ORP (mV)	-21.1	14.6	169.2%
	mg/L	mg/L	%
COD	1925	1642	14.7%
Alkalinity	4200	2600	38.1%
Ammonia	925	502	45.7%
Chloride	2715	3407	-25.5%
Nitrate <sup>a</sup>	0.05	0.05	0.0%
Nitrite <sup>b</sup>	2	2	0.0%
Phosphate	2.7	3.2	-15.8%
Sulfate	8	15	-83.0%
Total Phosphorus	4.9	5	-0.4%

<sup>a</sup> 0.05 Detection Limit    <sup>b</sup> 2.0 Detection Limit



Table 4.10 Leachate characterization, Square MFC, cycle 3a (2/11/08 – 2/22/08)

	Influent	Effluent	% Difference
Temperature (°C)	20.9	20.3	2.9%
pH	7.8	8.9	-14.0%
Conductivity (mS/cm)	15.0	13.5	9.7%
DO (mg/L)	0.35	0.58	-65.7%
ORP (mV)	-25.7	41.2	260.3%
	mg/L	mg/L	%
COD	1950	1600	17.9%
Alkalinity	4200	2700	35.7%
Ammonia	898	358	60.1%
Chloride	2597	3197	-23.1%
Nitrate <sup>a</sup>	0.93	0.05	0.0%
Nitrite <sup>b</sup>	2	2	0.0%
Phosphate	3.3	2.8	16.6%
Sulfate	8.5	14.4	-70.5%
Total Phosphorus	5.8	4.4	23.5%

<sup>a</sup> 0.05 Detection Limit    <sup>b</sup> 2.0 Detection Limit

Table 4.11 Leachate characterization, Square MFC, cycle 4b (8/7/08 – 8/18/08)

	Influent	Effluent	% Difference
Temperature (°C)	21.7	21.4	1.3%
pH	7.4	8.8	-17.9%
Conductivity (mS/cm)	17.3	14.7	15.3%
DO (mg/L)	0.14	0.38	-171.4%
ORP (mV)	-117	-52.5	55.1%
	mg/L	mg/L	%
COD	3204	2422	24.4%
Alkalinity	5200	4200	19.2%
Ammonia	940	490	47.9%
Chloride	1800	2200	-22.2%
Nitrate <sup>a</sup>	0.05	0.05	0.0%
Nitrite <sup>b</sup>	2	2	0.0%
Phosphate	8.6	7.6	11.6%
Sulfate	38	42	-10.5%
Total Phosphorus	52	7.5	85.6%

<sup>a</sup> 0.05 Detection Limit    <sup>b</sup> 2.0 Detection Limit

Table 4.12 Leachate characterization, Square MFC, cycle 5b (8/18/08 – 9/5/08)

	Influent	Effluent	% Difference
Temperature (°C)	17.6	20.9	-18.6%
pH	8.2	8.6	-5.4%
Conductivity (mS/cm)	16.2	14.5	10.4%
DO (mg/L)	0.36	0.91	-152.8%
ORP (mV)	-191.5	39.5	120.6%
	mg/L	mg/L	%
COD	3006	2533	15.7%
Alkalinity	5200	4500	13.5%
Ammonia	940	290	69.1%
Chloride	1800	2600	-44.4%
Nitrate <sup>a</sup>	0.05	0.05	0.0%
Nitrite <sup>b</sup>	2	2	0.0%
Phosphate	8.6	8.1	5.8%
Sulfate	38	66	-73.7%
Total Phosphorus	52	4.9	90.6%

<sup>a</sup> 0.05 Detection Limit    <sup>b</sup> 2.0 Detection Limit

Table 4.13 Leachate characterization, Square MFC, cycle 6b (9/16/08–9/24/08)

	Influent	Effluent	% Difference
Temperature (°C)	15.1	20.2	-33.6%
pH	7.8	8.7	-10.7%
Conductivity (mS/cm)	11.2	11	2.4%
DO (mg/L)	1.2	1.9	-59.2%
ORP (mV)	52.5	12.9	75.4%
	mg/L	mg/L	%
COD	908	732	19.4%
BOD	140	NR*	NR*
TOC	310	230	25.8%
Alkalinity	3800	3600	5.3%
Ammonia	1000	820	18.0%
Chloride	1200	1500	-25.0%
Nitrate <sup>a</sup>	0.05	0.05	0.0%
Nitrite <sup>b</sup>	2	9.6	-7.6%
Phosphate	2.3	3.2	-39.1%
Sulfate	39	68	-74.4%
Sulfide	NR*	NR*	NR*
Total Phosphorus	3.3	3.6	-9.1%

\*NR = No Result    <sup>a</sup> 0.05 Detection Limit    <sup>b</sup> 2.0 Detection Limit

Table 4.14 Leachate characterization, Square MFC, cycle 7b (9/24/08–10/3/08)

	Influent	Effluent	% Difference
Temperature (°C)	8.7	21.1	-142.9%
pH	7.8	8.6	-9.8%
Conductivity (mS/cm)	11.8	10.6	10.6%
DO (mg/L)	0.83	1.27	-53.0%
ORP (mV)	73	79.4	-8.8%
	mg/L	mg/L	%
COD	1075	614	42.9%
BOD	NR*	NR*	NR*
TOC	NR*	NR*	NR*
Alkalinity	3800	3300	13.2%
Ammonia	1000	520	48.0%
Chloride	1200	1500	-25.0%
Nitrate <sup>a</sup>	0.05	0.05	0.0%
Nitrite <sup>b</sup>	2	2	0.0%
Phosphate	2.3	2.7	-17.4%
Sulfate	39	66	-69.2%
Sulfide	NR*	NR*	NR*
Total Phosphorus	3.3	3.6	-9.1%

\*NR = No Result <sup>a</sup> 0.05 Detection Limit <sup>b</sup> 2.0 Detection Limit

### **4.3.2 Circle MFC**

Data from initial testing of the Circle MFC, cycles 1-4b, is displayed in Tables 4.15, 4.16, 4.17 and 4.18. This testing was completed using leachate from the TLR III, Phase 1. Further cycles were completed to test for COD, BOD, TOC, and sulfide characteristics of influent and effluent leachate into the system. A full set of BOD, TOC, and sulfide data was not collected in the previous cycles due to numerous constraints and equipment failures. Testing in these cycles, 1-3c, was completed using landfill leachate from TLR III, Phase 2. Data from these tests can be found in Tables 4.19, 4.20 and 4.21. All of these results will be discussed at length in section 4.3.4, however all of the influent values were within

the range that leachate from municipal solid waste landfills is typically observed (Table 2.1, Kjeldsen et al. 2002)

Table 4.15 Leachate characterization, Circle MFC, cycle 1b (8/7/08 – 8/23/08)

	Influent	Effluent	% Difference
Temperature (°C)	21.7	21.3	2.0%
pH	7.4	8.6	-16.1%
Conductivity (mS/cm)	17.3	14.4	17.0%
DO (mg/L)	0.14	1.06	-657.1%
ORP (mV)	-117	26.3	122.5%
	mg/L	mg/L	%
COD	3204	2042	36.3%
Alkalinity	5200	4300	17.3%
Ammonia	940	690	26.6%
Chloride	1800	2100	-16.7%
Nitrate <sup>a</sup>	0.05	0.05	0.0%
Nitrite <sup>b</sup>	2	2	0.0%
Phosphate	8.6	9.8	-14.0%
Sulfate	38	250	-557.9%
Total Phosphorus	52	9.9	81.0%

<sup>a</sup> 0.05 Detection Limit    <sup>b</sup> 2.0 Detection Limit

Table 4.16 Leachate characterization, Circle MFC, cycle 2b (8/23/08 – 9/9/08)

	Influent	Effluent	% Difference
Temperature (°C)	9.9	20.4	-104.8%
pH	8.5	8.3	2.7%
Conductivity (mS/cm)	6.7	14.7	-121.2%
DO (mg/L)	0.6	0.61	-1.7%
ORP (mV)	-18.7	-4.1	78.1%
	mg/L	mg/L	%
COD	3017	2161	28.4%
Alkalinity	5200	3900	25.0%
Ammonia	940	870	7.4%
Chloride	1800	2000	-11.1%
Nitrate <sup>a</sup>	0.05	0.05	0.0%
Nitrite <sup>b</sup>	2	2	0.0%
Phosphate	8.6	8.6	0.0%
Sulfate	38	64	-68.4%
Total Phosphorus	52	5.3	89.8%

<sup>a</sup> 0.05 Detection Limit <sup>b</sup> 2.0 Detection Limit

Table 4.17 Leachate characterization, Circle MFC, cycle 3b (9/15/08 – 9/24/08)

	Influent	Effluent	% Difference
Temperature (°C)	15.1	20.5	-35.8%
pH	7.8	8.6	-9.8%
Conductivity (mS/cm)	11.2	10.5	6.1%
DO (mg/L)	1.2	0.85	29.2%
ORP (mV)	52.5	NR	NR
	mg/L	mg/L	%
COD	908	773	14.9%
BOD	140	NR*	NR*
TOC	310	200	35.5%
Alkalinity	3800	3600	5.3%
Ammonia	1000	820	18.0%
Chloride	1200	1300	-8.3%
Nitrate <sup>a</sup>	0.05	0.05	0.0%
Nitrite <sup>b</sup>	2	2	0.0%
Phosphate	2.3	3.6	-56.5%
Sulfate	39	58	-48.7%
Sulfide	NR*	NR*	NR*
Total Phosphorus	3.3	3.8	-15.2%

\*NR = No Result <sup>a</sup> 0.05 Detection Limit <sup>b</sup> 2.0 Detection Limit

Table 4.18 Leachate characterization, Circle MFC, cycle 4b (9/24/08 –10/3/08)

	Influent	Effluent	% Difference
Temperature (°C)	8.7	20.2	-132.8%
pH	7.8	8.6	-9.1%
Conductivity (mS/cm)	11.8	10.4	12.4%
DO (mg/L)	0.83	1.12	-34.9%
ORP (mV)	73	59.2	18.9%
	mg/L	mg/L	%
COD	1075	556	48.3%
Alkalinity	3800	3500	7.9%
Ammonia	1000	710	29.0%
Chloride	1200	1400	-16.7%
Nitrate <sup>a</sup>	0.05	0.05	0.0%
Nitrite <sup>b</sup>	2	2	0.0%
Phosphate	2.3	2.9	-26.1%
Sulfate	39	61	-56.4%
Total Phosphorus	3.3	3.2	3.0%

<sup>a</sup> 0.05 Detection Limit    <sup>b</sup> 2.0 Detection Limit

Table 4.19 Leachate characterization, Circle MFC, cycle 1c (1/16/09 – 2/2/09)

	Influent	Effluent	% Difference
Temperature (°C)	23.3	19.8	15.2%
pH	7.6	8.6	-12.2%
Conductivity (mS/cm)	19.3	19.1	0.9%
DO (mg/L)	0.18	0.28	-55.6%
ORP (mV)	-49.2	-67.7	-37.6%
	mg/L	mg/L	%
COD	1934	2265	-17.1%
BOD	200	65	67.5%
TOC	1200	1300	-8.3%
Sulfide	0.28	0.13	54.5%

Table 4.20 Leachate characterization, Circle MFC, cycle 2c (2/2/09 – 2/16/09)

	Influent	Effluent	% Difference
Temperature (°C)	21	19.4	7.7%
pH	7.8	8.2	-5.9%
Conductivity (mS/cm)	16.9	16.4	3.1%
DO (mg/L)	0.63	0.16	74.6%
ORP (mV)	-30	-85.6	-185.3%
	mg/L	mg/L	%
COD	2054	1900	7.5%
BOD	180	84	53.3%
TOC	1200	1000	16.7%
Sulfide	0.23	0.15	34.8%

Table 4.21 Leachate characterization, Circle MFC, cycle 3c (2/16/09 – 3/12/09)

	Influent	Effluent	% Difference
Temperature (°C)	22.8	19.9	12.7%
pH	7.6	8.1	-7.1%
Conductivity (mS/cm)	17.2	16.7	2.8%
DO (mg/L)	0.25	0.41	-64.0%
ORP (mV)	-17.7	-73.7	-316.4%
	mg/L	mg/L	%
COD	2718	2765	-1.8%
BOD	430	120	72.1%
TOC	1400	660	52.9%
Sulfide	0.21	0.02	88.9%

### **4.3.3 Larger Scale MFC**

Data from testing of the Larger Scale MFC, cycles 1-2c, is displayed in Tables 4.22 and 4.23. This testing was completed using leachate from the TLR III, Phase 2. All of these results will be discussed at length in section 4.3.4, however all of the influent values were within the range that leachate from

municipal solid waste landfills is typically observed (Table 2.1, Kjeldsen et al. 2002)

Table 4.22 Leachate characterization, Larger Scale MFC, cycle 1c (2/2/09–2/16/09)

	Influent	Effluent	% Difference
Temperature (°C)	201	18.5	11.7%
pH	7.8	8.5	-9.7%
Conductivity (mS/cm)	16.9	15.4	8.6%
DO (mg/L)	0.63	0.16	74.6%
ORP (mV)	-30	-32	-6.7%
	mg/L	mg/L	%
COD	2054	1990	3.1%
BOD	180	95	47.2%
TOC	1200	1200	0.0%
Alkalinity	5500	4900	10.9%
Ammonia	1000	1200	-20.0%
Chloride	1800	1900	-5.6%
Nitrate*	0.05	0.05	0.0%
Nitrite**	2	2	0.0%
Phosphate	7.7	8.6	-11.7%
Sulfate	140	170	-21.4%
Sulfide	0.23	0.15	33.9%
Total Phosphorus	12	8.7	27.5%

<sup>a</sup> 0.05 Detection Limit    <sup>b</sup> 2.0 Detection Limit



Table 4.23 Leachate characterization, Larger Scale MFC, cycle 2c (2/16/09 – 4/9/09)

	Influent	Effluent	% Difference
Temperature (°C)	22.8	19.3	15.5%
pH	7.6	8.6	-12.5%
Conductivity (mS/cm)	17.2	16.1	5.9%
DO (mg/L)	0.25	0.2	20.0%
ORP (mV)	-17.7	-277	-1465.0%
	mg/L	mg/L	%
COD	2718	2897	-6.6%
BOD	430	61	85.8%
TOC	1400	710	50.7%
Alkalinity	5700	4700	17.5%
Ammonia	1300	520	60.0%
Chloride	1500	2400	-60.0%
Nitrate*	0.05	0.05	0.0%
Nitrite**	2	2	0.0%
Phosphate	12	6.1	49.2%
Sulfate	69	140	-102.9%
Sulfide	0.21	0.21	0.0%
Total Phosphorus	11	3.6	67.3%

<sup>a</sup> 0.05 Detection Limit    <sup>b</sup> 2.0 Detection Limit

#### **4.3.4 Leachate Characterization Analysis**

A large amount of data was recorded from all of the cycles of the three MFC designs. The following section will focus on analyzing the percent differences in influent and effluent values and the reasons behind these changes. Similarities and differences between the data of the three designs will also be discussed. Percent difference summary tables for all cycles of the MFC designs are in Tables 4.24, 4.25, 4.26, 4.27 and 4.28.

Table 4.24 Percent difference for Square MFC, cycles 1-3 a

	1 a % Difference	2 a % Difference	3 a % Difference
Temperature (°C)	13.4%	5.9%	2.9%
pH	-13.5%	-14.5%	-14.0%
Conductivity (mS/cm)	16.3%	1.8%	9.7%
DO (mg/L)	-40.7%	42.2%	-65.7%
ORP (mV)	230.0%	169.2%	260.3%
COD	1.7%	14.7%	17.9%
BOD	49.2%	NR*	NR*
Alkalinity	37.8%	38.1%	35.7%
Ammonia	45.4%	45.7%	60.1%
Chloride	-25.3%	-25.5%	-23.1%
Nitrate	0.0%	0.0%	0.0%
Nitrite	0.0%	0.0%	0.0%
Phosphate	23.0%	-15.8%	16.6%
Sulfate	-39.0%	-83.0%	-70.5%
Total Phosphorus	4.4%	-0.4%	23.5%

\*NR = No Result

Table 4.25 Percent difference for Square MFC, cycles 4-7 b

	4 b % Difference	5 b % Difference	6 b % Difference	7 b % Difference
Temperature (°C)	1.3%	-18.6%	-33.6%	-142.9%
pH	-17.9%	-5.4%	-10.7%	-9.8%
Conductivity (mS/cm)	15.3%	10.4%	2.4%	10.6%
DO (mg/L)	-171.4%	-152.8%	-59.2%	-53.0%
ORP (mV)	55.1%	120.6%	75.4%	-8.8%
COD	24.4%	15.7%	19.4%	42.9%
Alkalinity	19.2%	13.5%	5.3%	13.2%
Ammonia	47.9%	69.1%	18.0%	48.0%
Chloride	-22.2%	-44.4%	-25.0%	-25.0%
Nitrate	0.0%	0.0%	0.0%	0.0%
Nitrite	0.0%	0.0%	0.0%	0.0%
Phosphate	11.6%	5.8%	-39.1%	-17.4%
Sulfate	-10.5%	-73.7%	-74.4%	-69.2%
Total Phosphorus	85.6%	90.6%	-9.1%	-9.1%

\*NR = No Result

Table 4.26 Percent difference for Circle MFC, cycles 1-4 b

	1 b % Difference	2 b % Difference	3 b % Difference	4 b % Difference
Temperature (°C)	2.0%	-104.8%	-35.8%	-132.8%
pH	-16.1%	2.7%	-9.8%	-9.1%
Conductivity (mS/cm)	17.0%	-121.2%	6.1%	12.4%
DO (mg/L)	-657.1%	-1.7%	29.2%	-34.9%
ORP (mV)	122.5%	78.1%	NR*	18.9%
COD	36.3%	28.4%	14.9%	48.3%
Alkalinity	17.3%	25.0%	5.3%	7.9%
Ammonia	26.6%	7.4%	18.0%	29.0%
Chloride	-16.7%	-11.1%	-8.3%	-16.7%
Nitrate	0.0%	0.0%	0.0%	0.0%
Nitrite	0.0%	0.0%	0.0%	0.0%
Phosphate	-14.0%	0.0%	-56.5%	-26.1%
Sulfate	-557.9%	-68.4%	-48.7%	-56.4%
Total Phosphorus	81.0%	89.8%	-15.2%	3.0%

\*NR = No Result

Table 4.27 Percent difference for Circle MFC, cycles 1-3 c

	1 c % Difference	2 c % Difference	3 c % Difference
Temperature (°C)	15.2%	7.7%	12.7%
pH	-12.2%	-5.9%	-7.1%
Conductivity (mS/cm)	0.9%	3.1%	2.8%
DO (mg/L)	-55.6%	74.6%	-64.0%
ORP (mV)	-37.6%	-185.3%	-316.4%
COD	-17.1%	7.5%	-1.8%
BOD	67.5%	53.3%	72.1%
TOC	-8.3%	16.7%	52.9%
Sulfide	54.5%	34.8%	88.9%

Table 4.28 Percent difference for Larger Scale MFC, cycles 1-2 c

	1 c % Difference	2 c% Difference
Temperature (°C)	11.7%	15.5%
pH	-9.7%	-12.5%
Conductivity (mS/cm)	8.6%	5.9%
DO (mg/L)	74.6%	20.0%
ORP (mV)	-6.7%	-1465.0%
COD	3.1%	-6.6%
BOD	47.2%	85.8%
TOC	0.0%	50.7%
Alkalinity	10.9%	17.5%
Ammonia	-20.0%	60.0%
Chloride	-5.6%	-60.0%
Nitrate	0.0%	0.0%
Nitrite	0.0%	0.0%
Phosphate	-11.7%	49.2%
Sulfate	-21.4%	-102.9%
Sulfide	33.9%	0.0%
Total Phosphorus	27.5%	67.3%

### pH.

There were a total of 15 cycles of operation completed for this research. In every cycle except one, there was an increase in pH, independent from design or size of the MFC (Figure 4.20). These increases were in the range of 5.4% to 17.9%, with the one decrease occurring in the Circle MFC (2.7%). While it is common for the pH to change at the anode of an MFC during operation; it is generally a decrease to a more acidic level. This is due to incomplete transfer of protons to the cathode and a resulting build up at the anode which reduces the pH. However in other research using landfill leachate, a slight increase in pH was also observed during MFC operation. This was attributed to a possible

removal of acid components present in the leachate, such as volatile fatty acids, during MFC operation (Greenman et al. 2009). Leachate is a highly buffered system as well and sulfides in the leachate can accept protons and limit pH decrease (Jambeck, Townsend, and Solo-Gabriele 2008).

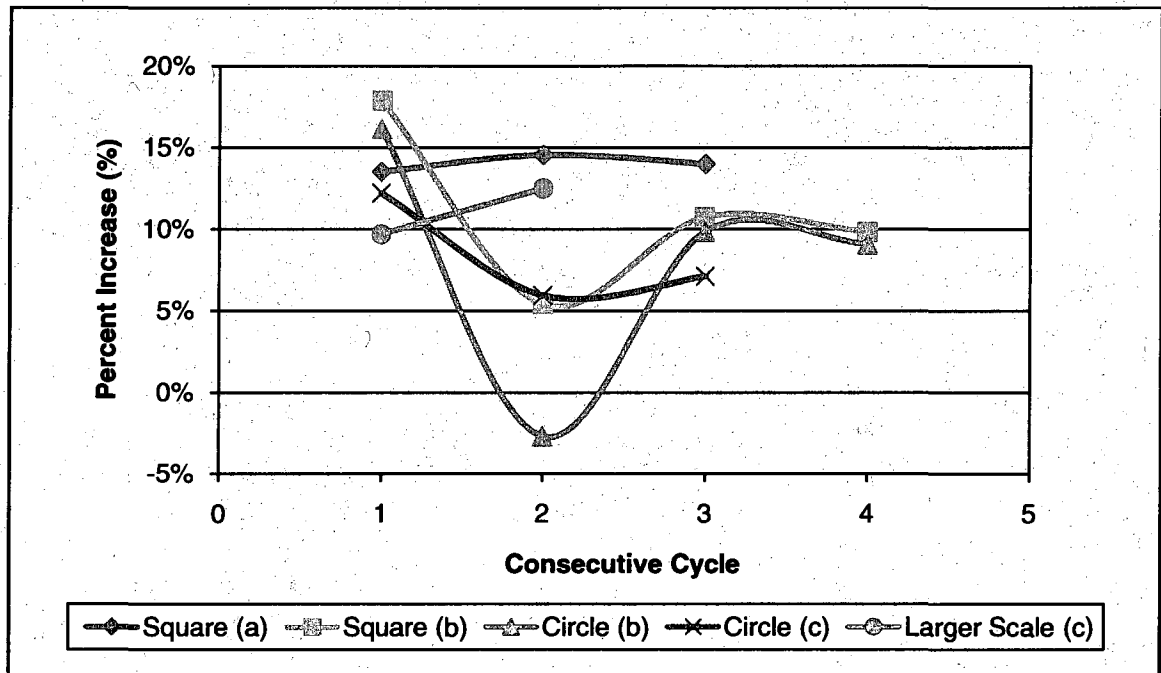


Figure 4.20 Percent increase of pH for all cycles of MFC designs

### Conductivity.

The ability of a solution to conduct current is based upon the ions in solution and has been termed conductivity. The movement of ions in the solution transports the current, thus conductivity increases as the ion concentrations increase (Snoeyink and Jenkins 1980). There has been substantial research done in recent years that shows conductivity is a key factor in the efficiency of the MFC system. Conductivity, through the increase in ionic strength, has had to

be increased in many wastewaters and artificial substrates that are used in MFCs (Huang and Logan 2008; Liu, Cheng and Logan 2005; Liu et al 2008; Logan et al. 2007; Oh and Logan 2006) This is one of the major benefits to using landfill leachate as a substrate in MFCs for conductivity is at high levels initially. Influent conductivity was in the range of 11.22 – 19.26 mS/cm, with one low reading of 6.66 mS/cm. Effluent readings were in the range of 10.57-10.09 mS/cm, creating a range of decrease in levels from 0.9 – 16.3% (with one exception in cycle 2b where conductivity was increased).

#### Dissolved Oxygen.

Figure 4.21 shows the influent and effluent concentrations of DO for all cycles of all MFC designs. Landfill leachate is generally an anaerobic substrate with low DO levels, which were variable throughout sampling and testing of the MFCs in this research. Increases in DO concentrations within the MFC systems during operation would be due to the system being open to the air. An aerobic zone could have formed near the cathode and resulted in increases of DO. For the cycles where a decrease in DO occurred, anaerobic conditions within the system were more efficient and a larger anaerobic zone was allowed to control the system and reduce DO.

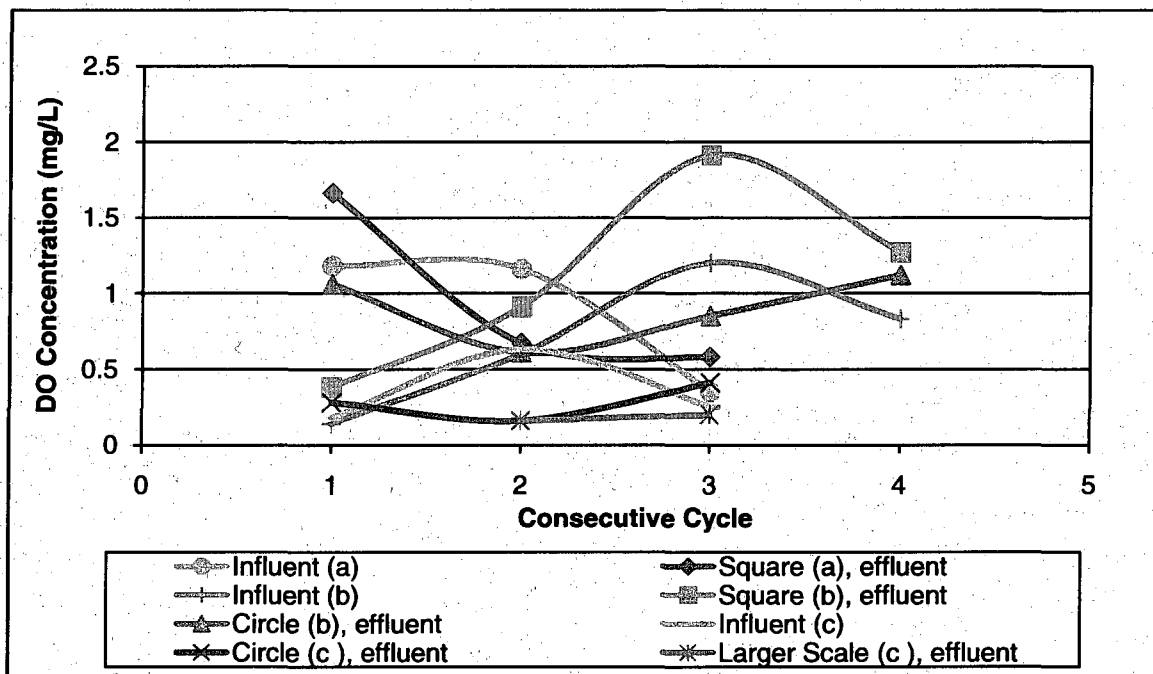


Figure 4.21 DO concentration of influent and effluent leachate for all cycles

### Oxidation Reduction Potential (ORP)

ORP is a useful measure of the state of the system being tested, as well as the degree of treatment. An aerobic system (oxygen present) will be displayed as a positive reading, while an anaerobic system (no oxygen) will display a negative ORP reading. ORP measures the tendency of a solution to gain or lose electrons (Snoeyink and Jenkins 1980). Landfills are generally anaerobic systems, so the leachate flowing through them is usually anaerobic with negative ORP values. Two exceptions to this anaerobic condition were the influent leachate from TLR II, Phase 2 during cycle 3 and 4b for the Circle MFC and cycle 5 and 7 b for the Square MFC. These influent values were +52.5 mV and +73 mV respectively for the Square and Circle MFCs. This suggests that the leachate entering the MFC was actually aerobically active. Interestingly, these

cycles also had significantly shorter total cycle time for both of the MFC designs, as shown in Tables 4.2 and 4.3, and Figure 4.22. However, a connection cannot be definitively made between ORP and cycle time due to the concomitant changing values of other constituents.

For all other incoming leachate samples, a range of negative ORP values were obtained, however ORP values of effluent leachate did vary and were sometimes positive. Cycles 1-3a and 5b of the Square MFC as well as cycle 1b of the Circle MFC had these positive effluent ORP values. While this would suggest that the MFC was operating under aerobic conditions; this may not be the case entirely. To produce electricity, MFCs must have anaerobic conditions for the appropriate bacteria to grow within the system. These results do suggest that the systems could have had relatively large aerobic zones.

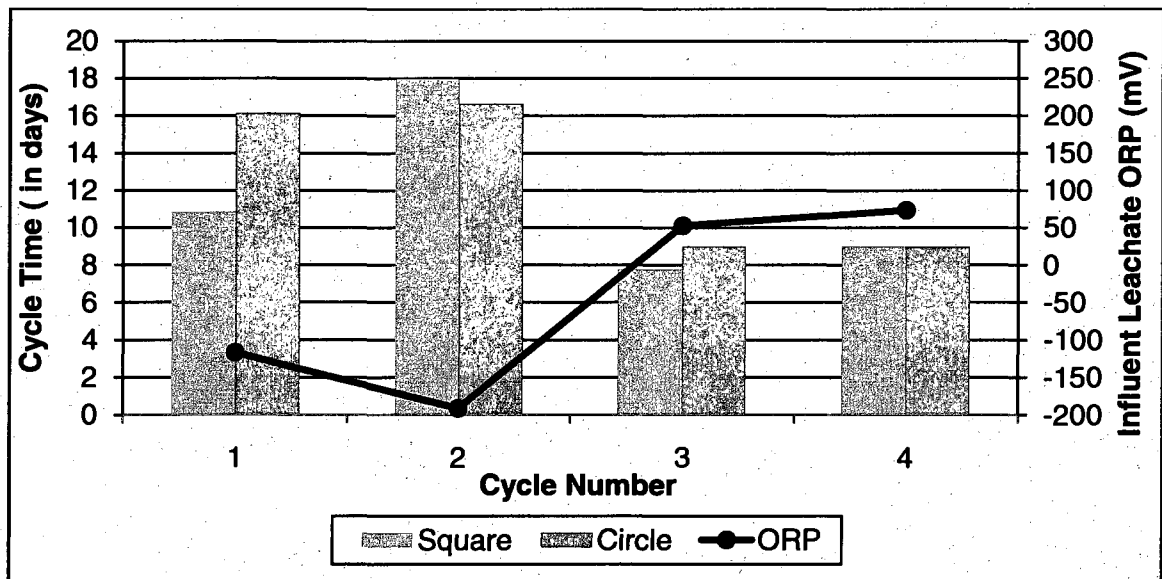


Figure 4.22 Cycle time and influent leachate ORP (Square and Circle MFCs)



### COD, BOD, and TOC.

Chemical oxygen demand, biochemical oxygen demand, and total organic carbon are all measures of the amount of organics in the leachate. Chemical oxygen demand is measure of the amount of organic compounds in a substance while BOD measures the amount of molecular oxygen that is utilized during a period of time for microbial degradation of organic matter as well as inorganic material. TOC is the total amount of organic carbon in a substrate. COD, BOD, and TOC removals for the Circle and Larger Scale MFC are shown in Figure 4.23.

COD differences for the Square design were in the range of 1.7-43%, which is a very broad range for removals. The Circle COD removal range was 15-49%, however, in cycles 1-3c, COD actually increased during the cycle of the MFC. For the same leachate c, the Larger Scale MFC had an increase in COD of 6.6% and a decrease of 3.1%. There are several inorganics that can exhibit COD in leachate, such as sulfides, that can interfere in COD being a measure of just the organics of a system (Jambeck, Townsend, and Solo-Gabriele 2008). BOD removals for these same cycles were 53-72% for the Circle MFC, and 47-86% for the Larger Scale.

While the COD removals are lower than those recorded by other landfill leachate in MFC research (70-98%), BOD is in the range of 57-66% removal that has been previously reported (Greenman et al. 2009; You et al. 2006). COD removals for other MFC systems utilizing different wastewaters are shown in Table 4.6, however they should not be directly compared to this research

because of highly variable operating conditions and architectures. Small volume systems have COD removals of 42-87% while larger systems of 300-400 mL volumes, have 50-70% COD removals. Almost all MFC treatment efficiencies in the literature are only reported in COD removals, however a BOD removal of 78% was found for a tubular MFC system using domestic wastewater (Liu, Ramarayanan and Logan 2004).

TOC removals for the Circle and Larger Scale MFC increased with each cycle of operation (Figure 4.23.) TOC removals of the Larger Scale MFC were minimal for the first cycle of operation and 50.7% during the second cycle.

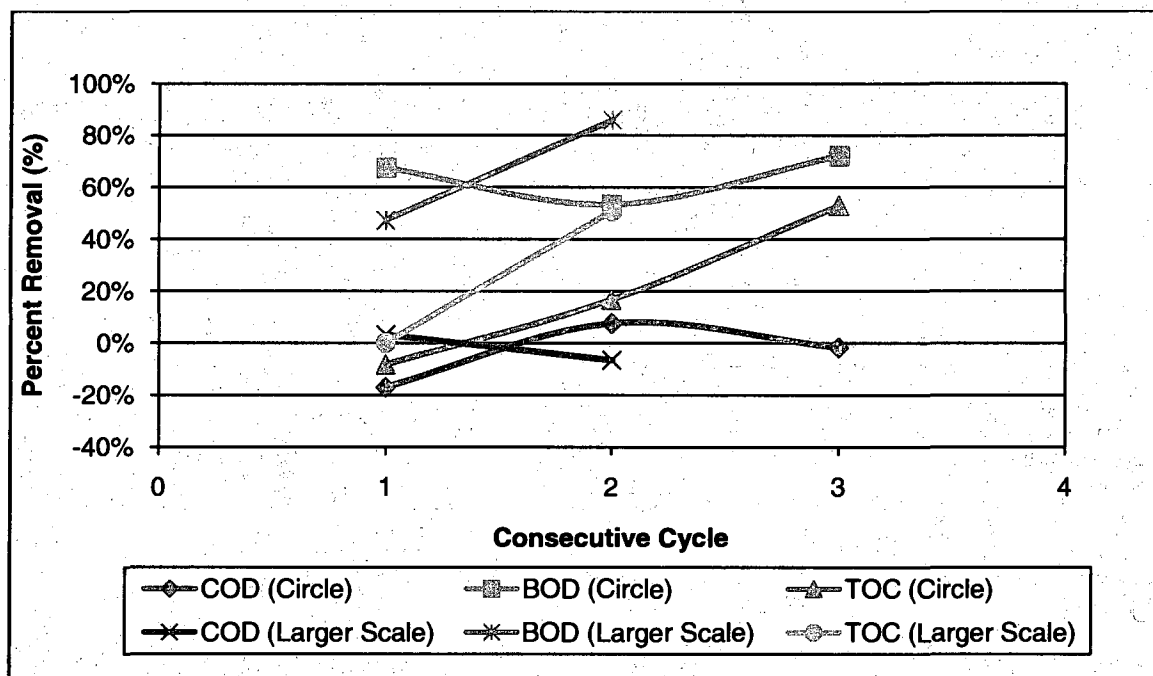


Figure 4.23. COD, BOD, and TOC removals for Circle and Large Scale MFCs

### Alkalinity.

The alkalinity of a solution is that solution's ability to neutralize a strong acid and is attributed to strong buffers such as  $\text{HCO}_3^-$ ,  $\text{CO}_3^{2-}$ , and  $\text{OH}^-$ . Other species such as ammonia, phosphate, silicate, borate and organic bases can also contribute to alkalinity (Snoeyink and Jenkins 1980). For all designs and cycles of the MFCs, there was a consistent decrease in alkalinity during the total cycle time. This would suggest that buffering of the system was occurring while the MFC was operating. Decreases in pH are not uncommon in anode compartments of MFCs because not all protons reach the cathode. If protons are accumulating, a decrease in pH can occur and therefore a decrease in alkalinity as the system is attempting to remain in equilibrium. Furthermore, ammonia and phosphate are being removed in some cycles, so if these were contributing to alkalinity, this would cause a decrease. Sulfide can also accept protons in leachate, which would contribute to alkalinity (Jambeck, Townsend, and Solo-Gabriele 2008).

### Ammonia.

In every cycle of the Circle and Square MFCs, ammonia was removed in differing amounts. There are four common removal mechanisms that could be occurring within this system to remove ammonia. If nitrifying bacteria were present, ammonia could be oxidized by nitrification in the aerobic region near the cathode and coupled with denitrification. Ammonia oxidizing bacteria could also be oxidizing the ammonia in conjunction with ammonia oxidation and nitrite reduction by anaerobic ammonia oxidation bacteria. Ammonia oxidizing bacteria

could also be reducing nitrite and oxidizing ammonia. Lastly, a new unidentified bacteria could be oxidizing ammonia while reducing the anode of the MFC system. A fifth mechanism, which has not been studied at great length, is the chemical/physical removal of ammonia from the system (Kim et al. 2007).

In research with a single chamber MFC treating animal wastewater, it was determined that ammonia loss in that system was due to ammonia volatilization at the elevated pHs near the cathode. A localized pH at this location could cause a shift in ammonium ions to ammonia, resulting in nitrogen losses through the cathode. It was found that this ammonia loss increased as power production of the system increased. While it is possible that there was still some ammonia loss due to nitrification at the cathode by ammonia oxidizing bacteria and oxygen that has diffused into the system, limited appropriate bacterial communities were found (Kim et al. 2007).

While it is unclear what mechanisms were taking place within the designs of this research; it is plausible to assume that a mixture of all of the above mechanisms accounted for the ammonia removal. There is a high probability that an aerobic zone occurred near the cathode of the MFCs due to the porous nature of the carbon cloth. This could support an aerobic nitrifying bacterial community along with an anaerobic ammonia oxidation bacterial community in the rest of the MFC. Volatilization of ammonia was also possible with the increased surface area of the cathode in the designs of this research. For the Square MFC, removals of ammonia were seen from 45-70%, with one cycle only removing 18%. The Circle MFC had removals in the range of 7-29%. The

Larger Scale MFC had an increase in ammonia in the first cycle, yet a 60% reduction in the 52 day cycle. The removals for all MFCs and cycles, except cycles 1-3a of the Circle are shown in Figure 4.24.

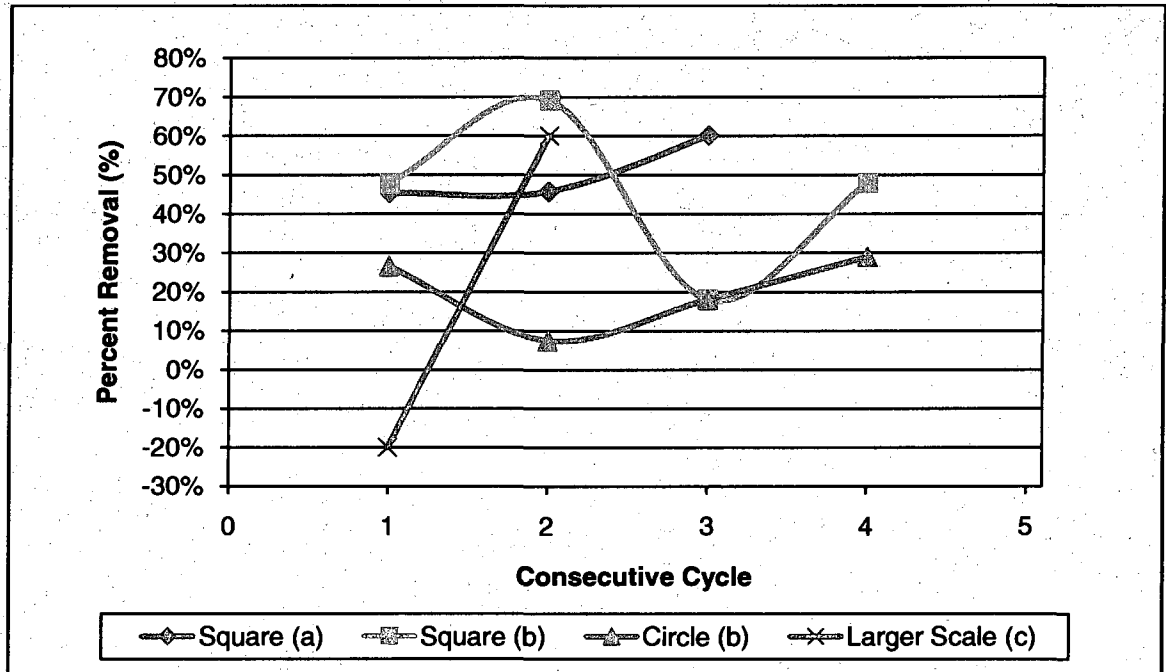


Figure 4.24 Ammonia removal for all MFC designs

Chloride.

An increase in chloride concentration for each cycle was common for both the Square and Circle MFC designs in the range of 22-26% and 8-17% respectively. Cycle 2b of the Square design had an increase of 44% and the Larger Scale MFC saw a large increase of 60% in cycle 2c with only a small increase in cycle 1c. This consistent increase could be due to both the evaporation and utilization of the leachate out of these systems that were open to the air. As can be seen on page 136-138 of the Appendix, continuous additions

of leachate were needed as volume was lost over time in both the Square and Circle design. As the leachate evaporated and was utilized, chloride likely remained in the system and accumulated since these were not continuous flow designs. This explanation is supported by the fact that the Square and Larger Scale MFC has higher accumulations of chloride and more evaporation/utilization, as shown by the amount of additions of leachate that had to be made. The Circle MFC, while still experiencing evaporation/utilization, experienced it at a much slower rate, and had less chloride accumulation. Cycle 2b of the Square MFC had a cycle time of 7-10 days longer than cycles 1, 3, and 4b while the Larger Scale MFC had a 52 day cycle with a 60% increase of chloride. This would account for the larger chloride accumulation for there was a longer time for evaporation/utilization and chloride accumulation to occur. Furthermore, a mass balance was completed on each system, taking into account the additions of leachate and subsequent increase in chloride concentrations (page 144 of Appendix D). Calculated final concentrations of chloride were close in value to the concentrations measured for each system, which suggests that evaporation and utilization of water from the system was the cause for the increasing levels of chloride.

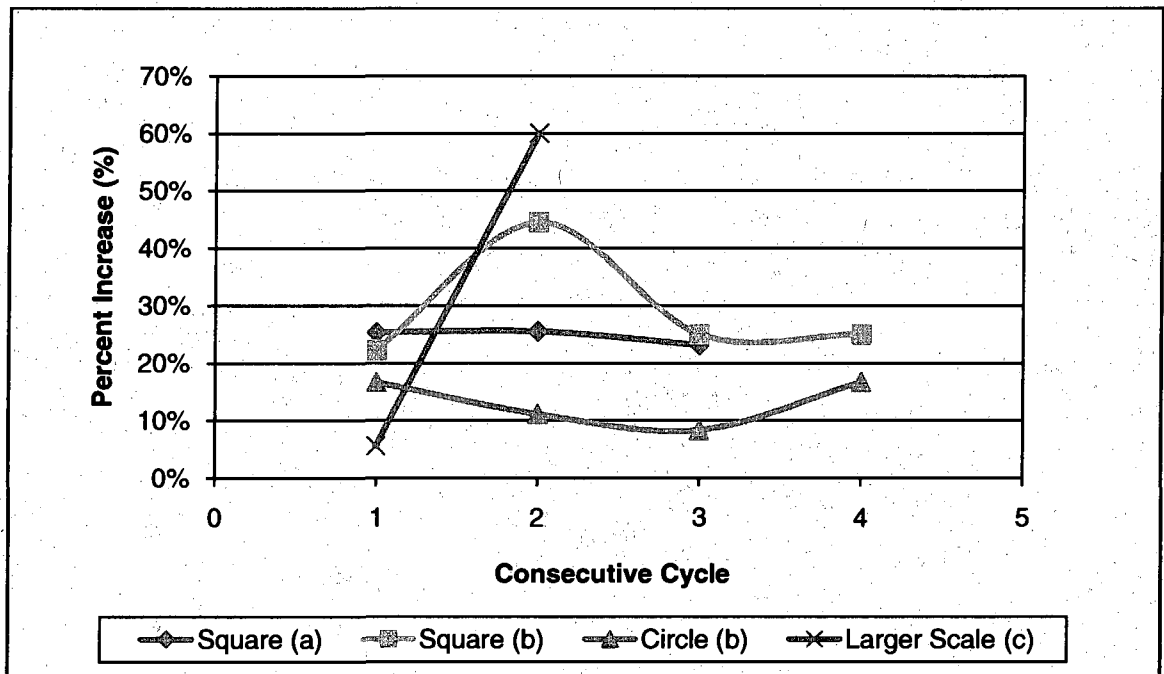


Figure 4.25 Chloride increase for all MFC designs

#### Nitrate/Nitrite.

In all influent leachate from this landfill, there were no detectable levels of nitrate or nitrite. It is not uncommon for leachate to have low levels of these constituents and have all nitrogen as ammonia in the system due to the biological process of the landfill, as discussed in section 2.2.

#### Phosphate/Total Phosphorus.

Phosphorus can be removed through biological processes by incorporating it into cell biomass which is then removed from the system. This biological process involves both an anaerobic and aerobic zone for treatment. For MFC systems, part of this reaction would have to occur in the small aerobic zone near the cathode of the MFC. When dissolved degradable organic matter (bsCOD) is fermented, acetate is formed. This acetate is used by phosphorus

accumulating organisms in an anaerobic zone to produce intracellular polyhydroxybutyrate (PHB) storage products. When these products are created, orthophosphate is released from the cell and into solution, along with magnesium, potassium and calcium cations.

In the aerobic zone of treatment, this PHB storage product is metabolized, which creates energy and carbon for cell growth. When this energy is released, it is used to form polyphosphate bonds in cell storage. This results in orthophosphate uptake from the solution as it is used within the bacterial cell. When this biomass is removed from the system, stored phosphorus is concurrently removed, resulting in biological phosphorus removal.

The MFC anaerobic system is not designed to remove phosphorus, however, because aerobic and anaerobic zones do exist, it is reasonable to assume that phosphorus uptake and release were occurring within the MFCs. These inconsistent conditions would account for the inconsistent measurements of both phosphate and total phosphorus in each of the MFC designs. The Square MFC had decreases of phosphate of 23 and 16.6 %, and an increase of 15.8% during initial testing with corresponding decreases of 4.4 and 23.5% and an increase of 0.4% in total phosphorus (Table 4.24).

For landfill leachate 'b', using the Square and Circle designs, variation in removals and increase were also seen. Figure 4.26 illustrates the percent difference of total phosphorus levels for each design on the left vertical axis (Square, cycles 4-7b, Circle, cycles 1-4b, jointly numbered 1-4 in consecutive order). The right vertical axis is influent ORP readings from the leachate. As



discussed earlier, the leachate for the last two cycles was positive. This graph suggests that there could be a relationship between the total phosphorus increase and a positive ORP reading. An explanation for this occurrence would be biological phosphorus removal beginning in the leachate prior to sampling. If the leachate experienced aerobic conditions, phosphorus and phosphate could have been sequestered by microbes in solution. Once the leachate entered the MFC systems and started to become anaerobic, these phosphates and phosphorus could have been released by the bacteria; increasing these levels in the effluent leachate. The Larger Scale MFC had similar removals and increases with a phosphate increase of 11.7% and a removal of 49%; and a total phosphorus removal of 27.5-67.3%.

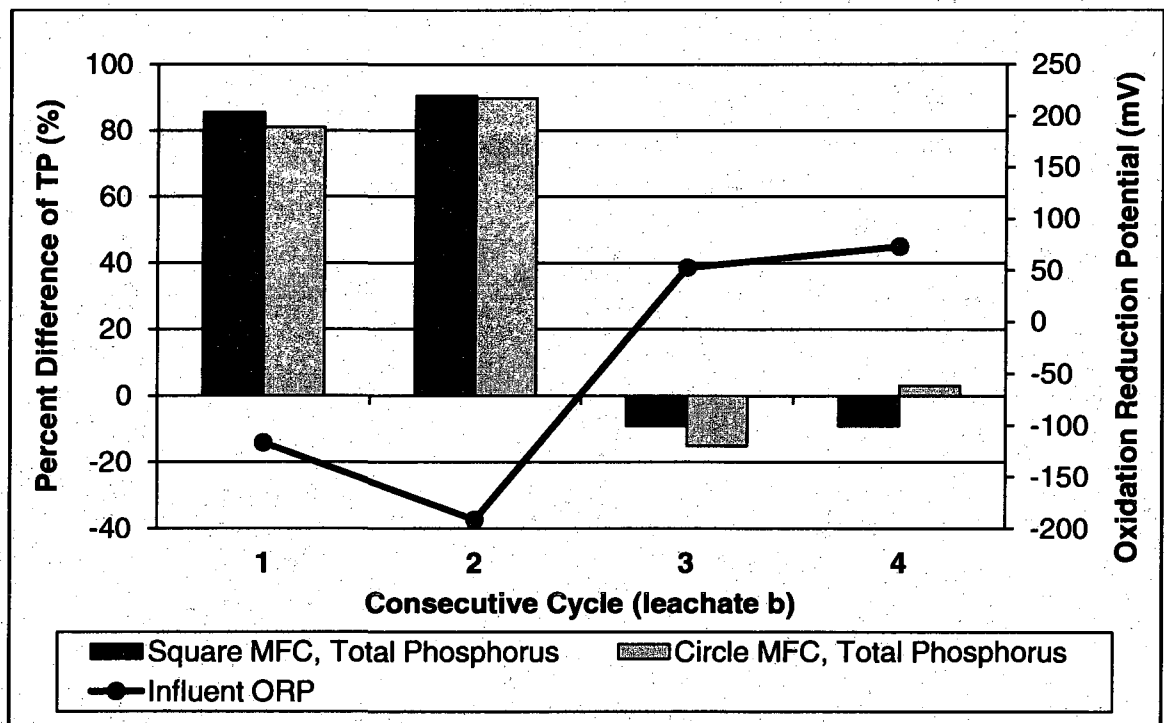
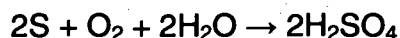
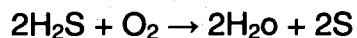


Figure 4.26 % Difference of TP and ORP for Square and Circle MFC

### Sulfate/Sulfide.

Every cycle of the MFCs in this research produced an increase in sulfate levels in the effluent leachate (10.5% to 83% for the Square MFC to 49-68% for the Circle MFC). The Larger Scale MFC experienced increases of 21% and 102.9%. At the same time as the sulfate increased, a reduction in sulfides was seen in the Circle MFC from 35-89% and 0-34% for the Larger Scale MFC. This was most likely due to sulfur oxidation occurring within the MFC. In each sample of leachate that was taken from the landfill; small black particulates were suspended in solution. These particulates could be sulfide precipitation in the solution. Chemolithotrophic bacteria use hydrogen sulfide as well as elemental sulfur as a source of energy in the following reactions;



These reactions are aerobic processes, thus they would have to be occurring near the cathode in the MFC, where an aerobic region is likely present due to diffusion through the carbon cloth. This would account for both the increase in sulfate as well as the utilization of sulfide. Graphite can contain small levels of sulfur, thus sulfur could also be entering the system through slow release from the anodes of the system. If this reaction was occurring, it would suggest that the pH of these systems should decrease with the production of sulfuric acid, which was not observed in the leachate MFCs and could be due to the substantial buffering capacity that is present through alkalinity of the influent leachate.

A mass balance of sulfate concentrations was completed for each of the MFC systems, based upon initial levels and the increase due to leachate additions (to account for evaporation and utilization of the leachate). For the Square, Circle, and Larger Scale MFC systems, accumulation of sulfate due to evaporation/utilization was not the major cause of sulfate concentration increases within the MFC system, as can be seen from the mass balance (page 145 of Appendix D).

#### Cations.

An analysis of cations in influent and effluent leachate was completed using ICP, as discussed in Chapter 3 of this document. These analyses were done using the Circle MFC to determine if any major changes in cation concentration occurred during MFC operation. As can be seen in Tables 4.29 and 4.30, amounts of cations did vary, however all concentrations were low and remained low, with the exception of calcium and magnesium. While these two elements were at increased levels, the values remained in the typical range of values for landfill leachate (Table 2.1). It should be noted that there was a 28-72% reduction in iron during the operation of the MFCs. This coincides with a finding in the microbial analysis section (4.4) that Firmicutes were found in the MFC environment and increased in population during operation. This phylum is known to contain iron-reducing bacteria.

Table 4.29 Cation conc. for influent and effluent leachate of Square MFC

<b>Cation</b>	<b>Initial (mg/L)</b>	<b>Final (mg/L)</b>	<b>% Difference</b>
Arsenic (As)	1.25	1.49	-19%
Barium (Ba)	0.14	0.062	56%
Cobalt (Co)	0.012	0.015	-25%
Chromium (Cr)	0.125	0.151	-21%
Iron (Fe)	5.418	3.894	28%
Manganese (Mn)	0.274	0.116	58%
Nickel (Ni)	0.091	0.117	-29%
Antimony (Si)	0.019	0.021	-11%
Vanadium (V)	0.054	0.115	-113%
Zinc (Zn)	0.078	0.056	28%

Table 4.30 Cation conc. for influent and effluent leachate of Circle MFC

<b>Cation</b>	<b>Initial</b>	<b>Final</b>	<b>% Difference</b>
Silver (Ag)	0.006	0.014	-60.7%
Aluminum (Al)	0.453	0.274	65.1%
Arsenic (As)	1.400	1.301	7.6%
Barium (Ba)	0.106	0.090	17.5%
Calcium (Ca)	45.566	42.238	7.9%
Cobalt (Co)	0.015	0.018	-15.9%
Chromium (Cr)	0.102	0.127	-19.4%
Iron (Fe)	3.710	2.121	74.9%
Magnesium (Mg)	47.898	56.789	-15.7%
Manganese (Mn)	0.102	0.137	-25.5%
Nickel (Ni)	0.080	0.103	-22.4%
Antimony (Sb)	0.042	0.054	-22.0%
Selenium (Se)	0.040	0.054	-25.6%
Vanadium (V)	0.067	0.092	-27.6%
Zinc (Zn)	0.034	0.036	-6.4%

#### **4.4 Microbial Analysis**

The microbial communities that are present in MFC environments and facilitate voltage production are phylogenetically diverse. In the beginning stages of microbial fuel cell research, it was thought that only metal-reducing bacteria, such as *Shewanella* and *Geobacter* contributed to the exocellular electron transfer that is needed in MFCs. However, it has been determined that many different types of bacteria can take part in electricity production. Common phylum's of bacteria that have been shown to be dominant in MFC microbial communities are alpha-, beta-, gamma-, and delta- proteobacteria along with firmicutes (Logan 2008).

Four different leachate/biofilm samples were tested by David B. Ringelberg of the US Army Corps of Engineers at the Cold Regions Research and Engineering Laboratory, Engineer Research and Development Center as detailed in section 3.2.3. A sample of leachate from TLR II, Phase 1 which was unable to produce electricity (Non-Producing), was tested to determine if the microbial community could be inhibiting electrical results. Leachate from TLR III, Phase 2 was also analyzed prior (Pre-MFC) to entering the MFC system as well as after (Post-MFC) running a complete cycle in the Circle MFC. A sample of biofilm from the anode of the Circle MFC was also tested. This MFC had been consistently running for approximately 2 months with landfill leachate. Results are stated as TLFA percentage of total area for each phylum of bacteria that are present. Pie chart representations of this data are in Figures 4.28 – 4.31.

A comparison of these four analyses can be found in Figure 4.27, with only the major phyla listed (> 1 %). A large difference in beta-proteobacteria populations between leachate that is conducive to voltage production and that which was not, can be seen. This suggests that beta-proteobacteria is not a major contributor to electron transfer in this system, for a large population did not stimulate any electrical production. Firmicutes and Bacteroidetes were microbial populations that were only present within the voltage producing MFCs; with a small population of Firmicutes pre-MFC. This suggests that there are conditions within the MFC that facilitate growth of these types of bacteria. Firmicutes and bacteroidetes are bacteria that have been found in MFC communities in previous literature (Logan 2008; Logan and Regan 2006a). Alpha- and gamma-proteobacteria seem to be inhibited by the MFC environment.

While this microbial analysis is only a beginning step in understanding the microbial aspects of the MFC within landfill leachate systems; it is important to note that landfill leachate contains many of the bacteria that are necessary for voltage production in MFCs (Logan 2008; Logan and Regan 2006a). This validates the finding of this research as well as others that inoculation of the MFC with anaerobic bacteria is not necessary when using landfill leachate as a substrate (Greenman et al. 2009).

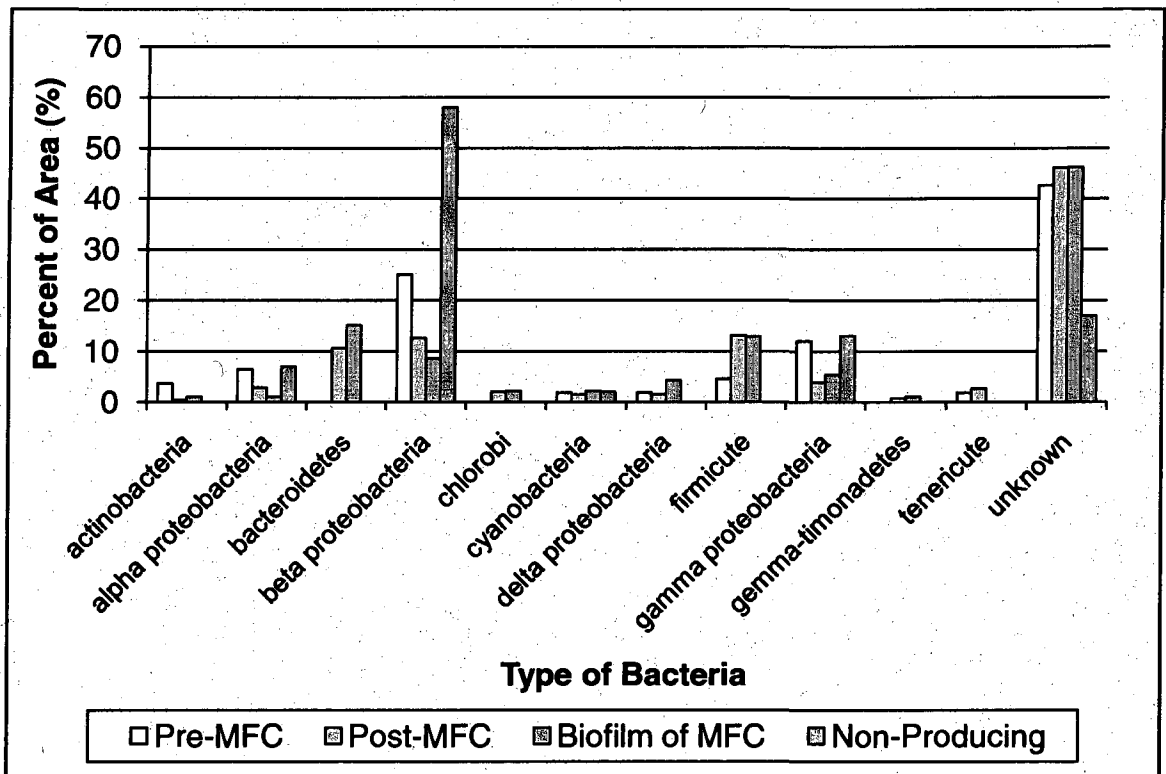


Figure 4.27 Comparison of microbial communities (Major Phyla)

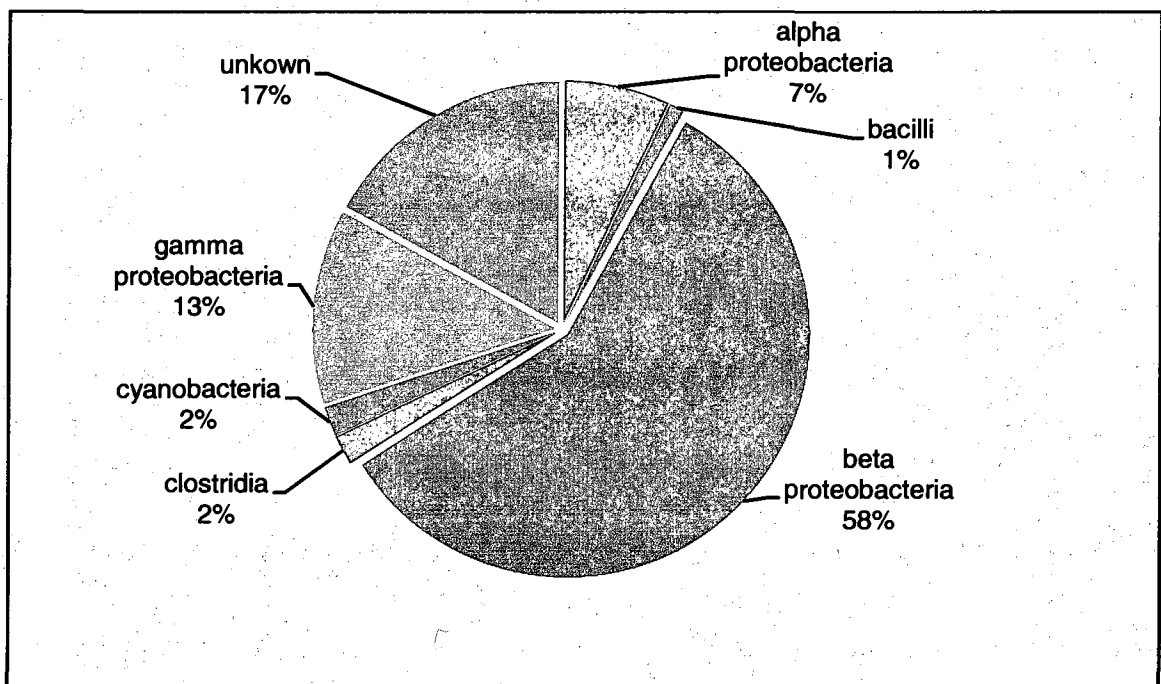


Figure 4.28 Microbial community analysis, Non-Producing, in % of total area

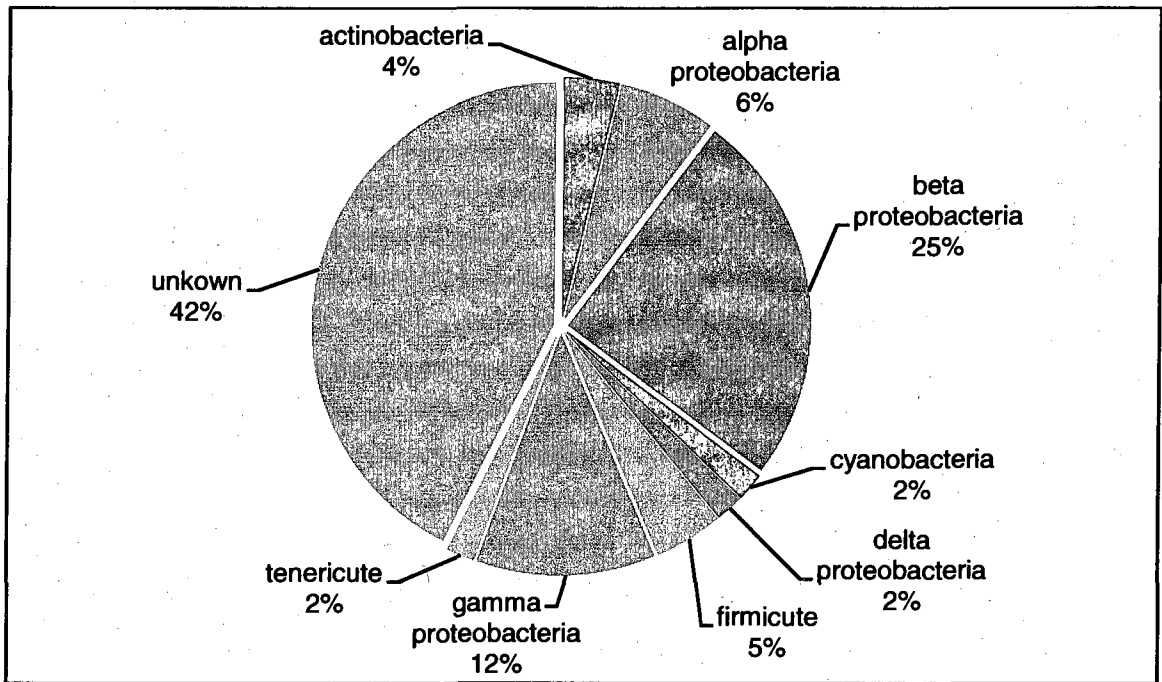


Figure 4.29 Microbial community analysis, Pre-MFC, in % of total area

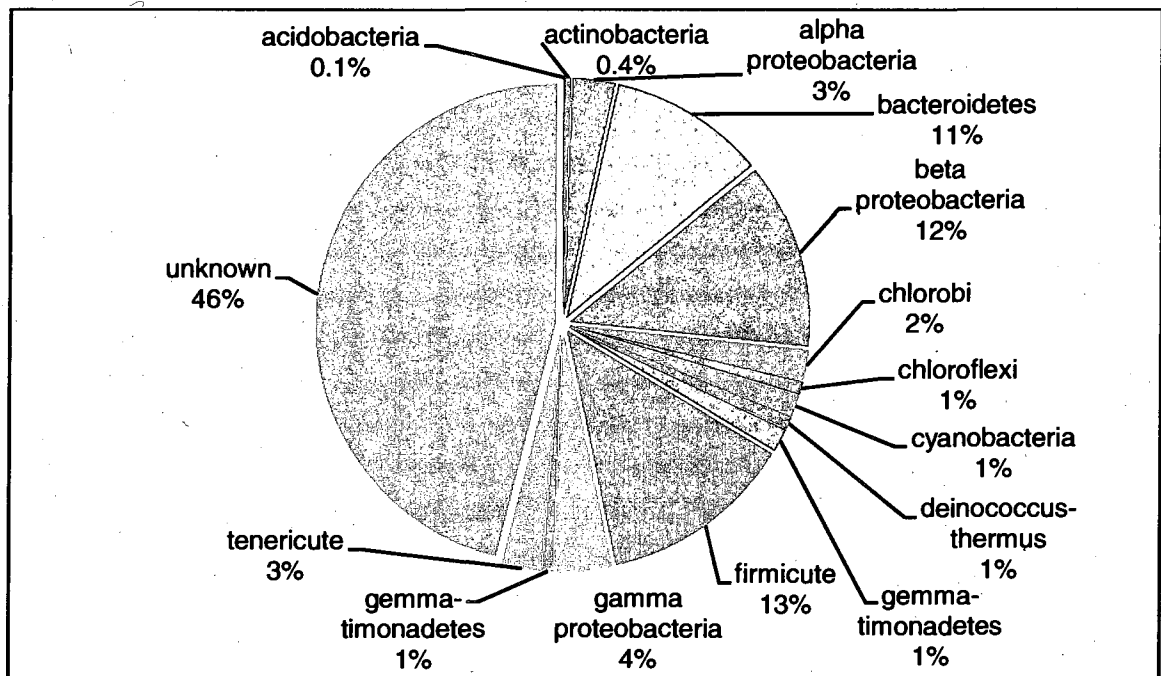


Figure 4.30 Microbial community analysis, Post-MFC, in % of total area



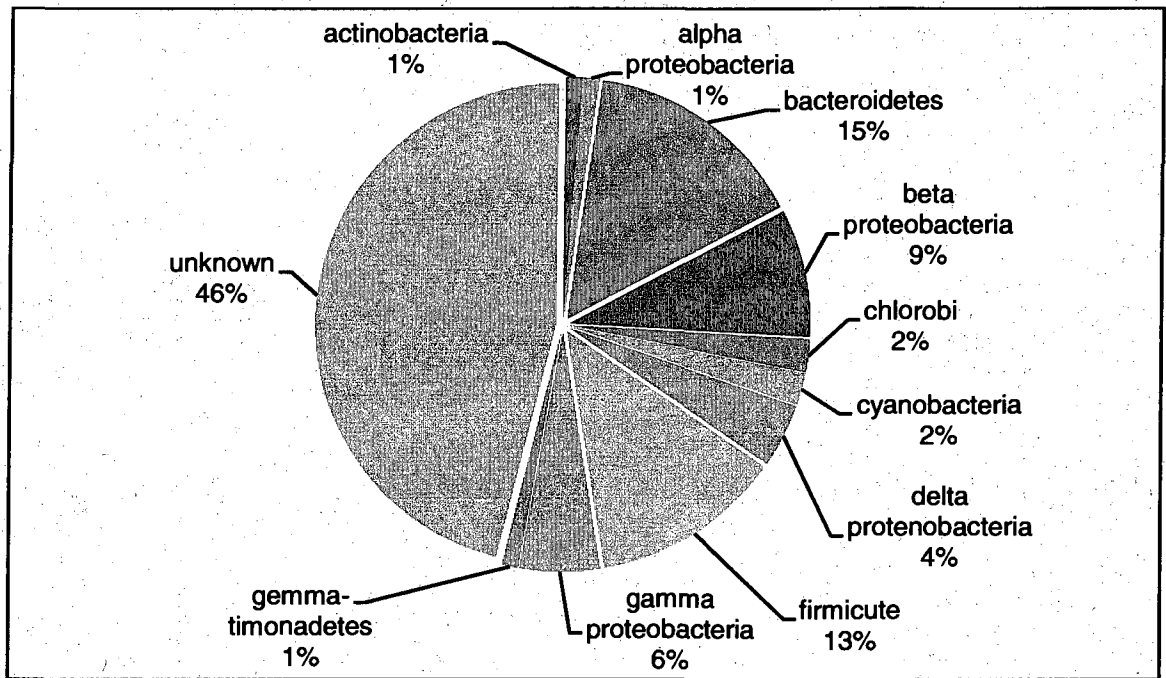


Figure 4.31 Microbial community analysis, Biofilm of MFC, in % of total area

## CHAPTER 5

### SUMMARY AND CONCLUSIONS

Microbial fuel cells are a new technology that can be used for treating landfill leachate and simultaneously producing electricity. Three designs were tested in batch cycles using landfill leachate (908-3200 mg/L COD): a Square MFC (995 mL), Circle MFC (934 mL) and a Large Scale MFC (18.3 L). Each system was a single chamber design using graphite (anode) and carbon cloth with Pt catalyst (cathode). No outside source of inoculation was utilized for any of the designs. A total of seven cycles were completed for each the Square MFC and Circle MFC. A total of two cycles were completed for the Large Scale MFC. No additional inoculation of the MFC was needed because exoeletrogens were already present within the leachate. A maximum power density of 24-31 mW/m<sup>2</sup> (653-824 mW/m<sup>3</sup>) was achieved using the Circle MFC design. Removals of BOD, TOC, and ammonia were in the range of 50-72%, 17-53% and 7-69% respectively. With a larger scale MFC, a maximum voltage of 635 mV was achieved with BOD removals of 47-86%, TOC removals of 50.7% and ammonia removals of 60%. This cycle of operation lasted over 52 days and was still producing 484 mV when taken offline.

Leachate is a well-matched substrate for use in a microbial fuel cell because of its relatively high amount of organics, conductivity, and buffering capacity, yet minimal solids. All of these characteristics, with the exception of high organics, can limit the utilization of other wastewaters for use in MFCs. Even though substrates such as wastewater and leachate will not provide equal

power production to MFCs utilizing pure substrates such as acetate; use of a substrate like leachate mimics more realistic conditions. MFCs utilizing landfill leachate also need no outside source of inoculation due to the presence of the appropriate mixed bacterial community. The results of this research are promising for future developments in using leachate as a substrate in MFCs for simultaneous leachate treatment and electricity generation. The Larger Scale MFC in this study showed that the MFC technology can be scaled-up to treat larger volumes of substrate without decreasing treatment efficiencies. While power production did not increase linearly with the volume increase, power production was higher than the small-scale cells and was maintained longer (over 52 days versus the typical 14-20 days for small scale cells).

The removal of major constituents such as BOD, TOC, and ammonia suggest that this technology could be a viable option for leachate treatment. An MFC system could be utilized as a pre-treatment for recirculation or to reduce energy use of further treatment. It could also be used as a standalone treatment process. For landfills in the postclosure monitoring period of operation, an MFC could be an option for a low operation and maintenance system to treat leachate to levels acceptable for direct discharge into surface water or groundwater.

Further research will be needed to find more efficient and less expensive cathode materials if MFCs are to be applied to even greater volumes of substrate. Advances such as graphite fiber brushes for anodes have provided the necessary surface area and conditions that are needed in the anode compartment, producing power densities of  $2400 \text{ mW/m}^2$  (normalized to cathode

surface area) (Logan et al. 2007). Currently, the cathode is the aspect of MFC design that limits power production and scale-up possibilities. In addition, the minimal increase of the Large Scale design power production over the small scale cells illustrates the need for improved design of larger MFC systems to minimize the internal resistance.

Further research on landfill leachate treatment using microbial fuel cells is needed. Different leachate from various landfills should be utilized to further examine leachate as a substrate and evaluate treatment efficiencies. Larger MFCs could be piloted at landfills needing leachate treatment, however improved cathode materials and design would be needed to complete this task. A larger MFC system could be an ideal system for remote landfill locations due to minimal energy input and minimal necessary operations. A more in-depth microbial analysis should also be completed to examine characteristics of the community within the leachate and MFC environment in detail. It is still unknown what specific bacterial species are providing the exocellular electron transfer in the landfill leachate MFC system.

## LIST OF REFERENCES

- Aelterman, Peter, Korneel Rabaey, Hai The Pham, Nico Boon, & Willy Verstraete. (2006a). Continuous electricity generation at high voltages and currents using stacked microbial fuel cells. *Environmental Science and Tehcnology*, 40, 3388-3394.
- Aelterman, Peter, Korneel Rabaey, Peter Clauwaert, & Willy Verstraete. (2006b). Microbial fuel cells for wastewater treatment. *Water Science and Technology*, 54(8), 9-15.
- Aelterman, Peter, Mathias Versichele, Massimo Marzorati, Nico Boon, & Willy Verstraete. (2008a). Loading rate and external resistance control the electricity generation of microbial fuel cells with different three-dimensional anodes. *Bioresource Technology*, 99, 8895-8902.
- Aelterman, Peter, Stefano Freguia, Jurg Keller, Willy Verstraete, & Korneel Rabaey. (2008b). The anode potential regulates bacterial activity in microbial fuel cells. *Applied Microbiology and Biotechnology*, 78, 409-418.
- Barlaz, Morton A., Alix P. Rooker, Peter Kjeldsen, Mohammed A. Gabr, and Robert C. Borden. (2002). Critical evaluation of factors required to terminate the postclosure monitoring period at solid waste landfills. *Environmental Science and Technology*, 36(16), 3457-3464.
- Biffinger, Justin C., and Bradley R. Ringeisen. (2008). Engineering microbial fuels cells: Recent patents and new directions. *Recent Patents on Biotechnology*, 2, 150-155.
- Bond, Daniel R., and Derek R. Lovley. (2005). Evidence for involvement of an electron shuttle in electricity generation by *Geothrix fermentans*. *Applied and Environmental Microbiology*, 71(4), 2186-2189.
- Call, Douglas & Bruce E. Logan. (2008). Hydrogen production in a single chamber microbial electrolysis cell lacking a membrane. *Environmental Science and Technology*, 42, 3401-3406.
- Chae, Kyu Jung, Mijin Choi, Folusho F. Ajayi, Wooshin Park, In Seop Chang, & In S. Kim. (2008). Mass transport through a proton exchange membrane (Nafion) in microbial fuel cells. *Energy and Fuels*, 22, 169-176.
- Chang, In Seop, Jae Kyung Jang, Geun Cheol Gil, Mia Kim, Hyung Joo Kim, Byung Won Cho, & Byung Hong Kim. (2004). Continuous determination of biochemical oxygen demand using microbial fuel cell type biosensor. *Biosensors and Bioelectronics*, 19, 607-613.

Chapelle, Francis H. (2001). *Groundwater Microbiology and Geochemistry 2<sup>nd</sup> Edition*. New York: John Wiley and Sons, Inc.

Chaudhuri, Swades K., and Derek R. Lovley. (2003). Electricity generation by direct oxidation of glucose in mediatorless microbial fuel cells. *Nature Biotechnology*, 21(10), 1229-1232.

Cheng, Shaoan, Brian A. Dempsey, & Bruce E. Logan. (2007). Electricity generation from synthetic acid-mine drainage (AMD) water using fuel cell technologies. *Environmental Science and Technology*, 41, 8149-8153.

Cheng, Shaoan, & Bruce E. Logan. (2007). Ammonia treatment of carbon cloth anodes to enhance power generation of microbial fuel cells. *Electrochemistry Communications*, 9, 492-496.

Cheng, Shaoan, Hong Liu, & Bruce E. Logan. (2006a). Increased performance of single-chamber microbial fuel cells using an improved cathode structure. *Electrochemistry Communications*, 8, 489-494.

Cheng, Shaoan, Hong Liu & Bruce E. Logan. (2006b). Increased power generation in a continuous flow MFC with advective flow through the porous anode and reduced electrode spacing. *Environmental Science and Technology*, 40, 2426-2432.

Cheng, Shaoan, Hong Liu, & Bruce Logan. (2006c). Power densities using different cathode catalysts (Pt and CoTMP) and polymer binders (Nafion and PTFE) in single chamber microbial fuel cells. *Environmental Science and Technology*, 40, 364-369.

Clauwaert, Peter, David van der Ha, Nico Boon, Kim Verbeken, Marc Verhaege, Korneel Rabaey, & Willy Verstraete. (2007a). Open air biocathode enables effective electricity generation with microbial fuel cells. *Environmental Science and Technology*, 41, 7564-7569.

Clauwaert, Peter, Korneel Rabaey, Peter Aelterman, Liesje de Schampelaire, The Hai Pham, Pascal Boeckx, Nico Boon, & Willy Verstraete. (2007b). Biological denitrification in microbial fuel cells. *Environmental Science and Technology*, 41, 3354-3360.

Clesceri, Lenore S., Arnold E. Greenberg, and Andrew D. Eaton, eds. (1998). *Standard Methods for the Examination of Water and Wastewater, 20<sup>th</sup> Edition*. USA: American Public Health Association, American Water Works Association, and Water Environment Federation.

- Fan, Yanzhen, Evan Sharbrough, & Hong Liu. (2008). Quantification of the internal resistance distribution of microbial fuel cells. *Environmental Science and Technology*, 42(21), 8101-8107.
- Feng, Yujie, Xin Wang, Bruce E. Logan & He Lee. (2008). Brewery wastewater treatment using air-cathode microbial fuel cells. *Environmental Biotechnology*, 78, 873-880.
- Garrity, M. George (Editor in chief), Don J. Brenner, Noel R. Krieg, and James T. Staley, Eds. (2005). *Bergey's Manual of Systematic Bacteriology, 2<sup>nd</sup> Edition, Volume 2: The Proteobacteria*, New York: Springer.
- Greenman, John, Antonia Galvez, Lorenzino Giusti, and Ioannis Ieropoulos. (2009). Electricity from landfill leachate using microbial fuel cells: Comparison with a biological aerated filter. *Enzyme and Microbial Technology*, 44, 112-119.
- Gregory, Kelvin B., Daniel R. Bond, & Derek R. Lovely. (2004). Graphite electrodes as electron donors for anaerobic respiration. *Environmental Microbiology*, 6(6), 596-604.
- Ghangrekar, M.M., & V.B. Shinde. (2007). Performance of membrane-less microbial fuel cell treating wastewater and effect of electrode distance and area on electricity production. *Bioresource Technology*, 98, 2879-2885.
- Gorby, Yuri A., Svetlana Yanina, Jeffery S. McLean, Kevin M. Rosso, Dianne Moyles, Alice Dohnaikova, Terry J. Beveridge, In Deop Chang, Byung Hong Kim, Kyung Shik Kim, David E. Culley, Samantha B. Reed, Margaret F. Romine, Daad A. Saffarin, Eric A. Hill, Liang Shi, Dwayne A. Elias, David Kennedy, Grigory Pinchuk, Kazuya Watanabe, Shun'ichi Ishii, Bruce Logan, Kenneth H. Nealson, & Jim K. Fredrickson. (2006). Electrically conductive bacterial nanowires produced by *Shewanella oneidensis* strain MR-1 and other microorganisms. *Proceedings of the National Academy of Sciences of the United States of America*, 103(30), 11358-11363.
- Halliday, David, Robert Resnick, and Jearl Walker. (2003). *Fundamentals of Physics 6<sup>th</sup> Edition*. New York: John Wiley and Sons, Inc.
- He, Zhen, Shelley D. Minteer, & Largus T. Angenent. (2005). Electricity generation from artificial wastewater using an upflow microbial fuel cell. *Environmental Science and Technology*, 39, 5262-5267.
- Heilmann, Jenna, & Bruce E. Logan. (2006). Production of electricity from proteins using a microbial fuel cell. *Water Environment Research*, 78(5), 531-537.

Huang, Liping, and Bruce E. Logan. (2008). Electricity generation and treatment of paper recycling wastewater using a microbial fuel cell. *Environmental Biotechnology*, 80, 349-355.

Ieroloulos, Ioannis, John Greenman, and Chris Melhuish. (2008). Microbial fuel cells based on carbon veil electrodes: Stack configuration and scalability. *International Journal of Energy Research*, 32, 1228-1240.

IPCC (Core Writing Team, Pachauri, R.K and Reisinger, A. (eds.)). (2007). Climate Change 2007: Synthesis Report. *Contribution of Working Groups I, II and III to the Fourth Assessment Report of the Intergovernmental Panel on Climate Change*. Geneva, Switzerland: IPCC.

Jambeck, Jenna R., Timothy G. Townsend, Helena M. Solo-Gabriele. (2008). Landfill disposal of CCA-treated wood with construction and demolition (C&D) debris: Arsenic, Chromium, and Copper concentrations in leachate. *Environmental Science & Technology*, 42 (15), 5740-5745.

Jang, Jae Kyung, The Hai Pham, In Seop Chang, Kui Hyun Kang, Hyunsoo Moon, Kyung Suk Cho, & Byung Hong Kim. (2004). Construction and operation of a novel mediator- and membrane-less microbial fuel cell. *Process Biochemistry*, 39, 1007-1012.

Kim, Jung Rae, Booki Min, & Bruce E. Logan. (2005). Evaluation of procedures to acclimate a microbial fuel cell for electricity production. *Applied Microbiology and Biotechnology*, 68, 23-30.

Kim, Jung Rae, Jerzy Dec, Mary Ann Bruns, & Bruce E. Logan. (2008). Removal of odors from swine wastewater by using microbial fuel cells. *Applied and Environmental Microbiology*, 74(8), 2540-2543.

Kim, Jung Rae, Jonh M. Regan, & Bruce E. Logan. (2007). Analysis of ammonia loss mechanisms in microbial fuel cells treating animal wastewater. *Biotechnology and Bioengineering*, 99(5), 1120-1127.

Kim, Jung Rae, Shaoan Cheng, Sang-Eun Oh, & Bruce E. Logan. (2007). Power generation using different cation, anion, and ultrafiltration membranes in microbial fuel cells. *Environmental Science and Technology*, 41, 1004-1009.

Kjeldsen, Peter, Morton A. Barlaz, Alix P. Rooker, Anders Baun, Anna Ledin, & Thomas H. Christensen. (2002). Present and long-term composition of MSW landfill leachate: A Review. *Critical Reviews in Environmental Science and Technology*, 32(4), 297-336.



Lanthier, Martin, Kelvin B. Gregory, & Derek R. Lovley. (2007). Growth with high planktonic biomass in *Shewanella oneidensis* fuel cells. *FEMS Microbial Letters*, 278, 29-35.

Liu, Hong & Bruce E. Logan. (2004). Electricity generation using an air-cathode single chamber microbial fuel cell in the presence and absence of a proton exchange membrane. *Environmental Science and Technology*, 38, 4040-4046.

Liu, Hong, Ramanathan Ramarayanan, & Bruce E. Logan. (2004). Production of electricity during wastewater treatment using a single chamber microbial fuel cell. *Environmental Science and Tehcnology*, 38, 2281-2285.

Liu, Hong, Shaoan Cheng, & Bruce E. Logan. (2005). Power generation in fed-batch microbial fuel cells as a fuction of ionic strenth, temperature, and reactor configuration. *Environmental Science and Technology*, 39, 5488-5493.

Liu, Hong, Shaoan Cheng, Liping Huang, & Bruce E. Logan. (2008). Scale-up of membrane-free single chamber microbial fuel cells. *Journal of Power Sources*, 179, 274-279.

Logan, Bruce E. (2008). *Microbial Fuel Cells*. New Jersey: John Wiley and Sons, Inc.

Logan Bruce E., Bert Hamelers, Rene Rozendal, Uwe Schroder, Jurg Keller, Stefano Reguia, Peter Aelterman, Willy Verstraete, & Korneel Rabaey. (2006). Microbial fuel cells: Methodology and technology. *Environmental Science and Technology*, 40(17), 5181-5192.

Logan, Bruce E., & John M. Regan. (2006). Electricity-producing bacterial communities in microbial fuel cells. *TRENDS in Mirobiology*, 14(12), 512-518.

Logan, Bruce, Shaoan Cheng, Valerie Watson, & Garrett Estadt. (2007). Graphite fiber brush anodes for increased power production in air-cathode microbial fuel cells. *Environmental Science and Technology*, 41, 3341-3346.

Lovley, Derek R. (2006). Bug Juice:harvesting electricity with microorganisms. *Nature Reviews*, 4, 497-508.

Microcellutions, UNH Senior Design Team. (2007). The MOR-2007 microbial fuel cell technology: An innovative and sustainable technology for manure management and electricity, *WERC Competition, Task 4*.

Min, Booki & Bruce E. Logan. (2004) Continuous electricity generation from domestic wastewater and organic substrates in a flat plate microbial fuel cell. *Environmental Science and Technology*, 38, 5809-5814.

Min, Booki, JungRae Kim, SangEun Oh, John M. Regan, & Bruce E. Logan. (2005). Electricity generation from swine wastewater using microbial fuel cells. *Water Research*, 39, 4961-4968.

Moon, Hyunsoo, In Seop Chang, & Byung Hong Kim. (2006). Continuous electricity production from artificial wastewater using a mediator-less microbial fuel cell. *Bioresource Technology*, 97, 621-627.

Moon, Hyunsoo, In Seop Chang, Jae Kyung Jang, & Byung Hong Kim. (2005). Residence time distribution in microbial fuel cell and its influence on COD removal with electricity generation. *Biochemical Engineering Journal*, 27, 59-65.

Nevin, K.P., H. Richter, S.F. Covalla, J.P. Johnson, T.L. Woodard, A.L. Orioff, H. Jia, M. Zang, & D.R. Lovley. (2008). Power output and columbic efficiencies from biofilms of *Geobacter sulfurreducens* comparable to mixed community microbial fuel cells. *Environmental Microbiology*, 10, 2505-2514.

Oh, SangEun, Booki Min & Bruce Logan. (2004). Cathode performance as a factor in electricity generation in microbial fuel cells. *Environmental Science and Technology*, 38, 4900-4904.

Oh, SangEun, & Bruce E. Logan. (2006). Proton exchange membrane and electrode surface areas as factors that affect power generation in microbial fuel cells. *Biotechnological Products and Process Engineering*, 70, 162-169.

Oldham, Keith B. and Jan C. Myland. (1994). *Fundamentals of Electrochemical Science*. San Diego: Academic Press, Inc.

Park, Doo Hyun, & J. Gregory Zeikus. (2003). Improved fuel cell and electrode designs for producing electricity from microbial degradation. *Biotechnology and Bioengineering*, 81(3), 348-355.

Pfaff, John D. (1993). Method 300.0 Determination of Inorganic Anions by Ion Chromatography. *Environmental Monitoring Systems Laboratory, Office of Research and Development, USEPA*. Washington, D.C.: USEPA.

Potter, M.C. (1911). Electrical effects accompanying the decomposition of organic compounds. *Proceedings of the Royal Society of London, Series B, Containing Papers of a Biological Character*, 84(571), 260-276.

Rabaey, Korneel, Kirsten Van De Sompel, Loi Maignien, Nico Boon, Peter Aelterman, Peter Clauwaert, Liesje De Schamphelaire, Hai The Pham, Jan Vermeulen, Marc Verhaege, Piet Lens, & Willy Verstraete. (2006). Microbial fuel cells for sulfide removal. *Environmental Science and Technology*, 40, 5218-5224.

Rabaey, Korneel, Nico Boon, Steven D. Siciliano, Marc Verhaege, & Willy Verstraete. (2004). Biofuel cells select for microbial consortia that self-mediate electron transfer. *Applied and Environmental Microbiology*, 70(9), 5373-5382.

Rabaey, Korneel, Nico Boon, Monica Hofte, & Willy Verstraete. (2005a). Microbial phenazine production enhances electron transfer in biofuel cells. *Environmental Science and Technology*, 39, 3401-3408.

Rabaey, Korneel, Peter Clauwaert, Peter Aelterman, & Willy Verstraete. (2005b). Tubular microbial fuel cells for efficient electricity generation. *Environmental Science and Technology*, 39, 8077-8082.

Ramasamy, Ramaraja P., Zhiyong Ren, Matthew M. Mench, & John M. Regan. (2008). Impact of initial biofilm growth on the anode impedance of microbial fuel cells. *Biotechnology and Bioengineering*, 101, 101-108.

Reguera, Gemma, Kelly P. Nevin, Julie S. Nicoll, Sean F. Covalla, Trevor L. Woodard, & Derek R. Lovley. (2006). Biofilm and nanowire production leads to increased current in *Geobacter sulfurreducens* fuel cells. *Applied and Environmental Microbiology*, 72(11), 7345-7348.

Rozendal, Rene A., Hubertus V.M. Hamelers, & Cees J.N. Buisman. (2006). Effects of membrane cation transport on pH and microbial fuel cell performance. *Environmental Science and Technology*, 40, 5206-5211.

Schroder, Uew. (2007). Anodic electron transfer mechanisms in microbial fuel cells and their energy efficiency. *Physical Chemistry Chemical Physics*, 9, 2619-2629.

Schamphelaire, Liesje de, Lenn van den Bossche, Hai son dang, Monica Hofte, Nico Boon, Korneel Rabaey, & Willy Verstraete. (2008). Microbial fuel cells generating electricity from rhizodeposits of rice plants. *Environmental Science and Technology*, 42, 3053-3058.

Shimoyama, Takefumi, Shoko Komukai, Akira Yamazawa, Yoshiyuki Ueno, Bruce E. Logan & Kazuya Watanabe. (2008). Electricity generation from model organic wastewater in a cassette-electrode microbial fuel cell. *Applied Microbiology and Biotechnology*, 80, 325-330.

Snoeyink, Vernon L. and David Jenkins. (1980). *Water Chemistry*. New York: John Wiley and Sons, Inc.

Strik, David P.B.T.B., Hilde Terlouw, Hubertus V.M. Hamelers, & Cees J.N. Buisman. (2008). Renewable sustainable biocatalyzed electricity production in a photosynthetic algal microbial fuel cell (PAMFC). *Applied Microbiology and Biotechnology*, 81, 659-668.

Tchobanoglous, George, Hilary Theisen, and Samuel Vigil. (1993). *Integrated Solid Waste Management, Engineering Principles and Management Issues*. Boston, Mass: Irwin McGraw Hill.

Torres, Cesar I., Andrew Kato Marcus, & Bruce E. Rittmann. (2008). Proton transport inside the biofilm limits electrical current generation by anode-respiring bacteria. *Biotechnology and Bioengineering*, published online 5 Feb.

USEPA (United States Environmental Protection Agency). (1991). Criteria for Municipal Solid Waste Landfills. *Code of Federal Regulations, Title 40, parts 257 and 258*.

USEPA (United States Environmental Protection Agency). (2007). *Municipal Solid Waste Generation, Recycling, and Disposal in the United States: Facts and Figures for 2007*. (EPA 530-F-08-018). Washington, DC: author.

USEPA (United States Environmental Protection Agency). (2009). *Phosphorous, all forms, Method 365.3*. Washington, DC: author.

Xing, Defeng, Ti Zuo, Shaoan Cheng, John M. Regan, & Bruce E. Logan. (2008). Electricity generation by *Rhodospseudomonas palustris* DX-1. *Environmental Science and Technology*, 42, 4146-4151.

You, Shijie, Qingliang Zhao, Jinna Zhang, Junqiu Jiang, Chunli Wan, Maoan Du, & Shiqi Zhao. (2007). A graphite-granule membrane-less tubular air-cathode microbial fuel cell for power generation under continuously operational conditions. *Journal of Power Sources*, 173, 172-177.

You, Shi J., Qing L. Zhao, Jun Q. Jiang, Jin N. Zhang, & Shi Q. Zhao. (2006). Sustainable approach for leachate treatment: electricity generation in microbial fuel cell. *Journal of Environmental Science and Health Part A*, 41, 2721-2734.

Yu, Eileen Hao, Shaoan Cheng, Keith Scott, & Bruce Logan. (2007). Microbial fuel cell performance with non-Pt cathode catalysts. *Journal of Power Sources*, 171, 275-281.

Zuo, Yi, Pin-Ching Maness, & Bruce E. Logan. (2006). Electricity production from steam-exploded corn stover biomass. *Energy and Fuels*, 20, 1716-1721.

Zuo, Yi, Shaoan Cheng, Doug Call, & Bruce E. Logan. (2007). Tubular membrane cathodes for scalable power generation in microbial fuel cells. *Environmental Science and Technology*, 41, 3347-3353.

Zuo, Yi, Shaoan Cheng, & Bruce E. Logan. (2008). Ion exchange membrane cathodes for scalable microbial fuel cells. *Environmental Science and Technology*, 42, 6967-6972.

## **APPENDICES**

## APPENDIX A

### Landfill Leachate Additions

#### Square MFC Landfill Leachate Additions

Date	Volume (mL)
Cycle 1a	
1/13/2008	40
1/15/2008	40
1/18/2008	40
1/19/2008	40
Cycle 2a	
2/1/2008	40
2/3/2008	40
Cycle 3a	
2/12/2008	40
2/16/2008	40
2/19/2008	40
Cycle 4b	
8/11/2008	40
8/12/2008	40
8/13/2008	40
8/15/2008	40
Cycle 5b	
8/21/2008	40
8/23/2008	40
8/25/2008	40
8/28/2008	40
9/3/2008	90
Cycle 6b	
9/18/2008	40
9/19/2008	40
9/22/2008	80
Cycle 7b	
9/26/2008	80
9/29/2008	40

### Circle MFC Landfill Leachate Additions

Date	Volume (mL)
Cycle 1b	
8/15/2008	40
Cycle 2b	
8/28/2008	40
9/3/2008	50
Cycle 3b	
9/22/2008	40
Cycle 4b	
9/29/2008	30
Cycle 1c	
1/19/2009	50
1/21/2009	30
1/26/2009	70
Cycle 2c	
2/5/2009	40
2/6/2009	20
2/9/2009	40
2/13/2009	50
Cycle 3c	
2/20/2009	55
2/23/2009	45
2/24/2009	50
2/26/2009	48
3/1/2009	47
3/8/2009	60

### Larger Scale MFC Landfill Leachate Additions

Date	Volume (mL)
Cycle 1b	
2/5/2009	500
2/8/2009	600
2/13/2009	200
2/15/2009	200
Cycle 1b	
2/18/2009	200
2/20/2009	400
2/21/2009	200
2/23/2009	300
2/24/2009	300
2/25/2009	200
2/26/2009	300
2/27/2009	250
3/1/2009	360
3/3/2009	400
3/4/2009	250
3/5/2009	200
3/6/2009	200
3/8/2009	300
3/9/2009	200
3/10/2009	200
3/12/2009	200
3/13/2009	200
3/14/2009	300
3/16/2009	400
3/17/2009	200
3/18/2009	200
3/19/2009	200
3/20/2009	300
3/21/2009	200
3/22/2009	50
3/24/2009	200
3/26/2009	300
3/28/2009	400
3/30/2009	300
4/1/2009	500
4/3/2009	300
4/4/2009	700
4/8/2009	300
4/10/2009	55



## APPENDIX B

### Instrument Accuracy and Precision Data

**Sulfide Analyzer, Spectrophotometer: DR/2000 by HACH (Manufacturer Reported)**

Accuracy :  $\pm 2\%$

**COD Analyzer, Spectrophotometer: DR/2400 by HACH (Manufacturer Reported)**

Range: 20-1500 mg/L

Accuracy: 778-822 mg/L COD, 95% confidence limits of distribution

**YSI 556 Multi Probe System (Manufacturer Reported)**

DO Meter-Steady State Polarographic Probe

Range: 0-20 mg/L

Accuracy:  $\pm 2\%$  of reading or 0.2 mg/L (whichever is greater)

Range : 20-50 mg/L

Accuracy:  $\pm 6\%$  of reading

Temperature –YSI Precision® Thermistor

Range: -50- 400° C

Accuracy:  $\pm 0.15^\circ$  C

Conductivity- Four Electrode Cell with Auto Ranging

Range: 0-200 mS/cm

Accuracy:  $\pm 0.5\%$  of reading or 0.001 mS/cm (whichever is greater)

pH- Glass Combo Electrode

Range: 0-14 units

Accuracy:  $\pm 0.2$  units

ORP- Platinum Bottom Probe

Range: -999- 999 mV

Accuracy:  $\pm 20$  mV

### Resource Laboratories Instrument Data for Analyses

<b>Parameter</b>	<b>Quantitation Limit* (mg/L)</b>	<b>Instrument Dilution Factor**</b>
Alkalinity	5	1
Ammonia	250	1
BOD	5	1
Chloride	25	50
Nitrate	0.5	5
Nitrite	2.0	20
Phosphate	0.5	5
Sulfate	25	50
TOC	20	20
Total	0.50	1

\* The quantitation limit is the lowest concentration that can be detected

\*\* The instrument dilution factor is the dilution performed at the instrument.; a 1 means that there was no dilution necessary.

## APPENDIX C

### Power Density and Polarization Curve Calculation Example

#### Power Density Equation:

$$P_{\text{an/cat}} = \frac{E_{\text{MFC}}^2}{A_{\text{an/cat}} R_{\text{ext}}}$$

Where: E = Cell Voltage (V)

v = Volume of anode compartment (L)

R<sub>ext</sub> = External Resistance (Ω)

A<sub>an/cat</sub> = Surface Area of Anode or Cathode electrode

$$P_v = \frac{E_{\text{MFC}}^2}{v R_{\text{ext}}}$$

#### Example:

For the Circle MFC, where A<sub>an/cat</sub> = 258 cm<sup>2</sup> (0.0258 m<sup>2</sup>) and v = 934 mL (0.000934 m<sup>3</sup>) with an external resistance of 10 Ω, the cell voltage was recorded as 0.026 V (see Table A-1) so,

$$P_{\text{an}} = \frac{(0.026 \text{ V})^2}{(0.0258 \text{ m}^2) * 10 \Omega} = 2.62 \text{ mW/m}^2$$

Or

$$P_{\text{an}} = \frac{(0.026 \text{ V})^2}{(0.000934 \text{ m}^3) * 10 \Omega} = 72.38 \text{ mW/m}^3$$

Calculations for each external resistance tested can be seen in Table A-1

### Polarization Curve:

The Polarization curve is the current density vs. the Power Density. The Current Density is simply:

$$\text{Current Density} = \frac{I}{A_{An}} \quad \text{where } I = \text{current (A)}, I = \frac{\text{Voltage (V)}}{\text{Resistance}_{\text{ext}}(\Omega)}$$

$$A_{An} = \text{Surface area of the anode (cm}^2\text{)}$$

Example:

For the Circle MFC, at  $R_{\text{ext}}$  of 10  $\Omega$ , voltage = 0.026 V, so

$$I = \frac{0.026 \text{ (V)}}{10(\Omega)} \frac{1000 \text{ mA}}{1 \text{ A}} = 2.6 \text{ mA}$$

And

$$\text{Current Density} = \frac{2.6 \text{ mA}}{258 \text{ cm}^2} = 0.0101 \text{ mA/cm}^2$$

Calculations for each external resistance test can be seen in Tale A-1

Table A-1 Data/Calculations of Circle MFC Power Density/Polarization Curves

External Resistance ( $\Omega$ )	Cell Voltage (mV)	Cell Voltage (V)	Cell Current (mA)	Current density (mA/cm <sup>2</sup> )	Power density (mW/m <sup>2</sup> )	Power density (mW/m <sup>3</sup> )
10	26	0.026	2.60	0.0101	2.62	72.38
20	56	0.056	2.80	0.0109	6.08	167.88
40	122	0.122	3.05	0.0118	14.42	398.39
80	201	0.201	2.51	0.0097	19.57	540.70
100	248	0.248	2.48	0.0096	23.84	658.50
200	397	0.397	1.99	0.0077	30.54	843.73
400	488	0.488	1.22	0.0047	23.08	637.43
800	536	0.536	0.67	0.0026	13.92	384.50
1000	548	0.548	0.55	0.0021	11.64	321.52
2000	579	0.579	0.29	0.0011	6.50	179.47
4000	600	0.600	0.15	0.0006	3.49	96.36
8000	616	0.616	0.08	0.0003	1.84	50.78
10000	620	0.620	0.06	0.0002	1.49	41.16
20000	630	0.630	0.03	0.0001	0.77	21.25
40000	635	0.635	0.02	0.0001	0.39	10.79
OCP	644	0.644	0.00	0.0000	0.00	0.00

### Coloumbic Efficiency Calculation Example

$$C_E = \frac{8 \cdot I \cdot t}{F v_{An} \Delta COD}$$

Where: I = average current over t (A)

t = total time of cycle (sec)

F = Faraday's constant (96,500 C/mol<sup>-</sup>)

v<sub>An</sub> = Volume of anode compartment (L)

ΔCOD = Change in COD concentration  
over time t (g/L)

Example:

For Cycle 3b of Circle MFC where v<sub>An</sub> = 934 mL (0.934 L); ΔCOD = 0.1354 g/L and t = 776,736 sec (8.99 days) and I = 0.0008043 A (average over t)

$$C_E = \frac{8 \cdot 0.0008043 \text{ A} \cdot 776,735 \text{ sec}}{96,500 \text{ C/mol} \cdot 0.934 \text{ L} \cdot 0.1354 \text{ g/L}}$$
$$= 41.0\%$$

## APPENDIX D

### Mass Balance of Chloride Concentrations in MFCs

<b>Square MFC Chloride Mas Balance</b>							
	Cycle 1a	Cycle 2a	Cycle 3a	Cycle 4b	Cycle 5b	Cycle 6b	Cycle 7b
Vol. of Leachate (mL)	1005	1005	1005	1005	1005	1005	1005
Initial Conc. (mg/mL)	2.2	2.7	2.6	1.8	1.8	1.2	1.2
Total Vol. Leachate added (mL)	160	80	120	160	250	160	120
Final Concentration calculated (mg/mL)	2.5	2.9	2.9	2.1	2.2	1.4	1.3
Final Concentration measured (mg/mL)	2.7	3.4	3.2	2.2	2.6	1.5	1.5

<b>Circle MFC Chloride Mass Balance</b>				
	Cycle 1b	Cycle 2b	Cycle 3b	Cycle 4b
Vol. of Leachate (mL)	934	934	934	934
Initial Conc. (mg/mL)	1.8	1.8	1.2	1.2
Total Vol. Leachate added (mL)	40	90	40	30
Final Concentration calculated (mg/mL)	1.9	2.0	1.3	1.2
Final Concentration measured (mg/mL)	2.1	2	1.3	1.4

<b>Larger Scale Chloride Mass Balance</b>		
	Cycle 1c	Cycle 2c
Vol. of Leachate (mL)	18327	18327
Initial Conc. (mg/mL)	1.8	1.5
Total Vol. Leachate added (mL)	1500	9565
Final Concentration calculated (mg/mL)	1.9	2.3
Final Concentration measured (mg/mL)	1.9	2.4

**Mass Balance of Sulfate Concentrations in MFCs**

<b>Square MFC Sulfate Mas Balance</b>							
	Cycle 1a	Cycle 2a	Cycle 3a	Cycle 4b	Cycle 5b	Cycle 6b	Cycle 7b
Vol. of Leachate (mL)	1005	1005	1005	1005	1005	1005	1005
Initial Conc. (mg/mL)	0.012	0.008	0.009	0.038	0.038	0.039	0.039
Total Vol. Leachate added (mL)	160	80	120	160	250	160	120
Final Concentration calculated (mg/mL)	0.014	0.009	0.009	0.044	0.047	0.045	0.044
Final Concentration measured (mg/mL)	0.017	0.015	0.014	0.042	0.066	0.068	0.066

<b>Circle MFC Sulfate Mass Balance</b>				
	Cycle 1b	Cycle 2b	Cycle 3b	Cycle 4b
Vol. of Leachate (mL)	934	934	934	934
Initial Conc. (mg/mL)	0.038	0.038	0.039	0.039
Total Vol. Leachate added (mL)	40	90	40	30
Final Concentration calculated (mg/mL)	0.040	0.042	0.041	0.040
Final Concentration measured (mg/mL)	0.250	0.064	0.058	0.061

<b>Larger Scale Sulfate Mass Balance</b>		
	Cycle 1c	Cycle 2c
Vol. of Leachate (mL)	18327	18327
Initial Conc. (mg/mL)	0.14	0.069
Total Vol. Leachate added (mL)	1500	9565
Final Concentration calculated (mg/mL)	0.151	0.105
Final Concentration measured (mg/mL)	0.170	0.140